Jorge Miguel Martins Santos

Master's degree in Chemical and Biochemical Engineering

A Novel Integrated Metabolic Activated Sludge Model for Enhanced Biological Phosphorus Removal Processes: Development, Calibration, Validation and Application

Dissertation submitted in the fulfilment of the requirements for the degree of Doctor (Ph.D) in Bioengineering Systems (MIT-Portugal)

Supervisor: Adrian Michael Oehmen, Senior Lecturer, School of Chemical Engineering, The University of Queensland

Co-Supervisor: Maria d'Ascensão Miranda Reis, Full-Professor, Faculty of Sciences and Technology, Universidade NOVA de Lisboa

President: Professor José Paulo Barbosa Mota

Examiners: Professor Ramón Barat Baviera
Professor Albert Guisasola Canudas

Members: Researcher Nídia Dana Mariano Lourenço
Senior Lecturer Adrian Michael Oehmen
PhD Pedro Ricardo Neto Póvoa

FACULDADE DE CIÊNCIAS E TECNOLOGIA
UNIVERSIDADE NOVA DE LISBOA

April 2020

2020

A Novel Integrated Metabolic Activated Sludge Model for Enhanced Biological Phosphorus Removal Processes: Development, Calibration, Validation and Application

Jorge Santos

Jorge Miguel Martins Santos

Master's degree in Chemical and Biochemical Engineering

A Novel Integrated Metabolic Activated Sludge Model for Enhanced Biological Phosphorus Removal Processes: Development, Calibration, Validation and Application

Dissertation submitted in the fulfilment of the requirements for the degree of Doctor (Ph.D) in Bioengineering Systems (MIT-Portugal)

Supervisor: Adrian Michael Oehmen, Senior Lecturer, School of Chemical Engineering, The University of Queensland

Co-Supervisor: Maria d'Ascensão Miranda Reis, Full-Professor, Faculty of Sciences and Technology, Universidade NOVA de Lisboa

President: Professor José Paulo Barbosa Mota

Examiners: Professor Ramón Barat Baviera
Professor Albert Guisasola Canudas

Members: Researcher Nídia Dana Mariano Lourenço
Senior Lecturer Adrian Michael Oehmen
PhD Pedro Ricardo Neto Póvoa

FACULDADE DE CIÊNCIAS E TECNOLOGIA
UNIVERSIDADE NOVA DE LISBOA

April 2020

A Novel Integrated Metabolic Activated Sludge Model for Enhanced Biological Phosphorus Removal Processes: Development, Calibration, Validation and Application

ACKNOWLEDGEMENTS

I acknowledge Fundação para a Ciência e Tecnologia for the PhD grant SFRH/BD/103492/2014, UCIBIO-REQUIMTE in Chemistry department of NOVA School of Science and Technology for hosting this PhD project, and MIT-Portugal for promoting best practices in innovation, entrepreneurship and leadership through the doctoral program in Bioengineering Systems.

I am deeply grateful to my supervisor, Professor Adrian Oehmen, for inspiring my interest in metabolic modelling and for all his time and effort in guiding me throughout this project. Adrian shared valuable thoughts on enhanced biological phosphorus removal and provided insightful comments for the development of a novel model in this research area. Professor Maria Reis, my co-supervisor, has inspired me with her leadership, passion and dedication to science and education. Maria welcomed me in her research group, encouraged me to pursue my dreams, and always supported the execution and dissemination of my PhD project. In addition to all experience and professional opportunities, I am very grateful to my supervisors for inspiring me to be a dedicated and humble professional. I have had the pleasure of doing research with the top leaders in the field of environmental/ industrial bioengineering.

I would also like to thank the co-authors of my scientific publications: Dr. Leiv Rieger, Dr. Ana Lanham, Dr. Mónica Carvalheira, Dr. António Martins and Eng. Sara Barreto. A special thank you goes to Dr. Leiv Rieger and inCTRL Solutions Inc. for the assistance in SIMBA# (ifak, Germany), as well as to Dr. António Martins, Eng. Sara Barreto and Águas do Algarve, S.A. from the group of Águas de Portugal for the sampling campaign at the Boavista Water Resource Recovery Facility and for sharing the plant's historical data.

Many thanks to the FCT NOVA's Research and Innovation Accelerator, represented by Dr. Marta Cerejo, and to Frontier IP group plc, represented by Rui Andrês and Sara Reis. Your assistance in intellectual property management and technology transfer was very important.

During this PhD, I was fortunate to work and share ideas with many brilliant people in the BIOENG group. A big thank you to everyone.

Por fim, gostaria de dedicar esta tese à minha família e amigos que muito me apoiaram durante todo o percurso académico. Aos meus amigos Mauro Luís, Mariana Matos e Joana Pereira, um muito obrigado pela vossa amizade e companheirismo. Aos meus queridos primos, pais e irmãos, agradeço todo o carinho, incentivo e motivação.

A todos,
Um muito obrigado!

ABSTRACT

Enhanced biological phosphorus removal (EBPR) facilities achieve low effluent phosphorus (P) levels (below 1 g $P.m^{-3}$) for long periods of time. However, these facilities are often affected by unpredictable upsets that increase their operational costs and reduce the potential to recover P from downstream processes. Thereby, these facilities need to have access to reliable tools, capable of dynamically predicting EBPR performance and diagnosing plant upsets. To address this need, a novel integrated metabolic activated sludge model, the META-ASM, was developed with a robust single set of default parameters to describe the activity of the key organisms and processes relevant to EBPR systems.

The advances regarding EBPR mechanisms investigated over the last twenty years were integrated in the META-ASM model to overcome various shortcomings of existing EBPR models. Special attention is given to the effect of operational conditions on the competition between polyphosphate accumulating organisms (PAOs) and glycogen accumulating organisms (GAOs), along with the capability of PAOs and GAOs to denitrify, the metabolic shifts as a function of storage polymer concentration for each group, the role of these polymers in endogenous processes, and a better description of the fermentation process.

The model was calibrated and validated against 34 data sets describing different EBPR dynamics obtained from bench-scale batch tests inoculated with lab-scale enriched PAO-GAO cultures and full-scale sludge from different EBPR facilities. The overall strong correlations obtained between the predicted and the measured EBPR profiles demonstrated that this new model reduces calibration efforts and is capable of predicting the microbial and chemical transformations over a wide range of operational and environmental conditions, supporting the robustness of the unique default parameter set that was generated. A performance comparison between META-ASM and literature models also demonstrated that existing models require extensive parameter changes and have limited predictive power to describe different EBPR dynamics.

The capacity of the META-ASM model to describe the long-term performance of a full-scale 3-stage Phoredox (A2/O) EBPR system and to be used as an operational diagnostic tool was evaluated in a 1336-day long-term dynamic simulation, while its performance was compared with the ASM-inCTRL model, a version based on the Barker & Dold model. Overall, the META-ASM provided a better description of PAOs active biomass and storage polymers and was a more powerful operational diagnostic tool for plant upsets. Viable troubleshooting scenarios were simulated to mitigate the upsets caused by the high aerobic hydraulic retention times (HRTs) and low organic loading rates (OLRs) of the plant.

This thesis demonstrates that the META-ASM model is a powerful operational diagnostic tool for EBPR systems, capable of predicting plant upsets, optimising performance and evaluating new process designs.

Keywords: Activated sludge model (ASM), Biological nutrient removal (BNR), Enhanced biological phosphorus removal (EBPR), metabolic modelling, polyphosphate accumulating organisms (PAOs) and process optimisation.

RESUMO

As estações de remoção biológica de fósforo (EBPR) são capazes de atingir baixos níveis de fósforo (P) no efluente (< 1 g $P.m^{-3}$) por longos períodos. No entanto, o processo EBPR poder ser afetado por perturbações inesperadas que aumentam os custos operacionais e reduzem o potencial de recuperação de P em processos a jusante. Por estas razões, estas estações precisam de ter acesso a ferramentas fidedignas, que sejam capazes de prever de forma dinâmica a eficiência do processo EBPR e de diagnosticar as suas perturbações. De forma a responder a esta necessidade, foi desenvolvido um novo modelo metabólico de lamas ativadas, META-ASM, que descreve com um único conjunto de parâmetros padrão a atividade dos principais organismos e processos relevantes nos sistemas EBPR.

Os avanços relativos aos mecanismos de EBPR investigados nos últimos vinte anos foram integrados no modelo META-ASM de forma a corrigir várias deficiências existentes nos modelos de EBPR. Esta tese foca-se principalmente no efeito das condições operacionais na competição entre organismos acumuladores de polifosfato (PAOs) e organismos acumuladores de glicogénio (GAOs), na capacidade de desnitrificação destes organismos, nas mudanças de vias metabólicas em função da concentração dos polímeros armazenados por cada grupo de organismo, no papel que estes polímeros exercem nos processos endógenos, e em fornecer uma descrição mais detalhada do processo de fermentação.

O modelo foi calibrado e validado por 34 conjuntos de dados, que descrevem diferentes dinâmicas do processo EBPR, obtidos por testes laboratoriais operados em *batch* e inoculados com lamas enriquecidas em culturas PAO-GAO e lamas provenientes de diferentes estações de EBPR de grande escala. As fortes correlações obtidas entre as previsões do modelo e os perfis de EBPR medidos demonstram que este novo modelo reduz os esforços de calibração, e é capaz de prever as transformações biológicas numa vasta gama de condições operacionais e ambientais, utilizando apenas um único conjunto de parâmetros padrão. Este resultado realça a robustez dos parâmetros gerados neste estudo. Adicionalmente, o desempenho do modelo META-ASM foi comparado ao dos modelos da literatura. Esta comparação revelou que os modelos existentes requerem extensas alterações de parâmetros, e por essa razão a sua capacidade preditiva é mais limitada a descrever diferentes dinâmicas do processo EBPR.

As capacidades do modelo META-ASM em descrever a eficiência a longo-prazo de um sistema de EBPR (de grande escala e configuração A2/O) e de ser utilizado como uma ferramenta de diagnóstico operacional foram testadas numa simulação dinâmica de 1336 dias. No mesmo estudo, a performance do modelo META-ASM foi comparada à do modelo ASM-inCTRL (versão baseada no modelo Barker & Dold). Os resultados obtidos demonstraram que o modelo META-ASM foi mais eficiente a descrever a biomassa ativa dos PAOs e a concentração dos seus polímeros de armazenamento, e também foi uma ferramenta de diagnóstico operacional mais eficaz. As perturbações ao processo EBPR causadas pelos

altos tempos de retenção hidráulicos aeróbios e pelas baixas cargas orgânicas da estação em estudo foram mitigadas através da simulação de cenários economicamente viáveis.

O trabalho desenvolvido neste doutoramento demonstra que o modelo META-ASM é uma ferramenta poderosa no diagnóstico operacional de sistemas EBPR, capaz de prever perturbações inesperadas, de otimizar a eficiência e de avaliar novos designs do processo.

Palavras-chave: Modelo de lamas ativadas, remoção biológica de nutrientes, remoção biológica de fósforo, modelação metabólica, organismos acumuladores de polifosfato e otimização de processo.

TABLE OF CONTENTS

LIST OF FIGURES

LIST OF TABLES

LIST OF ABBREVIATIONS

The notation used in this thesis is in accordance with the new guidelines for using activated sludge models created by the International Water Association Task Group on Good Modelling Practice (Rieger et al., 2012).

A/O	2-stage Phoredox	**NH_X-N**	Ammonium plus ammonia
A2/O	3-stage Phoredox	**NO_3^--N**	Nitrate
Adj. R^2	Adjusted R-squared	**NOO**	Nitrite oxidizing organism
ANO	Autotrophic nitrifying organism	**NO_x**	Nitrates plus nitrites
AOO	Ammonia oxidizing organism	**OHO**	Ordinary heterotrophic organism
ASM	Activated sludge model	**OLR**	Organic loading rate
ATU	Allyl-N thiourea	**P**	Phosphorus
Ax	Anoxic	**PAO**	Polyphosphate accumulating organism
BCFS®	Biological chemical P removal configuration	**PHA**	Poly-β-hydroxyalkanoates
BNR	Biological nutrient removal	**PO_4^{3-}-P**	Phosphate
BOD	Biochemical oxygen demand	**PP**	Polyphosphate (poly-P)
COD	Chemical oxygen demand	**PP_{Hi}**	Non-releasable stored polyphosphate
CPO	*Competibacter*-lineage GAO	***ppk1***	Polyphosphate kinase gene
CSTR	Continuous stirred tank reactor	**PP_{Lo}**	Releasable stored polyphosphate
δ	ATP produced per $NADH_2$ oxidized ratio	**PT**	Portugal
DCPO	Denitrifying CPO	**P_{Tot}**	Total phosphorus
DDFO	Denitrifying DFO	**Q**	Flow rate
DFO	*Defluviicoccus* genus GAO	**qFISH**	Quantitative fluorescence *in situ* hybridisation
DGAO	Denitrifying GAO	**R_{AN}**	Anaerobic tank
DK	Denmark	**R_{AN1}**	First stirred cell in anaerobic tank
DO	Dissolved oxygen	**R_{AN2}**	Second stirred cell in anaerobic tank
DOHO	Denitrifying OHO	**RAS**	Return activated sludge
DPAO	PAO subgroup capable of reducing nitrate	**R_{AX}**	Anoxic tank
ε	PO_4 transported per $NADH_2$ oxidized ratio	**R_{AX1}**	First stirred cell in anoxic tank
EBPR	Enhanced biological phosphorus removal	**R_{AX2}**	Second stirred cell in anoxic tank
EFF	Effluent	**rbCOD**	Readily biodegradable COD
f_{DCPO}	Fraction of DCPO	**R_{OX}**	Aerobic tank
f_{DDFO}	Fraction of DDFO	**RSS**	Side-stream hydrolysis tank
f_{DPAO}	Fraction of DPAO	**RW**	Reject water
F_e	Iron dosage	**S2EBPR**	Side-stream EBPR configuration
GAO	Glycogen accumulating organism	**SBR**	Sequencing batch reactor
Gly	Glycogen	**SRT**	Sludge retention time
H_2	Hydrogen	**TCA**	Tricarboxylic acid
HRT	Hydraulic retention time	**Tot**	Total
INF	Raw influent wastewater	**TSS**	Total suspended solids
ISS	Inorganic suspended solids	**TW**	Thickened WAS
IWA	International Water Association	**UCT**	University of Cape Town
JHB	Johannesburg	**UCTPHO+**	University of Cape Town model
K_1, K_2	ATP necessary for biomass synthesis	**VFA**	Volatile fatty acid
K_{O2}	Oxygen half-saturation coefficient	**VSS**	Volatile suspended solids
META-ASM	Integrated metabolic activated sludge model	**WAS**	Waste activated sludge

MLR	Mixed liquor recycle	**WRRF**	Water resource recovery facility
MLSS	Mixed liquor suspended solids	$\mathbf{X_{Bio}}$	Particulate state variable of total active biomass
MLVSS	Mixed liquor volatile suspended solids	$\mathbf{X_{PAO,stor}}$	State variable of PHA stored by PAOs in ASM2d and Barker & Dold models
N	Nitrogen	$\mathbf{X_{PHA,Tot}}$	State variable of total PHA

META-ASM STATE VARIABLES

$\mathbf{S_{O2}}$	Dissolved oxygen	$\mathbf{X_B}$	Slowly biodegradable substrate
$\mathbf{S_F}$	Fermentable organic matter	$\mathbf{X_{B,N}}$	Particulate biodegradable organic N
$\mathbf{S_{F,N}}$	Soluble biodegradable organic N from S_F	$\mathbf{X_{B,P}}$	Particulate biodegradable organic P
$\mathbf{S_{F,P}}$	Soluble biodegradable organic P from S_F	$\mathbf{X_E}$	Endogenous decay products
$\mathbf{S_{Ac}}$	Acetate	$\mathbf{X_{IG}}$	Inorganic suspended solids
$\mathbf{S_{Pr}}$	Propionate	$\mathbf{X_{OHO}}$	Ordinary heterotrophic organisms
$\mathbf{S_U}$	Soluble unbiodegradable organics	$\mathbf{X_{AOO}}$	Ammonia oxidizing organisms
$\mathbf{S_{U,N}}$	Soluble unbiodegradable organic N	$\mathbf{X_{NOO}}$	Nitrite oxidizing organisms
$\mathbf{S_{U,P}}$	Soluble unbiodegradable organic P	$\mathbf{X_{PAO}}$	*Accumulibacter* PAOs
$\mathbf{S_{NHx}}$	Ammonium plus ammonia nitrogen	$\mathbf{X_{CPO}}$	*Competibacter*-lineage GAOs
$\mathbf{S_{NO3}}$	Nitrate	$\mathbf{X_{DFO}}$	*Defluviicoccus* genus GAOs
$\mathbf{S_{NO2}}$	Nitrite	$\mathbf{X_{PAO,PHA}}$	Poly-β-hydroxyalkanoates stored by PAOs
$\mathbf{S_{N2}}$	Dissolved nitrogen gas	$\mathbf{X_{CPO,PHA}}$	Poly-β-hydroxyalkanoates stored by CPO
$\mathbf{S_{H2}}$	Hydrogen gas	$\mathbf{X_{DFO,PHA}}$	Poly-β-hydroxyalkanoates stored by DFO
$\mathbf{S_{PO4}}$	Soluble inorganic phosphorus	$\mathbf{X_{PAO,PP}}$	Stored polyphosphates in PAOs
$\mathbf{S_{Alk}}$	Alkalinity	$\mathbf{X_{PAO,Gly}}$	Glycogen stored by PAOs
$\mathbf{C_U}$	Colloidal unbiodegradable organics	$\mathbf{X_{CPO,Gly}}$	Glycogen stored by CPO
$\mathbf{X_U}$	Particulate unbiodegradable organics	$\mathbf{X_{DFO,Gly}}$	Glycogen stored by DFO
$\mathbf{X_{U,N}}$	Particulate unbiodegradable organic N	$\mathbf{X_{MeOH}}$	Metal-hydroxides
$\mathbf{X_{U,P}}$	Particulate unbiodegradable organic P	$\mathbf{X_{MeP}}$	Metal-phosphates
$\mathbf{C_B}$	Colloidal biodegradable organics		

1

INTRODUCTION

1.1 Motivation and problem statement

Phosphorus (P) is an essential and irreplaceable nutrient for the growth and metabolic function of all living organisms (Yang et al., 2017). It is a limited resource mined from phosphate rock, which is unevenly distributed globally, and used mainly to produce mineral fertilizers (Desmidt et al., 2015; Scholz et al., 2013). The European Union is the region most dependent on imports of phosphate rock, as it imports about 92% of its needs from a handful countries (Desmidt et al., 2015; European Commission, 2013), including politically unstable countries like Morocco and Western Sahara. However, it is estimated that about 3 million metric tons $P.year^{-1}$, equivalent to 15-20% of world demand for phosphate rock (Rittmann et al., 2011; Yang et al., 2017), are being lost as human waste through sewage waters and contributing severely to the eutrophication and deterioration of aquatic ecosystems (Selman et al., 2008). To address the risk of P supply and control the severe effects of eutrophication, many regions have been implementing increasingly stringent regulations for P removal (less than 0.1 $g.m^{-3}$) (Bunce et al., 2018; Oleszkiewicz and Barnard, 2006) and policies that make P recovery mandatory in water resource recovery facilities (WRRFs) (Günther et al., 2018).

P can be removed efficiently in WRRFs by chemical P precipitation and enhanced biological P removal (EBPR) processes, or by a combination of both, and potentially recovered at various points in the treatment line, such as: the liquid phase, sludge phase and mono-incinerated sludge ash. P recovery rates can reach 40-50% from the liquid phase, at most, and up to 90% from sewage sludge and sewage sludge ash (Cornel and Schaum, 2009; Desmidt et al., 2015). Compared to chemical P removal, EBPR produces less sludge but with more P content and less inert materials, and significantly reduces chemical and sludge disposal costs (Parsons and Smith, 2008). Thus, the EBPR is a more economical and sustainable process for removing P and potentially enhancing P recovery in downstream processes (Yuan et al., 2012).

Although EBPR facilities are able to achieve low P effluent levels (below 1 g $P.m^{-3}$) for long periods of time, many of them suffer from inconsistent performance due to the occurrence of upsets that can lead to temporary or even irreversible EBPR loss (Barnard et al., 2012; Barnard and Abraham, 2006; Barnard and Steichen, 2006; Bushee et al., 2019; Gu et al., 2008; Neethling, 2006; Oehmen et al., 2007). In response to an upset event, the EBPR facilities oftentimes fall back to chemical P precipitation to meet effluent limits. As most upsets are unpredictable, chemicals are often added constantly and in excess as a corrective measure, which increases the operational costs and reduces the potential to recover P from downstream processes.

Due to these reasons, EBPR facilities need to have access to reliable and robust tools, capable of dynamically predicting EBPR performance and diagnosing plant upsets, that provide strategies to maintain a more stable and consistent long-term EBPR operation. However, existing EBPR models are lacking detailed and dynamic process understanding and, therefore, they require extensive

stoichiometric and kinetic parameter changes (Dunlap et al., 2016; Menniti et al., 2016), which reduces their predictive power and limits their practical use, especially regarding the prediction of long-term EBPR performance.

1.2 Thesis objectives

The overall objective of this thesis is to develop a novel integrated metabolic activated sludge model, the META-ASM, that provides an overall platform to describe the activity of the key organisms and processes relevant to EBPR systems with a robust single-set of default parameters and that overcomes various shortcomings of existing EBPR models studied over the last twenty years. It is intended that this model will become an important tool for the EBPR industry, allowing researchers to improve their understanding of the mechanisms behind microbial population dynamics, and practitioners to optimize their operation and design through a more reliable, economical, and less time-consuming method.

The specific goals of this thesis were to:

1) Review existing EBPR models and identify their limitations.
2) Gather information from targeted experiments available in literature to overcome these limitations.
3) Develop a novel structure for an EBPR biokinetic model and demonstrate its effectiveness.
4) Calibrate and validate the novel model with different data sets from experiments using enriched lab polyphosphate accumulating organism (PAO) - glycogen accumulating organism (GAO) cultures, as well as full-scale sludge to provide a single set of default parameters.
5) Apply the model in a full-scale EBPR WRRF as a diagnostic tool for plant upsets.

1.3 Thesis outline

This thesis is divided into five chapters, organized as follows:

- **Chapter 1** presents an introduction to this work by defining the motivation, the problem statement, the objectives and the outline of this thesis.

- **Chapter 2** introduces the necessary background and current state-of-the-art of the EBPR process and EBPR model development. It focusses on describing EBPR microbiology and biochemistry, the factors influencing EBPR process performance, as well as on identifying the most well-known EBPR literature models and research needs in EBPR modelling.

- **Chapter 3** presents a novel integrated metabolic activated sludge model, the META-ASM, and describes the new model developments, highlighting the mechanisms that were simplified or are neglected by current models. It describes the procedure followed to derive a reliable default parameter set capable of predicting EBPR behaviour over a wide range of selected operational and environmental conditions. In addition, the effectiveness of this novel model is also demonstrated in comparison with the performance of the most well-known EBPR literature models. The chapter ends with the discussion of the challenges and limitations as well as the implications of the proposed approach for modelling full-scale EBPR systems.

  This work was published in an international peer reviewed scientific journal as:

  Santos, J.M.M., Rieger, L., Lanham, A.B., Carvalheira, M., Reis, M.A.M., Oehmen, A., 2020. A novel metabolic-ASM model for full-scale biological nutrient removal systems. Water Res. 171, 115373. doi:10.1016/J.WATRES.2019.115373

- **Chapter 4** describes the application of the model developed, calibrated and validated in the previous chapter as an operational diagnostic tool in a full-scale EBPR system with a 3-stage Phoredox (A2/O) configuration, suffering from inconsistent performance due to the occurrence of EBPR upsets. The capability of this model to predict the upsets without requiring further parameter calibration is assessed and the model is also used to provide solutions for mitigating the causes of these upsets.

  This work will be submitted to an international peer reviewed scientific journal as:

  Santos, J.M.M., Martins, A., Barreto, S., Rieger, L., Reis, M.A.M., Oehmen, A., 2020. Long-term simulation of a full-scale EBPR WRRF with a novel metabolic-ASM model and its use as a diagnostic tool for plant upsets (in preparation).

- **Chapter 5** describes the general conclusions of this PhD project as well as the perspectives and recommendations for future work on EBPR modelling and metabolic modelling.

Other relevant publications not included in this thesis:

- Ribeiro, J.M., Conca, V., Santos, J.M.M., Dias, D.F.C., Sayi-Ucar, N., Frison, N., Oehmen, A.. Expanding ASM models towards integrated processes for short-cut nitrogen removal and bioplastic recovery (in preparation).
- Marques, R., Ribera-Guardia, A., Santos, J., Carvalho, G., Reis, M.A.M., Pijuan, M., Oehmen, A., 2018. Denitrifying capabilities of *Tetrasphaera* and their contribution towards nitrous oxide production in enhanced biological phosphorus removal processes. Water Res. 137, 262–272. doi:https://doi.org/10.1016/j.watres.2018.03.010.
- Marques, R., Santos, J., Nguyen, H., Carvalho, G., Noronha, J.P., Nielsen, P.H., Reis, M.A.M., Oehmen, A., 2017. Metabolism and ecological niche of *Tetrasphaera* and *Ca. Accumulibacter* in enhanced biological phosphorus removal. Water Res. doi:10.1016/j.watres.2017.04.072.

2

BACKGROUND

2.1 Enhanced biological phosphorus removal

Enhanced biological phosphorus removal (EBPR) is an activated sludge process that relies on the activity of a specific group of bacteria, known as polyphosphate accumulating organisms (PAOs). These organisms remove phosphate (PO_4^{3-}-P) from wastewater in excess of their growth requirements and store it as intracellular granules of polyphosphate called volutins (Gebremariam et al., 2011; Oehmen et al., 2007; Yuan et al., 2012). The typical range of the amount of phosphorus (P) incorporated in the sludge mass reported in full-scale EBPR systems is around 0.06-0.15 mg P/mg VSS (0.05-0.10 mg P/mg TSS) (Henze et al., 2008). However, PAOs have potential to incorporate up to 0.38 mg P/mg VSS (0.17 mg P/mg TSS) compared to the 0.02 mg P/mg VSS (0.015 mg P/mg TSS) incorporated by the ordinary heterotrophic organisms (OHOs), non-PAOs (Gebremariam et al., 2011; Henze et al., 2008; Wentzel et al., 1989; Yuan et al., 2012). The greater the enrichment of PAOs in the activated sludge, the more P can be removed from the influent and incorporated into the sludge. EBPR activated sludge systems can typically remove more than 85% of the P from the influent (Bunce et al., 2018; Gebremariam et al., 2011), while non-EBPR activated sludge systems can only remove about 15 to 25% (Henze et al., 2008).

The good performance of the EBPR process is maintained by recycling the activated sludge under alternating anaerobic and aerobic (or anoxic) conditions. In full-scale EBPR systems, the activated sludge is recycled through the return activated sludge stream (RAS) and PO_4^{3-}-P is removed from the influent through the wastage of P-rich sludge in the waste activated sludge stream (WAS). Figure 2.1. (A) shows a 2-stage Phoredox (A/O) EBPR configuration that removes simultaneously biochemical oxygen demand (BOD) and P. The term biological nutrient removal (BNR) is often used for EBPR activated sludge systems that simultaneously remove BOD, nitrogen (N) and P (Oehmen et al., 2007). In these systems, an anoxic stage is needed and, therefore, the activated sludge is recycled under alternating anaerobic, anoxic and aerobic conditions. Examples of BNR configurations are shown in Figure 2.1. (B), (C), (D), (E), (F) and (G). Note that this literature review focusses only on the EBPR mechanisms, while other biological processes are discussed where appropriate.

Previous EBPR (or BNR) configurations (hereafter referred to as conventional EBPR or BNR configurations) were designed based on the concept that all primary effluent would first have to pass through an anaerobic zone to produce the carbon source, volatile fatty acids (VFAs), required for PAOs (Barnard et al., 2017). In recent years, these configurations have been upgraded by systems that enhance hydrolysis and fermentation of the primary settled sludge and/ or of (a fraction) of the RAS to overcome the issue of low availability of readily biodegradable COD (rbCOD) and VFAs in the influent (Barnard et al., 2017; Henze et al., 2008). The Danish side-stream EBPR (S2EBPR) configuration shown in Figure 2.1. (H) is one of the several S2EBPR configurations developed for this purpose.

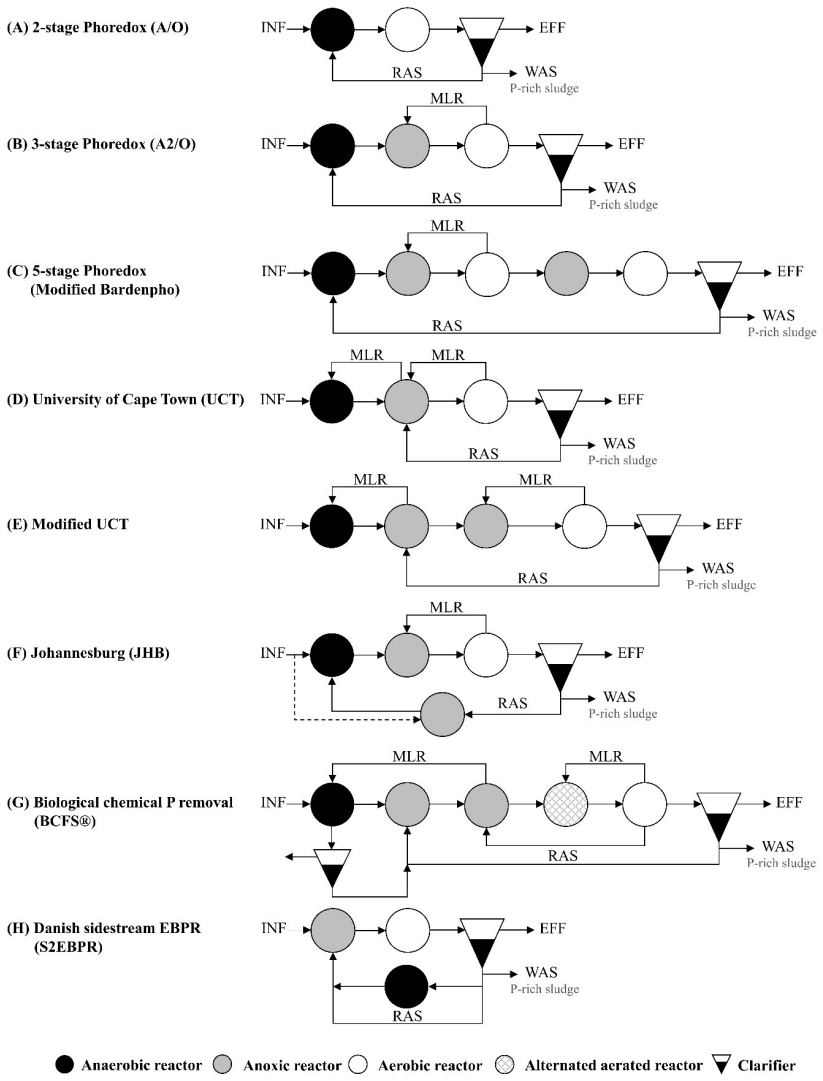

Figure 2.1. EBPR/ BNR full-scale configurations. INF: influent; EFF: effluent; RAS: return activated sludge; WAS: waste activated sludge; MLR: mixed liquor recycle. Adapted from Henze et al. (2008) and Meijer (2004).

2.1.1 EBPR microbiology and biochemistry

The most abundant PAOs in full-scale EBPR systems are members of the genera *Candidatus Accumulibacter* (hereafter referred to as *Accumulibacter*), *Candidatus Accumulimonas* (hereafter referred to as *Accumulimonas*) and *Tetrasphaera*. Wu et al. (2019) performed a global study on diversity and biogeography of bacterial communities in 269 water resource recovery facilities (WRRFs) from 23 countries and 6 continents and showed that the relative abundance of these organisms was 0.42 ± 0.04%, 0.42 ± 0.06% and 0.17 ± 0.02%, respectively.

Accumulibacter, genus member of the family *Rhodocyclaceae* of the *Betaproteobacteria* class, is the most studied PAO organism at lab-scale (Bond et al., 1995; Carvalheira et al., 2014a, 2014b; Crocetti et al., 2000; Hesselmann et al., 1999; Rubio-Rincón et al., 2017) and full-scale (Lanham et al., 2013; Saunders et al., 2003, 2013). These organisms were classified into two main groups (Types I and II), each divided into several clades (IA-E and IIA-G), using both the polyphosphate kinase gene (*ppk1*) and the 16S rRNA as a genetic marker (He et al., 2007; Peterson et al., 2008).

The metabolism of *Accumulibater* PAOs is very dynamic and relies on the role of three storage polymers: polyphosphate, poly-β -hydroxyalkanoates (PHA) and glycogen. Under anaerobic conditions, unlike most other organisms, they take-up VFAs and store them as PHAs using the energy produced from the hydrolysis of intracellular polyphosphate and release of PO_4^{3-}-P as well as the reducing power from either tricarboxylic acid (TCA) cycle or glycolysis of intracellular glycogen (Cokro et al., 2017; Lanham et al., 2013; Zhou et al., 2009). Moreover, polyphosphate and glycogen are used sequentially as energy sources for anaerobic maintenance. Under anoxic or aerobic conditions, PHA is oxidized for PO_4^{3-}-P uptake and polyphosphate production, glycogen regeneration and biomass growth. A net removal of PO_4^{3-}-P is observed because more PO_4^{3-}-P is taken up under aerobic conditions due to the growth of new cells compared to the PO_4^{3-}-P released under anaerobic conditions. PHA, glycogen and polyphosphate are sequentially used as energy sources for the aerobic and anoxic maintenance processes. Figure 2.2 shows the biochemical transformations of *Accumulibacter*, and this phenotype has been used to characterise the activity of other putative PAOs (hereafter referred to as classical PAOs).

Several *Accumulibacter* PAO clades in WRRFs have been found to have different denitrification capabilities. Some *Accumulibacter* species are capable of performing denitrifying PO_4^{3-}-P removal with nitrate, as suggested by recent studies (Camejo et al., 2019; Gao et al., 2019; Skennerton et al., 2015), while all known *Accumulibacter* clades are able to perform denitrification from nitrite onwards to dinitrogen gas, as suggested by previous research in this area (Camejo et al., 2016; Flowers et al., 2013; Martín et al., 2006).

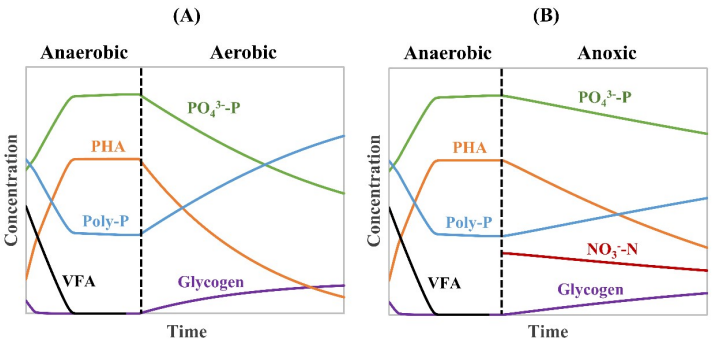

Figure 2.2. Schematic diagram showing the typical phenotype of classical PAOs. The graph shows the typical profiles of PO_4^{3-}-P, VFAs, PHA, polyphosphate (poly-P), glycogen, nitrate (NO_3^--N) occurred in an alternating anaerobic/ aerobic (A) and alternating anaerobic/ anoxic (B) sequencing batch reactors. Adapted from Henze et al. (2008).

The impact of the genera *Accumulimonas* and *Tetrasphaera* PAOs in EBPR systems requires further research as well as an understanding of the underlying mechanisms. *Accumulimonas,* is a genus member of the family *Halomonadaceae* of the *Gammaproteobacteria* class, and has been suggested to behave similarly to the classical PAO phenotype, while *Tetrasphaera*, a genus member of the family *Intrasporangiaceae* of the *Actinobacteria* class, appear to show a different phenotype (Stokholm-Bjerregaard et al., 2017).

In recent years, the role of *Tetrasphaera* PAOs in EBPR systems has aroused much research interests because these organisms have been found in significant abundance under certain EBPR configurations, especially in S2EBPR (Lanham et al., 2013; Liu et al., 2019; Stokholm-Bjerregaard et al., 2017; Wang et al., 2019; Wu et al., 2019), and sometimes outnumbering the classical PAO organisms. However, the quantification of its contribution to store intracellular P remains unclear and warrants further research. Available studies show that their metabolism does not rely on PHA and they appear to be less competitive for VFA uptake (Kong et al., 2008; Kristiansen et al., 2013; Nguyen et al., 2011), which is not consistent with the classical PAO phenotype. Instead, they can grow anaerobically by fermenting amino acids or sugars and aerobically through the oxidation of intracellular metabolites, such as amino acids, sugars and possibly fermentation products (Liu et al., 2019; Nielsen et al., 2019). The profile of PO_4^{3-}-P is still unclear in *Tetrasphaera* PAOs. An enriched lab-scale study showed that these organisms are able to uptake PO_4^{3-}-P anaerobically through energy generated by fermentation of some carbon sources (Marques et al., 2017), whereas other studies showed that they release PO_4^{3-}-P anaerobically, and uptake PO_4^{3-}-P aerobically and anoxically (Kristiansen et al., 2013; Nguyen et al., 2015). Although *Tetrasphaera* is able to denitrify, their ability to remove P under anoxic conditions is less significant compared to *Accumulibacter* PAOs (Marques et al., 2018).

2.1.2 Factors influencing EBPR process performance

WRRFs with the EBPR configurations shown in Figure 2.1 are able to achieve low P effluent levels (below 1 g $P.m^{-3}$) for long periods of time. However, several studies have reported that many of these EBPR facilities suffer from inconsistent performance or unpredictable upsets that can lead to temporary or even irreversible EBPR loss (Barnard et al., 2012; Barnard and Abraham, 2006; Barnard and Steichen, 2006; Bushee et al., 2019; Gu et al., 2008; Neethling, 2006; Oehmen et al., 2007; Rieger et al., 2001). In this section, examples of factors commonly reported as primary causes of EBPR upsets are described, highlighting their impact on the metabolism of *Accumulibacter* PAOs.

(a) Influent load dynamics. WRRFs are commonly affected by periods of limited availability of rbCOD and nutrients in the influent, occurring on weekends, rainfall events or changes in population flux (e.g. public vacation). A shift in influent loads affects the activity of *Accumulibacter* PAOs because their metabolism relies on the availability of VFAs. Under periods of low organic loading or starvation conditions, the aerobic (or anoxic) ability of PAOs to take up PO_4^{3-}-P and grow decreases, since less PHA is stored under anaerobic conditions. As a consequence, the endogenous activity of PAOs increases and PAOs tend to deplete their storage polymers prior to decay (Carvalheira et al., 2014c; Hao et al., 2010; Liu et al., 2017; Lopez et al., 2006; Lu et al., 2007; Stokholm-Bjerregaard, 2016; Vargas et al., 2013; Wang et al., 2012, 2015). This behaviour suggests that EBPR performance may be affected only temporarily if caused by the reduction in PAOs activity, or it may be lost if PAOs are exposed to long periods of starvation conditions that cause the exhaustion of their storage polymers and lead to their decay. As mentioned, the S2EBPR configuration shown in Figure 2.1. (H) was mainly developed to overcome this issue by enhancing the hydrolysis and fermentation of (a fraction) of the RAS, since many EBPR facilities are limited by the small size of their mainstream anaerobic reactors.

(b) Inhibition of fermentation. Recycling of electron acceptors (oxygen, nitrate and/ or nitrite) to the anaerobic zones inhibits the fermentation performed by OHOs and promotes their competition with PAOs for the carbon source. This effect reduces the EBPR efficiency in WRRFs that are limited in carbon source because less VFAs are available for PAOs. Figure 2.1. (B), (C), (D), (E) and (F) show examples of BNR configurations developed to overcome the issue of nitrate and nitrite entrainment in the anaerobic zone.

(c) PAO-GAO competition for substrate in anaerobic zones. Glycogen accumulating organisms **(**GAOs) compete with PAOs for the VFAs under anaerobic conditions, leading to EBPR deterioration due to the fact that most of the systems are carbon limited (Cech and Hartman, 1993; Satoh et al., 1994; Zeng et al., 2003a). These organisms are sometimes found in full-scale systems in similar abundance than *Accumulibacter* (Lanham et al., 2013; Saunders et al., 2003; Stokholm-Bjerregaard et al., 2017) and their presence affects the observed anaerobic EBPR yields and kinetic rates. The proliferation of these organisms can be controlled through the operational conditions discussed below.

The most studied GAOs at lab-scale (Carvalheira et al., 2014a; Crocetti R. et al., 2002; Kim et al., 2011; Kong et al., 2002; Dai et al., 2007; Wong et al., 2004; Wong and Liu, 2007) and full-scale systems (Kong et al., 2002, 2006; Mcilroy et al., 2015; Stokholm-Bjerregaard et al., 2017; Wong et al., 2005; Burow et al., 2007; McIlroy and Seviour, 2009; Meyer et al., 2006; Stokholm-Bjerregaard et al., 2017) are the genera *Candidatus Competibacter* and *Candidatus Contendobacter* (hereafter referred to as *Competibacter*-lineage), both belonging to the *Competibacteraceae* family (*Gammaproteobacteria* class), and the *Defluviicoccus* genus of the family *Rhodospirillaceae* (*Alphaproteobacteria* class). The *Competibacter*-lineage is recognized to be composed of 13 clades (Mcilroy et al., 2015) and the *Defluviicoccus* genus of four clusters (I-IV) (Stokholm-Bjerregaard et al., 2017). The phenotype identified for these classical GAOs is similar to that of *Accumulibacter*, except that polyphosphate is not cycled (Oehmen et al., 2007). These organisms rely solely on glycogen as source of energy and reducing power under anaerobic conditions (Liu et al., 1994; Mino et al., 1995).

(d) Effect of selected operational conditions and environmental factors. The most relevant operational and environmental conditions influencing full-scale EBPR performance are the: i) high influent $rbCOD_{INF}/P_{Tot,INF}$ ratio; ii) carbon composition; iii) low pH values; iv) high dissolved oxygen (DO); v) excessive return activated sludge (RAS) recycle rates; vi) long hydraulic retention times (HRTs) in aerobic tanks; vii) very low and very high sludge retention times (SRTs); viii) high environmental temperatures and ix) overdosing of metals. The individual or combined effect of these operational conditions may exert a selective pressure that favours the growth of other organisms over PAOs, as discussed below.

i) High influent $rbCOD_{INF}/P_{Tot,INF}$ ratio. Several studies indicate that a high $rbCOD_{INF}/P_{Tot,INF}$ ratio (e.g. >50 g COD/g P) in the influent tends to favour the growth of GAOs, whereas a low $rbCOD_{INF}/P_{Tot,INF}$ ratio (e.g. <13 g COD/g P) tends to be more favourable for the growth of PAOs (Gu et al., 2008; Oehmen et al., 2007). Ratios between these limits led to coexistence of both PAO and GAOs. Despite this influence on the PAO-GAO competition, high EBPR stability was positively correlated with higher influent $rbCOD_{INF}/P_{Tot,INF}$ ratios (Gu et al., 2008).

ii) Carbon composition. GAOs compete with PAOs for the VFAs, as previously described. Most available studies (Carvalheira et al., 2014b; Chen et al., 2005; Dai et al., 2007; Hollender et al., 2002; Oehmen et al., 2004, 2005b; Onuki et al., 2002; Pijuan et al., 2004; Wang et al., 2010) have focused mainly on the impact of acetate and propionate on the PAO-GAO competition because they are the most abundant VFAs (Oehmen et al., 2007) in wastewater. These experimental studies showed that the *Competibacter*-lineage and *Defluviicoccus* genus GAOs are able to take up acetate at a similar and about half of the *Accumulibacter* rate, respectively. On the other hand, the *Defluviicoccus* genus can take up propionate at a similar rate as *Accumulibacter*, while the *Competibacter*-lineage takes up this VFA at negligible rates. Lopez-Vazquez et al. (2009), through a metabolic model, and Carvalheira et al. (2014b),

through experimental studies, demonstrated that the combined mixture of acetate and propionate (75-25 and 50-50% acetate to propionate ratios) in the influent favours the metabolism of PAO over GAO.

In addition to these VFAs, other carbon sources, such as sugars, amino acids and alcohols, appear to have an impact on the EBPR performance. For instance, *Accumulibacter* type IIF was reported to be able to use ethanol (Skennerton et al., 2015), while recent studies (Liu et al., 2019; Nielsen et al., 2019) have shown that *Tetrasphaera* PAOs are capable of fermenting amino acids and sugars. However, other new putative GAOs, such as M*icropruina* (McIlroy et al., 2018; Shintani et al., 2000), appear to have the same capacity as *Tetrasphaera* PAOs and, therefore, the impact of these carbon sources on the PAO-GAO competition requires further research.

iii) Low pH values. Smolders et al. (1994a) found that the energy requirements for acetate uptake across the cell membrane of *Accumulibacter* PAOs increase linearly with the pH (in the range of 5.5-8.5) in order to compensate the increased electrical potential difference and maintain the proton motive force of the cell constant. Filipe et al. (2001) observed the same effect with an unidentified group of GAOs and demonstrated that GAOs use less energy for acetate uptake than PAOs, suggesting that low pH values promote the growth of GAOs. Therefore, higher pH values (>7.0) are used to outcompete GAOs because PAOs have polyphosphate and glycogen as sources of energy under anaerobic conditions, while GAOs only have glycogen (Gebremariam et al., 2011; Oehmen et al., 2007).

iv) High DO. Carvalheira et al. (2014a) showed that the growth of GAOs is favoured at high DO conditions. The authors concluded that PAOs have a higher affinity for oxygen, which provide them a kinetic advantage over GAOs at low DO levels (<1.5 $mg.L^{-1}$). The same effect was observed by Keene et al. (2017) in their pilot and full-scale experiments.

v) Excessive RAS recycle rates. EBPR systems operating with excessive RAS recycle rates promote the recycling of nitrate and nitrite to anaerobic zones, whose impact on the EBPR performance was described previously.

vi) Long HRTs in aerobic tanks. This effect tends to reduce the amount of polyphosphate in PAOs (Carvalheira et al., 2014a) and is worsened when an increase of the aerobic HRT accompanies the reduction of the organic loading rate (OLR). In these situations, an aerobic PO_4^{3-}-P release is typically observed in the aerobic tanks due to the fact that PAOs, after depleting their PHA and glycogen pools, consume polyphosphate (and release PO_4^{3-}-P) as a survival strategy. This reduction of polyphosphate content offers a competitive advantage for the growth of other organisms because PAOs have less energy available for the consumption of VFA either under anaerobic or anoxic or aerobic conditions. Another relevant effect is that PAOs can use alternative pathways for the origin of reducing power in the anaerobic metabolism when glycogen is depleted, such as the TCA cycle (Cokro et al., 2017; Lanham et al., 2013; Pijuan et al., 2008; Zhou et al., 2009). This metabolic shift is often observed in full-scale EBPR processes with lower influent VFA concentrations and longer aerobic retention times, as

demonstrated by Lanham et al. (2014) through the application of mathematical models. Although this metabolic shift offers PAOs advantages over GAOs, it can also affect EBPR stability, because in both alternative pathways more PO_4^{3-}-P is released and less PHA is produced under anaerobic conditions. This means that less PHA is available for the removal of PO_4^{3-}-P under anoxic and aerobic conditions.

vii) Very low or high SRTs. The state of the art on the effect of the sludge age on EBPR performance as well as on the PAO-GAO competition remains unclear. Chan et al. (2017) tested various SRTs (from 14 to 3 days) on the long-term EBPR performance of three different A/O sequencing batch reactors (SBRs) and observed a washout of *Accumulibacter* at a SRT of 3 days. The authors suggested that EBPR can be sustained with a minimal SRT around 3.6-4 days at 25ºC. On the other hand, Rodrigo et al. (1999) studied the effect of SRT from 11 to 65 days on the performance of a bench scale continuous A2/O reactor and suggested that GAOs could be favoured at long SRTs. In line with this work, Whang and Park (2006) studied the effect of the temperature and SRT on the competition between PAOs and GAOs and observed that GAOs were able to outcompete PAOs in an A/O SBR at 30ºC and SRT of 10 days. Reducing the SRT from 10 to 5 days improved the EBPR efficiency, but GAOs and PAOs still coexisted at 30ºC. The authors concluded that the EBPR efficiency was only improved at 30ºC when the SRT was reduced from 5 to 3 days.

Theoretically, the minimum SRT of an EBPR process is not directly linked to the maximal growth rate of the microorganisms, as it occurs in activated sludge systems designed for the removal of COD and N. In EBPR systems, the dynamics of the storage polymers play an important role on the definition of the minimum SRT, especially the dynamics related with the PHA conversion kinetics, the maximum achievable PHA content in the cells (storage capacity) and the effects of temperature, carbon source, electron acceptors and other parameters on these kinetics (Brdjanovic et al., 1998b; Schauer et al., 2018). The range of SRTs chosen in various studies with lab-scale enriched PAO-GAO cultures has been between 5 to 20 days (Carvalheira et al., 2014a, 2014b; Carvalho et al., 2007; Chan et al., 2017; Lee et al., 2007; Li et al., 2008; Rubio-Rincón et al., 2017; Saad et al., 2016), suggesting that this range is sufficient to sustain the performance of PAOs.

viii) High environmental temperatures. This effect favours the growth of PAOs and GAOs. However, GAOs have competitive advantages over PAOs because their anaerobic, aerobic and anoxic kinetic rates are higher than PAOs, particularly at 25-30ºC (Brdjanovic et al., 1997, 1998a; Lopez-Vazquez et al., 2007, 2009; Meijer et al., 2002).

ix) Overdosing of metals. Adding high doses of metals can contribute to the reduction of EBPR performance because available metals precipitate PO_4^{3-}-P, which means that less polyphosphate is stored by PAOs and used as a source of energy for the consumption of VFAs. In fact, this effect was demonstrated by Lv et al. (2014), where GAOs ended up being favoured by the prolonged addition of chemical precipitants.

2.2 EBPR model development

Biokinetic models have been developed to summarise the current state-of-knowledge of the most relevant biochemical transformations occurring in activated sludge processes. These models are presented in a table format, known as the Gujer matrix or Petersen matrix, which is composed of a stoichiometric matrix and a kinetic vector. The stoichiometric matrix contains the stoichiometric coefficients of each process, where state variables (or components) are displayed in columns and processes are displayed in rows. The kinetic vector contains only one column and the same number of rows as the stoichiometric matrix and shows the kinetic rate expressions of each process. In addition, a composition matrix is also presented with the required conversion coefficients for all state variables (in rows) to check the continuity for conserved (e.g. chemical oxygen demand, COD, elements and charge) and observable (e.g. TSS) (in columns) elements for each process. Readers are referred to Rieger et al. (2012) for more details on the structure of the Gujer matrix and guidelines for the development of activated sludge models.

Currently there are three different model concepts used in the literature to describe EBPR activated sludge systems: (i) the activated sludge models, ASMs, (ii) the metabolic models and (iii) the combination of these two approaches. The biokinetic models shown in Table 2.1 have become the state-of-the-art reference for modelling EBPR activated sludge processes in engineering applications and its implementation in process simulators has provided a less time-consuming and less costly methodology to understand, design, control and optimise EBPR systems.

Table 2.1. List of the most known EBPR biokinetic models used in activated sludge systems. Comparison in terms of number (#) of state variables and processes as well as a list of standard processes. Adapted from Hauduc et al. (2013).

	Barker & Dold (Barker and Dold, 1997a)	**ASM2d** (Henze et al., 1999)	**ASM3+BioP** (Rieger et al., 2001)	**UCTPHO+** (Hu et al., 2007a)	**ASM2d + TUD** (Meijer, 2004)
# of state variables	**19**	**19**	**17**	**16**	**18**
# of processes	**36**	**21**	**23**	**35**	**22**
Standard processes					
Hydrolysis	5	3	1	-	3
Fermentation	1	1		1	1
OHO growth	8	4	2	12	4
-Adsorption	-	-	-	1	-
-Storage	-	-	2	-	-
ANO[a] growth	1	1	1	1	1
OHO decay	1	1	4	1	1
ANO decay	1	1	2	1	1
PHA storage	1	1	1	1	2
Glycogen storage	-	-	-	-	2
Poly-P[b] storage	{5	2	2	{6	2
PAO growth		2	2		2
PAO decay	13	3	6	11	3
Phosphorus precipitation	-	2	-	-	-

[a] Autotrophic nitrifying organisms and [b] polyphosphate.

2.2.1 ASM models

ASM models have been proposed as mechanistic models that represent the biochemical transformations in activated sludge through several simplified process descriptions (Hauduc et al., 2013). The stoichiometric coefficients in these models are obtained through mass balances of chemical equations that describe the bulk biochemical transformations of the processes. In this approach, the initial substrates (e.g. VFAs) and final products (e.g. PHAs) are only considered in the mass balances, neglecting the effect of cell intermediates (e.g. reducing power, NADH, and energy, ATP). The kinetic expressions are based on the Monod equation, where the kinetic coefficients need to be rigorously calibrated and validated by appropriate experimental tests (Oehmen et al., 2007). The ASM models are published with their stoichiometric and kinetic parameters. These parameters are considered default only if they were validated on different WRRFs and have a clear explanation of how each proposed value was obtained, as well as the boundaries where they remain valid (Rieger et al., 2012).

Examples of ASMs developed, as knowledge on EBPR mechanisms evolved, are: i) the ASM2 model (Henze et al., 1995)/ ASM2d model (Henze et al., 1999); ii) the Barker & Dold model (Barker and Dold, 1997a); iii) the ASM3+BioP (Rieger et al., 2001) and iv) the most recent version of the University of Cape Town model, UCTPHO+ (Hu et al., 2007a). These models were developed to

describe EBPR together with COD and N removal, oxygen consumption and sludge production by incorporating the activity of the following three microbial groups: the ordinary heterotrophic organisms (X_{OHO}), the autotrophic nitrifying organisms (X_{ANO}) and PAOs (X_{PAO}). Table 2.1 summarises the standard processes incorporated in each model.

The ASM2 model (Henze et al., 1995), developed by the International Water Association (IWA), was extended from the ASM1 model (Henze et al., 1987) to incorporate the EBPR processes based on the UCTPHO model (Wentzel et al., 1992) and other literature information available at the time. In addition, a simple chemical P removal model via precipitation was also included. The ASM2 model assumes that PAOs only grow under aerobic conditions and, therefore, it was extended in 1999 into the ASM2d model (Henze et al., 1999) to include the knowledge acquired on denitrifying PAOs, where two additional anoxic PAO processes were incorporated. The authors intended to provide a conceptual platform that could be used for further model development, recognising that these models were a compromise between complexity and simplicity, and between different points of view on what the correct EBPR model should look like (Henze et al., 2000). Moreover, the model parameter set presented was not validated extensively against experimental data (Hu et al., 2003), although since the original publications, many studies have proposed new default parameter sets (Hauduc et al., 2011). In parallel to these efforts, a more complex biokinetic model was presented, calibrated and validated by Barker & Dold in 1997 (Barker and Dold, 1997a, 1997b). The authors also used as a starting point the same models used for ASM2 and also included the activity of denitrifying PAOs.

To overcome some of the shortcomings of ASM1, the IWA presented the ASM3 model (Gujer et al., 1999) as the new standard model for describing hydrolytic, heterotrophic and autotrophic processes in activated sludge systems. This model replaced the death-regeneration process for heterotrophic organisms by an endogenous respiration process and also introduced the role of organic substrates. Later, Rieger et al. 2001 added to the ASM3 an EBPR module based on modified processes from the ASM2d. The resulting model, ASM3+BioP (Rieger et al., 2001), neglects the fermentation of readily biodegradable COD, the chemical P removal via precipitation model was not included, and PAO decay is modelled as endogenous respiration. This model was calibrated and validated with experimental data from batch, pilot and full-scale WRRF experiments.

Increasing interest in BNR activated sludge systems led Hu et al. 2007a to develop a new ASM, UCTPHO+. The authors reviewed the state-of-the-art for BNR activated sludge models and selected the UCTPHO model (Wentzel et al., 1992) as the most suitable model for further development, using also information from available literature and other models, such as the ASM2 model (Henze et al., 1995)/ ASM2d model (Henze et al., 1999) and the Barker & Dold model (Barker and Dold, 1997a). They focused mainly on improving the description of the anoxic growth of PAOs, with associated PAO denitrification and anoxic P uptake and on the PAO anoxic death/ maintenance. The model was calibrated and validated against a large number of data sets (Hu et al., 2007b).

2.2.2 Metabolic models

Metabolic models are mechanistic models that rely on the understanding of the metabolic pathways active in the process in order to explain the biochemical transformations that take place within the cells, providing a better definition of the biological processes (Oehmen et al., 2010a). In this approach, most of the yield coefficients are calculated theoretically through substrate, energy and reducing power balances on internal cellular reactions defined based on well-established biochemical pathways for the processes involved in PAO and GAO metabolism. As opposed to ASMs, an overall stoichiometric reaction is determined for each anaerobic, anoxic and aerobic condition by correlating unknown internal cellular reaction rates with observable rates outside the cell, assuming that the reaction intermediates, such as ATP and NADH, do not accumulate within the cells (i.e. their production rates are equal to their consumption rates) (Oehmen et al., 2007). The overall stoichiometric reaction is expressed as a function of initial substrates and final products and the kinetic expressions are also based on the Monod equation. This approach not only increases the consistency and reliability of the model, but also facilitates the calibration process by reducing the number of parameters that require calibration, since the kinetic parameters are the only parameters that require calibration.

Application of advanced molecular tools into lab-scale PAO-GAO enriched cultures and full-scale EBPR systems contributed to the development of various metabolic models (Oehmen et al., 2010a). In this section, the most relevant EBPR metabolic models are described. Smolders et al. (1994a, 1994b, 1995) proposed the first metabolic models for the anaerobic and aerobic metabolism of PAOs on acetate based on PAO lab-scale enriched cultures. Following the same kinetic structure, Kuba et al. (1996) proposed a metabolic model for denitrifying EBPR systems. Subsequently, Murnleitner et al. (1997) integrated the previous anaerobic, aerobic and anoxic PAO metabolic models in a single model, known as the "Delft model", and reformulated its kinetic structure. Metabolic models for the anaerobic and aerobic metabolism of GAOs on acetate were also proposed by Filipe et al. (2001) and Zeng et al. (2002, 2003a). Later, Oehmen et al. (2005c, 2006) adapted the previous models to describe the anaerobic and aerobic metabolism of PAOs and GAOs on propionate. Based on the state of the art available, Lopez-Vazquez et al. (2009) developed an overall PAO-GAO metabolic model by incorporating the effect of the carbon source (such as acetate and propionate), temperature (from 10 to 30ºC) and pH (from pH 6.0 to 7.5) on the competition between the genera *Accumulibacter*, *Competibacter* lineage and *Defluviicoccus*. Following the same kinetic structure, Oehmen et al. (2010b) extended the previous model to describe the different denitrification capabilities of *Accumulibacter* Types I and II as well as denitrifying and non-denitrifying *Competibacter* and *Defluviicoccus* GAOs. The authors modelled denitrification as a multi-step process (NO_3->NO_2->N_2O->N_2). Building on the same research, Lanham et al. (2014) adapted the previous PAO-GAO metabolic models to describe the anaerobic and aerobic biochemical transformations observed in bench-scale batch tests inoculated with full-scale sludge from four different WRRFs. The authors needed to incorporate the TCA cycle as a source of reducing power

in the anaerobic metabolism of PAOs, since previous PAO-GAO metabolic models only considered the glycolysis pathway. They also modified the aerobic maintenance processes in PAOs to describe the sequential dependence on PHA, glycogen and polyphosphate.

The PAO-GAO metabolic models of Lopez-Vazquez et al. (2009) and Oehmen et al. (2010b) have been widely used in research applications to assess whether the anaerobic, anoxic and aerobic biochemical transformations observed in EBPR experiments correlate with the classical phenotypes of PAOs and GAOs. In fact, several lab and field studies have reported that the stoichiometric yields estimated in these models are able to describe a wide range of operational and environmental conditions (Carvalheira et al., 2014a, 2014b; Carvalho et al., 2007; Lanham et al., 2013; Lu et al., 2006; Oehmen et al., 2005a, 2005b; Pijuan et al., 2004, 2008; Zeng et al., 2003b). Furthermore, their calibrated kinetic parameters only require minor adjustments when the overall stoichiometric reactions and kinetic structure of these models are modified to incorporate new process understanding.

Despite the fact that PAO-GAO metabolic models summarise the current state-of-knowledge of EBPR processes, their use in engineering applications is not straightforward because they only describe the activity of PAOs and GAOs.

2.2.3 Combined metabolic-ASM models

Combining EBPR metabolic models with the heterotrophic, hydrolytic and autotrophic processes from ASMs is considered as the most promising approach, since it provides an overall platform to describe the activity of the key organisms and processes relevant to WRRFs over a wide range of operational and environmental conditions with a fully reliable stoichiometry. This approach recognises the benefits of using metabolic models to describe the EBPR processes.

The most referenced example of this combination is the ASM2d + TUD model developed by the Delft University of Technology (Meijer, 2004), which is the last published version of the integrated ASM-TUD model. This model combines the ordinary heterotrophic, hydrolytic and autotrophic processes from ASM2d (Henze, et al., 1999) with the metabolic model for denitrifying and non-denitrifying EBPR developed by Murnleitner et al. (1997). Table 2.1 summarises the standard processes incorporated in this model. The application of the ASM2d + TUD model in full-scale systems demonstrated to indeed reduce the number of parameters requiring calibration (Van Veldhuizen, et al., 1999; Brdjanovic, et al., 2000; Hao et al., 2001; Meijer, et al., 2001). However, this model does not describe the activity of GAOs neither the mechanisms underlying PAO-GAO competition, since they were only integrated later by Lopez-Vazquez et al. (2009), Oehmen et al. (2010b) and Lanham et al. (2014) in their PAO-GAO metabolic models. According to an international survey, this model is one of the least used in practice (Hauduc et al., 2009), probably because it is lacking detailed and dynamic

process understanding to predict EBPR upsets and has a complex biokinetic structure compared to other literature models.

2.3 Research needs in EBPR modelling

The understanding of EBPR mechanisms has been evolving since the first description of the PAO metabolism in 1975 (Barnard, 1975, 1976; Fuhs and Chen, 1975). Currently, it is known that EBPR is a highly dynamic process with complex biochemical transformations that are affected by a wide range of operational and environmental conditions as well as by the competition of other non-PAOs. However, the biokinetic models commonly used in engineering applications (see Table 2.1) were developed to describe mechanisms that at the time were not fully understood or were considered negligible or unlikely to occur in most available EBPR configurations. This lack of detailed and dynamic process understanding led to the formulation of simplified hypothesis, capable of providing an adequate description of the observed data, but only after extensive calibration procedures were employed.

Increasingly stringent regulations for P removal have challenged WRRFs to expand their limits and upgrade conventional EBPR configurations by novel technologies, such as S2EBPR, denitrifying EBPR and low DO EBPR. This shift of paradigm created the need to extend existing models with mechanisms that describe the effect of operational conditions on the PAO-GAO competition, the capability of PAOs and GAOs to denitrify, the metabolic shifts as a function of storage polymer concentrations, as well as the role of these polymers in endogenous processes and fermentation. The models shown in Table 2.1 lump impacts of GAOs into PAOs parameters; do not take into account the different denitrification capabilities of PAOs (and GAOs); neglect the impact of alternative metabolic pathways (such as the TCA cycle) as source of reducing power when glycogen is exhausted, and do not consider the use of different storage polymers by PAOs (and GAOs) as a survival strategy, prior to cell decay. As a consequence, these EBPR models are not capable of dynamically predicting long-term EBPR performance, diagnosing plant upsets and evaluating new process designs. In fact, some studies reported that these models require extensive stoichiometric and kinetic parameter changes (Dunlap et al., 2016; Menniti et al., 2016), which reduces their predictive power and limits their practical use.

In recent years, several experimental studies have improved the understanding of the above mechanisms and suggested modifications to the currently available EBPR metabolic models. Despite this available knowledge, these modifications have never been previously integrated into an overall activated sludge model and implemented in a commercial simulator. Therefore, the development of a valuable model (both in research and engineering) capable of covering EBPR dynamics in a predictive way is strongly needed and served as the motivation for the present thesis.

2.4 References

Barker, P.., Dold, P.L., 1997a. General model for biological nutrient removal activated-sludge systems: model presentation. Water Environ. Res. 69, 969–984. doi:doi:10.2175/106143097X125669

Barker, P.S., Dold, P.L., 1997b. General model for biological nutrient removal activated-sludge systems: model application. Water Environ. Res. doi:10.2175/106143097x125678

Barnard, J.L., Dunlap, P., Steichen, M., 2017. Rethinking the Mechanisms of Biological Phosphorus Removal. Water Environ. Res. doi:10.2175/106143017x15051465919010

Barnard, J., Houweling, D., Analla, H., Steichen, M., 2012. Saving phosphorus removal at the Henderson NV plant. Water Sci. Technol. doi:10.2166/wst.2012.022

Barnard, J.L., Abraham, K., 2006. Key features of successful BNR operation, in: Water Science and Technology. doi:10.2166/wst.2006.400

Barnard, J.L., Steichen, M.T., 2006. Where is biological nutrient removal going now? Water Sci. Technol. doi:10.2166/wst.2006.088

Barnard, J., 1976. A review of biological phosphorus removal in the activated sludge process. Water SA 2, 136–144.

Barnard, J.L., 1975. Biological nutrient removal without the addition of chemicals. Water Res. doi:10.1016/0043-1354(75)90072-X

Bond, P.L., Hugenholtz, P., Keller, J., Blackall, L.L., 1995. Bacterial community structures of phosphate-removing and non-phosphate-removing activated sludges from sequencing batch reactors. Appl. Environ. Microbiol.

Brdjanovic, D., 2000. Modeling COD, N and P removal in a full-scale wwtp Haarlem Waarderpolder. Water Res. 34, 846–858. doi:10.1016/S0043-1354(99)00219-5

Brdjanovic, D., Logemann, S., Van Loosdrecht, M.C.M., Hooijmans, C.M., Alaerts, G.J., Heijnen, J.J., 1998a. Influence of temperature on biological phosphorus removal: Process and molecular ecological studies. Water Res. 32, 1035–1048. doi:10.1016/S0043-1354(97)00322-9

Brdjanovic, D., Van Loosdrecht, M.C.M., Hooijmans, C.M., Alaerts, G.J., Heijnen, J.J., 1998b. Minimal aerobic sludge retention time in biological phosphorus removal systems. Biotechnol. Bioeng. 60, 326–332. doi:10.1002/(SICI)1097-0290(19981105)60:3<326::AID-BIT8>3.0.CO;2-J

Brdjanovic, D., Loosdrecht, M.C.M. van, Hooijmans, C.M., Alaerts, G.J., Heijnen, J.J., 1997. Temperature Effects on Physiology of Biological Phosphorus Removal. J. Environ. Eng. 123, 144–153. doi:10.1061/(ASCE)0733-9372(1997)123:2(144)

Bunce, J.T., Ndam, E., Ofiteru, I.D., Moore, A., Graham, D.W., 2018. A review of phosphorus removal technologies and their applicability to small-scale domestic wastewater treatment systems. Front. Environ. Sci. doi:10.3389/fenvs.2018.00008

Bushee, G., Schauer, P., Menniti, A., 2019. An assessment of operational tools for Characterizing BPR activity and evaluating process health. Proc. 92nd Water Environ. Fed. Tech. Exhib. Conf. (WEFTEC 2019) 2, 838–856.

Camejo, P.Y., Oyserman, B.O., McMahon, K.D., Noguera, D.R., 2019. Integrated Omic Analyses Provide Evidence that a “Candidatus Accumulibacter phosphatis” Strain Performs Denitrification under Microaerobic Conditions. mSystems. doi:10.1128/msystems.00193-18

Camejo, P.Y., Owen, B.R., Martirano, J., Ma, J., Kapoor, V., Santo Domingo, J., McMahon, K.D., Noguera, D.R., 2016. Candidatus Accumulibacter phosphatis clades enriched under cyclic anaerobic and microaerobic conditions simultaneously use different electron acceptors. Water Res. doi:10.1016/j.watres.2016.06.033

Carvalheira, M., Oehmen, A., Carvalho, G., Eusébio, M., Reis, M.A.M., 2014a. The impact of aeration on the competition between polyphosphate accumulating organisms and glycogen accumulating organisms. Water Res. 66C, 296–307. doi:10.1016/j.watres.2014.08.033

Carvalheira, M., Oehmen, A., Carvalho, G., Reis, M.A.M., 2014b. The effect of substrate competition on the metabolism of polyphosphate accumulating organisms (PAOs). Water Res. 64, 149–159. doi:10.1016/j.watres.2014.07.004

Carvalheira, M., Oehmen, A., Carvalho, G., Reis, M.A.M., 2014c. Survival strategies of polyphosphate accumulating organisms and glycogen accumulating organisms under conditions of low organic loading. Bioresour. Technol. 172, 290–296. doi:10.1016/j.biortech.2014.09.059

Carvalho, G., Lemos, P.C., Oehmen, A., Reis, M.A.M., 2007. Denitrifying phosphorus removal: Linking the process performance with the microbial community structure. Water Res. 41, 4383–4396. doi:10.1016/j.watres.2007.06.065

Cech, J.S., Hartman, P., 1993. Competition between polyphosphate and polysaccharide accumulating bacteria in enhanced biological phosphate removal systems. Water Res. 27, 1219–1225. doi:10.1016/0043-1354(93)90014-9

Chan, C., Guisasola, A., Baeza, J.A., 2017. Enhanced Biological Phosphorus Removal at low Sludge Retention Time in view of its integration in A-stage systems. Water Res. doi:10.1016/j.watres.2017.04.010

Chen, Y., Liu, Y., Zhou, Q., Gu, G., 2005. Enhanced phosphorus biological removal from wastewater - Effect of microorganism acclimatization with different ratios of short-chain fatty acids mixture. Biochem. Eng. J. 27, 24–32. doi:10.1016/j.bej.2005.06.003

Cokro, A.A., Law, Y., Williams, R.B.H., Cao, Y., Nielsen, P.H., Wuertz, S., 2017. Non-denitrifying polyphosphate accumulating organisms obviate requirement for anaerobic condition. Water Res. 111, 393–403. doi:10.1016/j.watres.2017.01.006

Cornel, P., Schaum, C., 2009. Phosphorus recovery from wastewater: Needs, technologies and costs. Water Sci. Technol. doi:10.2166/wst.2009.045

Crocetti, G.R., Hugenholtz, P., Bond, P.L., Schuler, A., Keller, J., Jenkins, D., Blackall, L.L., 2000. Identification of polyphosphate-accumulating organisms and design of 16S rRNA-directed probes for their detection and quantitation. Appl. Environ. Microbiol. doi:10.1128/AEM.66.3.1175-1182.2000

Crocetti R., G., Banfield F., J.F., Keller, J., Bond, P.L., Blackall, L.L., 2002. Glycogen-accumulating organisms in laboratory-scale and full-scale wastewater treatment processes. Microbiology. doi:10.1099/00221287-148-11-3353

Dai, Y., Yuan, Z., Wang, X., Oehmen, A., Keller, J., 2007. Anaerobic metabolism of Defluviicoccus vanus related glycogen accumulating organisms (GAOs) with acetate and propionate as carbon sources. Water Res. doi:10.1016/j.watres.2007.01.045

Desmidt, E., Ghyselbrecht, K., Zhang, Y., Pinoy, L., Van Der Bruggen, B., Verstraete, W., Rabaey, K., Meesschaert, B., 2015. Global phosphorus scarcity and full-scale P-recovery techniques: A review. Crit. Rev. Environ. Sci. Technol. doi:10.1080/10643389.2013.866531

Dunlap, P., Martin, K., Stevens, G., Tooker, N., Barnard, J., Gu, A., Takacs, I., Onnis-Hayden, A., Li, Y., 2016. Rethinking EBPR: What do you do when the model will not fit real- world evidence? 5th IWA/WEF Wastewater Treat. Model. Semin. Annecy, Fr. 39–62.

European Commission, 2013. Consultative Communication on the Sustainable Use of Phosphorus [WWW Document]. COM(2013) 517 Final. doi:10.1017/CBO9781107415324.004

Filipe, C.D., Daigger, G.T., Grady, C.P.J., 2001. A metabolic model for acetate uptake under anaerobic conditions by glycogen accumulating organisms: Stoichiometry, kinetics, and the effect of pH. Biotechnol. Bioeng. 76, 17–31.

Flowers, J.J., He, S., Malfatti, S., del Rio, T.G., Tringe, S.G., Hugenholtz, P., McMahon, K.D., 2013. Comparative genomics of two 'Candidatus Accumulibacter' clades performing biological phosphorus removal. ISME J. 7, 2301–2314. doi:10.1038/ismej.2013.117

Fuhs, G.W., Chen, M., 1975. Microbiological basis of phosphate removal in the activated sludge process for the treatment of wastewater. Microb. Ecol. doi:10.1007/BF02010434

Gao, H., Mao, Y., Zhao, X., Liu, W.-T., Zhang, T., Wells, G., 2019. Genome-centric metagenomics resolves microbial diversity and prevalent truncated denitrification pathways in a denitrifying PAO-enriched bioprocess. Water Res. 155, 275–287. doi:10.1016/J.WATRES.2019.02.020

Gebremariam, S.Y., Beutel, M.W., Christian, D., Hess, T.F., 2011. Research Advances and Challenges in the Microbiology of Enhanced Biological Phosphorus Removal-A Critical Review. Water Environ. Res. doi:10.2175/106143010x12780288628534

Gu, A.Z., Saunders, A., Neethling, J.B., Stensel, H.D., Blackall, L.L., 2008. Functionally Relevant Microorganisms to Enhanced Biological Phosphorus Removal Performance at Full-Scale Wastewater Treatment Plants in the United States. Water Environ. Res. doi:10.2175/106143008x276741

Gujer, W., Henze, M., Mino, T., Van Loosdrecht, M., 1999. Activated Sludge Model No. 3, in: Water Science and Technology. pp. 183–193. doi:10.1016/S0273-1223(98)00785-9

Günther, S., Grunert, M., Müller, S., 2018. Overview of recent advances in phosphorus recovery for fertilizer production. Eng. Life Sci. doi:10.1002/elsc.201700171

Hao, X., Wang, Q., Cao, Y., Van Loosdrecht, M.C.M., 2010. Experimental evaluation of decrease in the activities of polyphosphate/glycogen-accumulating organisms due to cell death and activity decay in activated sludge. Biotechnol. Bioeng. 106, 399–407. doi:10.1002/bit.22703

Hao, X., Van Loosdrecht, M.C., Meijer, S.C., Qian, Y., 2001. Model-based evaluation of two BNR processes--UCT and A2N. Water Res. 35, 2851–2860. doi:10.1016/S0043-1354(00)00596-0

Hauduc, H., Rieger, L., Oehmen, A., van Loosdrecht, M.C.M., Comeau, Y., Héduit, A., Vanrolleghem, P.A., Gillot, S., 2013. Critical review of activated sludge modeling: State of process knowledge, modeling concepts, and limitations. Biotechnol. Bioeng. doi:10.1002/bit.24624

Hauduc, H., Rieger, L., Ohtsuki, T., Shaw, A., Takács, I., Winkler, S., Héduit, A., Vanrolleghem, P.A., Gillot, S., 2011. Activated sludge modelling: Development and potential use of a practical applications database. Water Sci. Technol. doi:10.2166/wst.2011.368

Hauduc, H., Gillot, S., Rieger, L., Ohtsuki, T., Shaw, A., Takács, I., Winkler, S., 2009. Activated sludge modelling in practice: An international survey. Water Sci. Technol. 60, 1943–1951. doi:10.2166/wst.2009.223

He, S., Gall, D.L., McMahon, K.D., 2007. "Candidatus accumulibacter" population structure in enhanced biological phosphorus removal sludges as revealed by polyphosphate kinase genes. Appl. Environ. Microbiol. 73, 5865–5874. doi:10.1128/AEM.01207-07

Henze, M., van Loosdrecht, M.C.M., Ekama, G.A., Brdjanovic, D., 2008. Biological Wastewater Treatment: Principles, Modelling and Design. doi:10.2166/9781780401867

Henze, M., Gujer, W., Mino, T., van Loosdrecht, M.C.M., 2000. Activated Sludge Models ASM1, ASM2, ASM2d and ASM3. IWA Publ. 121. doi:10.1007/s13398-014-0173-7.2

Henze, M., Gujer, W., Mino, T., Matsuo, T., Wentzel, M.C., Marais, G.V.R., Van Loosdrecht, M.C.M., 1999. Activated Sludge Model No.2d, ASM2d, in: Water Science and Technology. pp. 165–182. doi:10.1016/S0273-1223(98)00829-4

Henze, M., Gujer, W., Mino, T., Matsuo, T., Wentzel, M. C. , Marais, G.V.R., 1995. Activated Sludge Model No. 2. IAWQ Scientific and Technical Report No. 3. IAWQ, London, UK., UK.

Henze, M., Grady, C., Gujer, W., Marais, G., Matsuo, T., 1987. Activated sludge model no. 1. London, UK IAWPRC Publ.

Hesselmann, R.P.X., Werlen, C., Hahn, D., van der Meer, J.R., Zehnder, A.J.B., 1999. Enrichment, phylogenetic analysis and detection of a bacterium that performs enhanced biological phosphate removal in activated sludge. Syst. Appl. Microbiol. doi:10.1016/S0723-2020(99)80055-1

Hollender, J., van der Krol, D., Kornberger, L., Gierden, E., Dott, W., 2002. Effect of different carbon sources on the enhanced biological phosphorus removal in a sequencing batch reactor. World J. Microbiol. Biotechnol. 18, 359–364. doi:10.1023/A:1015258308460

Hu, Z., Wentzel, M., Ekama, G., 2007a. A general kinetic model for biological nutrient removal activated sludge systems: Model development. Biotechnol. 98. doi:10.1002/bit21508

Hu, Z.R., Wentzel, M.C., Ekama, G.A., 2007b. A general kinetic model for biological nutrient removal activated sludge systems: Model evaluation. Biotechnol. Bioeng. doi:10.1002/bit.21507

Hu, Z.-R., Wentzel, M.C., Ekama, G.A., 2003. Modelling biological nutrient removal activated sludge systems—a review. Water Res. 37, 3430–3444. doi:10.1016/S0043-1354(03)00168-4

Keene, N.A., Reusser, S.R., Scarborough, M.J., Grooms, A.L., Seib, M., Santo Domingo, J., Noguera, D.R., 2017. Pilot plant demonstration of stable and efficient high rate biological nutrient removal with low dissolved oxygen conditions. Water Res. 121, 72–85. doi:10.1016/j.watres.2017.05.029

Kim, J.M., Lee, H.J., Lee, D.S., Lee, K., Jeon, C.O., 2011. Identification of a novel subgroup of uncultured gammaproteo bacterial glycogen-accumulating organisms in enhanced biological phosphorus removal sludge. Microbiology. doi:10.1099/mic.0.047779-0

Kong, Y., Xia, Y., Nielsen, P.H., 2008. Activity and identity of fermenting microorganisms in full-scale biological nutrient removing wastewater treatment plants. Environ. Microbiol. doi:10.1111/j.1462-2920.2008.01617.x

Kong, Y., Xia, Y., Nielsen, J.L., Nielsen, P.H., 2006. Ecophysiology of a group of uncultured Gammaproteobacterial glycogen-accumulating organisms in full-scale enhanced biological phosphorus removal wastewater treatment plants. Environ. Microbiol. doi:10.1111/j.1462-2920.2005.00914.x

Kong, Y., Ong, S.L., Ng, W.J., Liu, W.T., 2002. Diversity and distribution of a deeply branched novel proteobacterial group found in anaerobic-aerobic activated sludge processes. Environ. Microbiol. doi:10.1046/j.1462-2920.2002.00357.x

Kristiansen, R., Nguyen, H.T.T., Saunders, A.M., Nielsen, J.L., Wimmer, R., Le, V.Q., McIlroy, S.J., Petrovski, S., Seviour, R.J., Calteau, A., Nielsen, K.L., Nielsen, P.H., 2013. A metabolic model for members of the genus Tetrasphaera involved in enhanced biological phosphorus removal. ISME J. 7, 543–554. doi:10.1038/ismej.2012.136

Kuba, T., Murnleitner, E., Van Loosdrecht, M.C.M., Heijnen, J.J., 1996. A metabolic model for biological phosphorus removal by denitrifying organisms. Biotechnol. Bioeng. 52, 685–695. doi:10.1002/(SICI)1097-0290(19961220)52:6<685::AID-BIT6>3.3.CO;2-M

Lanham, A.B., Oehmen, A., Saunders, A.M., Carvalho, G., Nielsen, P.H., Reis, M.A.M., 2014. Metabolic modelling of full-scale enhanced biological phosphorus removal sludge. Water Res. 66C, 283–295. doi:10.1016/j.watres.2014.08.036

Lanham, A.B., Oehmen, A., Saunders, A.M., Carvalho, G., Nielsen, P.H., Reis, M.A.M., 2013. Metabolic versatility in full-scale wastewater treatment plants performing enhanced biological phosphorus removal. Water Res. 47, 7032–7041. doi:10.1016/j.watres.2013.08.042

Lee, D., Kim, M., Chung, J., 2007. Relationship between solid retention time and phosphorus removal in anaerobic-intermittent aeration process. J. Biosci. Bioeng. doi:10.1263/jbb.103.338

Li, N., Wang, X., Ren, N., Zhang, K., Kang, H., You, S., 2008. Effects of solid retention time (SRT) on sludge characteristics in enhanced biological phosphorus removal (EBPR) reactor. Chem. Biochem. Eng. Q.

Liu, R., Hao, X., Chen, Q., Li, J., 2019. Research advances of Tetrasphaera in enhanced biological phosphorus removal: A review. Water Res. doi:10.1016/j.watres.2019.115003

Liu, W., Peng, Y., Ma, B., Ma, L., Jia, F., Li, X., 2017. Dynamics of microbial activities and community structures in activated sludge under aerobic starvation. Bioresour. Technol. 244, 588–596. doi:10.1016/j.biortech.2017.07.131

Liu, W.T., Mino, T., Nakamura, K., Matsuo, T., 1994. Role of glycogen in acetate uptake and polyhydroxyalkanoate synthesis in anaerobic-aerobic activated sludge with a minimized polyphosphate content. J. Ferment. Bioeng. doi:10.1016/0922-338X(94)90124-4

Lopez-Vazquez, C.M., Oehmen, A., Hooijmans, C.M., Brdjanovic, D., Gijzen, H.J., Yuan, Z., van Loosdrecht, M.C.M., 2009. Modeling the PAO-GAO competition: Effects of carbon source, pH and temperature. Water Res. 43, 450–462. doi:10.1016/j.watres.2008.10.032

Lopez-Vazquez, C.M., Song, Y. Il, Hooijmans, C.M., Brdjanovic, D., Moussa, M.S., Gijzen, H.J., Van Loosdrecht, M.M.C., 2007. Short-term temperature effects on the anaerobic metabolism of glycogen accumulating organisms. Biotechnol. Bioeng. 97, 483–495. doi:10.1002/bit.21302

Lopez, C., Pons, M.N., Morgenroth, E., 2006. Endogenous processes during long-term starvation in activated sludge performing enhanced biological phosphorus removal. Water Res. 40, 1519–1530. doi:10.1016/j.watres.2006.01.040

Lu, H., Keller, J., Yuan, Z., 2007. Endogenous metabolism of Candidatus Accumulibacter phosphatis under various starvation conditions. Water Res. 41, 4646–4656. doi:10.1016/j.watres.2007.06.046

Lu, H., Oehmen, A., Virdis, B., Keller, J., Yuan, Z., 2006. Obtaining highly enriched cultures of Candidatus Accumulibacter phosphates through alternating carbon sources. Water Res. 40, 3838–3848. doi:10.1016/j.watres.2006.09.004

Lv, J.H., Yuan, L.J., Chen, X., Liu, L., Luo, D.C., 2014. Phosphorus metabolism and population dynamics in a biological phosphate-removal system with simultaneous anaerobic phosphate stripping. Chemosphere. doi:10.1016/j.chemosphere.2014.10.018

Marques, R., Ribera-Guardia, A., Santos, J., Carvalho, G., Reis, M.A.M., Pijuan, M., Oehmen, A., 2018. Denitrifying capabilities of Tetrasphaera and their contribution towards nitrous oxide production in enhanced biological phosphorus removal processes. Water Res. 137, 262–272. doi:https://doi.org/10.1016/j.watres.2018.03.010

Marques, R., Santos, J., Nguyen, H., Carvalho, G., Noronha, J.P., Nielsen, P.H., Reis, M.A.M., Oehmen, A., 2017. Metabolism and ecological niche of Tetrasphaera and Ca. Accumulibacter in enhanced biological phosphorus removal. Water Res. 122, 159–171. doi:10.1016/j.watres.2017.04.072

Martín, H.G., Ivanova, N., Kunin, V., Warnecke, F., Barry, K.W., McHardy, A.C., Yeates, C., He, S., Salamov, A.A., Szeto, E., Dalin, E., Putnam, N.H., Shapiro, H.J., Pangilinan, J.L., Rigoutsos, I.,

Kyrpides, N.C., Blackall, L.L., McMahon, K.D., Hugenholtz, P., 2006. Metagenomic analysis of two enhanced biological phosphorus removal (EBPR) sludge communities. Nat. Biotechnol. 24, 1263–1269. doi:10.1038/nbt1247

McIlroy, S.J., Onetto, C.A., McIlroy, B., Herbst, F.A., Dueholm, M.S., Kirkegaard, R.H., Fernando, E., Karst, S.M., Nierychlo, M., Kristensen, J.M., Eales, K.L., Grbin, P.R., Wimmer, R., Nielsen, P.H., 2018. Genomic and in Situ Analyses reveal the Micropruina spp. as Abundant fermentative glycogen accumulating organisms in enhanced biological phosphorus removal systems. Front. Microbiol. doi:10.3389/fmicb.2018.01004

Mcilroy, S.J., Nittami, T., Kanai, E., Fukuda, J., Saunders, A.M., Nielsen, P.H., 2015. Re-appraisal of the phylogeny and fluorescence in situ hybridization probes for the analysis of the Competibacteraceae in wastewater treatment systems. Environ. Microbiol. Rep. doi:10.1111/1758-2229.12215

Meijer, S., 2004. Theoretical and practical aspects of modelling activated sludge processes. Delft Univ. Technol. Netherlands 204.

Meijer, S.C.F., Van Loosdrecht, M.C.M., Heijnen, J.J., 2002. Modelling the start-up of a full-scale biological phosphorous and nitrogen removing WWTP. Water Res. 36, 4667–4682. doi:10.1016/S0043-1354(02)00192-6

Meijer, S.C.F., Van Loosdrecht, M.C.M., Heijnen, J.J., 2001. Metabolic modelling of full-scale biological nitrogen and phosphorus removing wwtp's. Water Res. 35, 2711–2723. doi:10.1016/S0043-1354(00)00567-4

Menniti, A., Schauer, P., Tackas, I., Shaw, A., 2016. Online Instrumentation for Monitoring and Control of Biological Phosphorus Removal. Proc. Water Environ. Fed. 2016, 3552–3561. doi:10.2175/193864716819713213

Mino, T., Liu, W.T., Kurisu, F., Matsuo, T., 1995. Modelling glycogen storage and denitrification capability of microorganisms in enhanced biological phosphate removal processes. Water Sci. Technol. doi:10.1016/0273-1223(95)00177-O

Murnleitner, E., Kuba, T., Van Loosdrecht, M.C.M., Heijnen, J.J., 1997. An integrated metabolic model for the aerobic and denitrifying biological phosphorus removal. Biotechnol. Bioeng. 54, 434–450. doi:10.1002/(SICI)1097-0290(19970605)54:5<434::AID-BIT4>3.0.CO;2-F

Neethling, J.B., 2006. Factors Influencing the Reliability of Enhanced Biological Phosphorus Removal. doi:10.2166/9781780404479

Nguyen, H.T.T., Kristiansen, R., Vestergaard, M., Wimmer, R., Nielsen, P.H., 2015. Intracellular Accumulation of Glycine in Polyphosphate-Accumulating Organisms in Activated Sludge, a Novel Storage Mechanism under Dynamic Anaerobic-Aerobic Conditions. Appl. Environ. Microbiol. doi:10.1128/aem.01012-15

Nguyen, H.T.T., Le, V.Q., Hansen, A.A., Nielsen, J.L., Nielsen, P.H., 2011. High diversity and abundance of putative polyphosphate-accumulating Tetrasphaera-related bacteria in activated sludge systems. FEMS Microbiol. Ecol. doi:10.1111/j.1574-6941.2011.01049.x

Nielsen, P.H., McIlroy, S.J., Albertsen, M., Nierychlo, M., 2019. Re-evaluating the microbiology of the enhanced biological phosphorus removal process. Curr. Opin. Biotechnol. 57, 111–118. doi:10.1016/J.COPBIO.2019.03.008

Oehmen, A, Carvalho, G., Lopez-Vazquez, C.M., van Loosdrecht, M.C.M., Reis, M.A.M., 2010a. Incorporating microbial ecology into the metabolic modelling of polyphosphate accumulating organisms and glycogen accumulating organisms. Water Res. 44, 4992–5004. doi:10.1016/j.watres.2010.06.071

Oehmen, A., Lopez-Vazquez, C.M., Carvalho, G., Reis, M.A.M., van Loosdrecht, M.C.M., 2010b. Modelling the population dynamics and metabolic diversity of organisms relevant in anaerobic/anoxic/aerobic enhanced biological phosphorus removal processes. Water Res. 44, 4473–4486. doi:10.1016/j.watres.2010.06.017

Oehmen, A., Lemos, P.C., Carvalho, G., Yuan, Z.G., Keller, J., Blackall, L.L., Reis, M.A.M., 2007. Advances in enhanced biological phosphorus removal: From micro to macro scale. Water Res. 41, 2271–2300. doi:DOI 10.1016/j.watres.2007.02.030

Oehmen, A., Zeng, R.J., Saunders, A.M., Blackall, L.L., Keller, J., Yuan, Z., 2006. Anaerobic and aerobic metabolism of glycogen-accumulating organisms selected with propionate as the sole carbon source. Microbiology. doi:10.1099/mic.0.28065-0

Oehmen, A., Vives, M.T., Lu, H., Yuan, Z., Keller, J., 2005a. The effect of pH on the competition between polyphosphate-accumulating organisms and glycogen-accumulating organisms. Water Res. 39, 3727–3737. doi:10.1016/j.watres.2005.06.031

Oehmen, A., Yuan, Z., Blackall, L.L., Keller, J., 2005b. Comparison of acetate and propionate uptake by polyphosphate accumulating organisms and glycogen accumulating organisms. Biotechnol. Bioeng. 91, 162–168. doi:10.1002/bit.20500

Oehmen, A., Zeng, R.J., Yuan, Z., Keller, J., 2005c. Anaerobic metabolism of propionate by polyphosphate-accumulating organisms in enhanced biological phosphorus removal systems. Biotechnol. Bioeng. 91, 43–53. doi:10.1002/bit.20480

Oehmen, A., Yuan, Z., Blackall, L.L., Keller, J., 2004. Short-term effects of carbon source on the competition of polyphosphate accumulating organsisms and glycogen accumulating organisms. Water Sci. Technol. doi:10.2166/wst.2004.0629

Oleszkiewicz, J.A., Barnard, J.L., 2006. Nutrient removal technology in North America and the European Union: A review. Water Qual. Res. J. Canada. doi:10.1002/chin.200734273

Onuki, M., Satoh, H., Mino, T., 2002. Analysis of microbial community that performs enhanced biological phosphorus removal in activated sludge fed with acetate. Water Sci. Technol. 46, 145–53.

Parsons, S.A., Smith, J.A., 2008. Phosphorus removal and recovery from municipal wastewaters. Elements. doi:10.2113/GSELEMENTS.4.2.109

Peterson, S.B., Warnecke, F., Madejska, J., McMahon, K.D., Hugenholtz, P., 2008. Environmental distribution and population biology of Candidatus Accumulibacter, a primary agent of biological phosphorus removal. Environ. Microbiol. 10, 2692–2703. doi:10.1111/j.1462-2920.2008.01690.x

Pijuan, M., Oehmen, A., Baeza, J.A., Casas, C., Yuan, Z., 2008. Characterizing the biochemical activity of full-scale enhanced biological phosphorus removal systems: A comparison with metabolic models. Biotechnol. Bioeng. 99, 170–179. doi:10.1002/bit

Pijuan, M., Guisasola, A., Baeza, J.A., Carrera, J., Casas, C., Lafuente, J., 2005. Aerobic phosphorus release linked to acetate uptake: Influence of PAO intracellular storage compounds. Biochem. Eng. J. 26, 184–190. doi:10.1016/j.bej.2005.04.014

Pijuan, M, Saunders, A.M., Guisasola, A., Baeza, J.A., Casas, C., Blackall, L.L., 2004. Enhanced biological phosphorus removal in a sequencing batch reactor using propionate as the sole carbon source. Biotechnol. Bioeng. 85, 56–67. doi:10.1002/bit.10813

Rieger, L., Gillot, S., Langergraber, G., Ohtsuki, T., Shaw, A., Takacs, I., Winkler, S., 2012. Guidelines for Using Activated Sludge Models: IWA Task Group on Good Modelling Practice., Scientific and Technical Report No. 22. IWA Publishing, London, UK.

Rieger, L., Koch, G., Kuhni, M., Gujer, W., Siegrist, H., 2001. The EAWAG Bio-P module for activated sludge model No. 3. Water Res. 35, 3887–3903.

Rittmann, B.E., Mayer, B., Westerhoff, P., Edwards, M., 2011. Capturing the lost phosphorus. Chemosphere. doi:10.1016/j.chemosphere.2011.02.001

Rodrigo, M.A., Seco, A., Ferrer, J., Penya-Roja, J.M., 1999. The effect of sludge age on the deterioration of the enhanced biological phosphorus removal process. Environ. Technol. (United Kingdom). doi:10.1080/09593332008616902

Rubio-Rincón, F.J., Lopez-Vazquez, C.M., Welles, L., van Loosdrecht, M.C.M., Brdjanovic, D., 2017. Cooperation between Candidatus Competibacter and Candidatus Accumulibacter clade I, in denitrification and phosphate removal processes. Water Res. 120, 156–164. doi:10.1016/j.watres.2017.05.001

Saad, S.A., Welles, L., Abbas, B., Lopez-Vazquez, C.M., van Loosdrecht, M.C.M., Brdjanovic, D., 2016. Denitrification of nitrate and nitrite by 'Candidatus Accumulibacter phosphatis' clade IC. Water Res. 105, 97–109. doi:10.1016/j.watres.2016.08.061

Satoh, H., Mino, T., Matsuo, T., 1994. Deterioration of enhanced biological phosphorus removal by the domination of microorganisms without polyphosphate accumulation, in: Water Science and Technology. pp. 203–211.

Saunders, A.M., Larsen, P., Nielsen, P.H., 2013. Comparison of nutrient-removing microbial communities in activated sludge from full-scale MBRs and conventional plants. Water Sci. Technol. 68, 366–371. doi:10.2166/wst.2013.183

Saunders, A.M., Oehmen, A., Blackall, L.L., Yuan, Z., Keller, J., 2003. The effect of GAOs (glycogen

accumulating organisms) on anaerobic carbon requirements in full-scale Australian EBPR (enhanced biological phosphorus removal) plants, in: Water Science and Technology. doi:10.2166/wst.2003.0584

Schauer, P., Bushee, G., Menniti, A., 2018. Characterizing BPR activity to understand overall process health. Proc. Water Environ. Fed. Nutr. Remov. Recover. 569–585.

Scholz, R.W., Ulrich, A.E., Eilittä, M., Roy, A., 2013. Sustainable use of phosphorus: A finite resource. Sci. Total Environ. doi:10.1016/j.scitotenv.2013.05.043

Selman, M., Sugg, Z., Greenhalgh, S., Diaz, R., 2008. Eutrophication and Hypoxia in Coastal Areas: A global assessment of the State of Knowledge. World Resour. Inst.

Shintani, T., Liu, W.T., Hanada, S., Kamagata, Y., Miyaoka, S., Suzuki, T., Nakamura, K., 2000. Micropruina glycogenica gen. nov., sp. nov., a new Gram-positive glycogen-accumulating bacterium isolated from activated sludge. Int. J. Syst. Evol. Microbiol. doi:10.1099/00207713-50-1-201

Skennerton, C.T., Barr, J.J., Slater, F.R., Bond, P.L., Tyson, G.W., 2015. Expanding our view of genomic diversity in *C andidatus* Accumulibacter clades. Environ. Microbiol. 17, 1574–1585. doi:10.1111/1462-2920.12582

Smolders, G.J.F., van Loosdrecht, M.C.M., Heijnen, J.J., 1995. A metabolic model for the biological phosphorus removal process. Water Sci. Technol. doi:10.1016/0273-1223(95)00182-M

Smolders, G.J., van der Meij, J., van Loosdrecht, M.C., Heijnen, J.J., 1994a. Model of the anaerobic metabolism of the biological phosphorus removal process: Stoichiometry and pH influence. Biotechnol. Bioeng. 43, 461–470. doi:10.1002/bit.260430605

Smolders, G.J., van der Meij, J., van Loosdrecht, M.C., Heijnen, J.J., 1994b. Stoichiometric model of the aerobic metabolism of the biological phosphorus removal process. Biotechnol. Bioeng. 44, 837–848. doi:10.1002/bit.260440709

Stokholm-Bjerregaard, M., 2016. Control of GAOs in wastewater treatment plants with enhanced biological phosphorus removal. PhD thesis. Aalborg University, Aalborg, Denmark, Denmark.

Stokholm-Bjerregaard, M., McIlroy, S.J., Nierychlo, M., Karst, S.M., Albertsen, M., Nielsen, P.H., 2017. A critical assessment of the microorganisms proposed to be important to enhanced biological phosphorus removal in full-scale wastewater treatment systems. Front. Microbiol. doi:10.3389/fmicb.2017.00718

Van Veldhuizen, H.M., Van Loosdrecht, M.C.M., Heijnen, J.J., 1999. Modelling biological phosphorus and nitrogen removal in a full scale activated sludge process. Water Res. 33, 3459–3468. doi:10.1016/S0043-1354(99)00064-0

Vargas, M., Yuan, Z., Pijuan, M., 2013. Effect of long-term starvation conditions on polyphosphate- and glycogen-accumulating organisms. Bioresour. Technol. 127, 126–131. doi:10.1016/j.biortech.2012.09.117

Wang, D., Tooker, N.B., Srinivasan, V., Li, G., Fernandez, L.A., Schauer, P., Menniti, A., Maher, C., Bott, C.B., Dombrowski, P., Barnard, J.L., Onnis-Hayden, A., Gu, A.Z., 2019. Side-stream enhanced biological phosphorus removal (S2EBPR) process improves system performance - A full-scale comparative study. Water Res. doi:10.1016/j.watres.2019.115109

Wang, Y., Zhou, S., Wang, H., Ye, L., Qin, J., Lin, X., 2015. Comparison of endogenous metabolism during long-term anaerobic starvation of nitrite/nitrate cultivated denitrifying phosphorus removal sludges. Water Res. 68, 374–386. doi:10.1016/j.watres.2014.09.044

Wang, Y., Geng, J., Peng, Y., Wang, C., Guo, G., Liu, S., 2012. A comparison of endogenous processes during anaerobic starvation in anaerobic end sludge and aerobic end sludge from an anaerobic/anoxic/oxic sequencing batch reactor performing denitrifying phosphorus removal. Bioresour. Technol. 104, 19–27. doi:10.1016/j.biortech.2011.09.049

Wang, Y., Jiang, F., Zhang, Z., Xing, M., Lu, Z., Wu, M., Yang, J., Peng, Y., 2010. The long-term effect of carbon source on the competition between polyphosphorus accumulating organisms and glycogen accumulating organism in a continuous plug-flow anaerobic/aerobic (A/O) process. Bioresour. Technol. 101, 98–104. doi:10.1016/j.biortech.2009.07.085

Wentzel, M.C., Ekama, G.A., Marai, G.V.R., 1992. Processes and modelling of nitrification denitrification biological excess phosphorus removal systems - A review, in: Water Science and Technology. pp. 59–82.

Wentzel, M.C., Ekama, G.A., Loewenthal, R.E., Dold, P.L., Marais, G., 1989. Enhanced polyphosphate

organism cultures in activated sludge systems. Part II: Experimental behaviour. Water S.A. 15, 71–88.

Whang, L., Park, J.K., 2006. Competition between Polyphosphate- and Glycogen-Accumulating Organisms in Systems : Effect of Temperature and Sludge Age. Water Environ. Res.

Wong, M.T., Mino, T., Seviour, R.J., Onuki, M., Liu, W.T., 2005. In situ identification and characterization of the microbial community structure of full-scale enhanced biological phosphorous removal plants in Japan. Water Res. doi:10.1016/j.watres.2005.05.015

Wu, Linwei, Ning, D., Zhang, B., Li, Y., Zhang, P., Shan, X., Zhang, Qiuting, Brown, Mathew, Li, Z., Van Nostrand, J.D., Ling, F., Xiao, N., Zhang, Ya, Vierheilig, J., Wells, G.F., Yang, Y., Deng, Y., Tu, Q., Wang, A., Acevedo, D., Agullo-Barcelo, M., Alvarez, P.J.J., Alvarez-Cohen, L., Andersen, G.L., de Araujo, J.C., Boehnke, K., Bond, P., Bott, C.B., Bovio, P., Brewster, R.K., Bux, F., Cabezas, A., Cabrol, L., Chen, S., Criddle, C.S., Deng, Y., Etchebehere, C., Ford, A., Frigon, D., Gómez, J.S., Griffin, J.S., Gu, A.Z., Habagil, M., Hale, L., Hardeman, S.D., Harmon, M., Horn, H., Hu, Z., Jauffur, S., Johnson, D.R., Keller, J., Keucken, A., Kumari, S., Leal, C.D., Lebrun, L.A., Lee, J., Lee, M., Lee, Z.M.P., Li, Y., Li, Z., Li, M., Li, X., Ling, F., Liu, Y., Luthy, R.G., Mendonça-Hagler, L.C., de Menezes, F.G.R., Meyers, A.J., Mohebbi, A., Nielsen, P.H., Ning, D., Oehmen, A., Palmer, A., Parameswaran, P., Park, J., Patsch, D., Reginatto, V., de los Reyes, F.L., Rittmann, B.E., Robles, A.N., Rossetti, S., Shan, X., Sidhu, J., Sloan, W.T., Smith, K., de Sousa, O.V., Stahl, D.A., Stephens, K., Tian, R., Tiedje, J.M., Tooker, N.B., Tu, Q., Van Nostrand, J.D., De los Cobos Vasconcelos, D., Vierheilig, J., Wagner, M., Wakelin, S., Wang, A., Wang, B., Weaver, J.E., Wells, G.F., West, S., Wilmes, P., Woo, S.-G., Wu, Linwei, Wu, J.-H., Wu, Liyou, Xi, C., Xiao, N., Xu, M., Yan, T., Yang, Y., Yang, M., Young, M., Yue, H., Zhang, B., Zhang, P., Zhang, Qiuting, Zhang, Ya, Zhang, T., Zhang, Qian, Zhang, W., Zhang, Yu, Zhou, H., Zhou, J., Wen, X., Curtis, T.P., He, Q., He, Z., Brown, Matthew, Zhang, T., He, Z., Keller, J., Nielsen, P.H., Alvarez, P.J.J., Criddle, C.S., Wagner, M., Tiedje, J.M., He, Q., Curtis, T.P., Stahl, D.A., Alvarez-Cohen, L., Rittmann, B.E., Wen, X., Zhou, J., Consortium, G.W.M., 2019. Global diversity and biogeography of bacterial communities in wastewater treatment plants. Nat. Microbiol. doi:10.1038/s41564-019-0426-5

Yang, Y., Shi, X., Ballent, W., Mayer, B.K., 2017. Biological Phosphorus Recovery: Review of Current Progress and Future Needs. Water Environ. Res. doi:10.2175/106143017x15054988926424

Yuan, Z., Pratt, S., Batstone, D.J., 2012. Phosphorus recovery from wastewater through microbial processes. Curr. Opin. Biotechnol. doi:10.1016/j.copbio.2012.08.001

Zeng, R.J., Van Loosdrecht, M.C.M., Yuan, Z., Keller, J., 2003a. Metabolic Model for Glycogen-Accumulating Organisms in Anaerobic/Aerobic Activated Sludge Systems. Biotechnol. Bioeng. 81, 92–105. doi:10.1002/bit.10455

Zeng, R.J., Yuan, Z., Keller, J., 2003b. Enrichment of denitrifying glycogen-accumulating organisms in anaerobic/anoxic activated sludge system. Biotechnol. Bioeng. doi:10.1002/bit.10484

Zeng, R., Yuan, Z., Van Loosdrecht, M.C.M., Keller, J., 2002. Proposed modifications to metabolic model for glycogen-accumulating organisms under anaerobic conditions. Biotechnol. Bioeng. doi:10.1002/bit.10370

Zhou, Y., Pijuan, M., Zeng, R.J., Yuan, Z., 2009. Involvement of the TCA cycle in the anaerobic metabolism of polyphosphate accumulating organisms (PAOs). Water Res. 43, 1330–1340. doi:10.1016/j.watres.2008.12.008

3

A NOVEL METABOLIC-ASM MODEL FOR FULL-SCALE BIOLOGICAL NUTRIENT REMOVAL SYSTEMS

SUMMARY:

This study demonstrates that META-ASM, a new integrated metabolic activated sludge model, provides an overall platform to describe the activity of the key organisms and processes relevant to biological nutrient removal (BNR) systems with a robust single-set of default parameters. This model overcomes various shortcomings of existing enhanced biological phosphorus removal (EBPR) models studied over the last twenty years. The model has been tested against 34 data sets from enriched lab polyphosphate accumulating organism (PAO)-glycogen accumulating organism (GAO) cultures and experiments with full-scale sludge from five water resource recovery facilities (WRRFs) with two different process configurations: 3-stage Phoredox (A2/O) and adapted Biodenitro™ combined with a return sludge side-stream hydrolysis tank (RSS). Special attention is given to the operational conditions affecting the competition between PAOs and GAOs, capability of PAOs and GAOs to denitrify, metabolic shifts as a function of storage polymer concentrations, as well as the role of these polymers in endogenous processes and fermentation. The overall good correlations obtained between the predicted versus measured EBPR profiles from different data sets support that this new model, which is based on in-depth understanding of EBPR, reduces calibration efforts. On the other hand, the performance comparison between META-ASM and literature models demonstrates that existing literature models require extensive parameter changes and have limited predictive power, especially in the prediction of long-term EBPR performance. The development of such a model able to describe in detail the microbial and chemical transformations of BNR systems with minimal adjustment to parameters suggests that the META-ASM model is a powerful tool to predict and mitigate EBPR upsets, optimise EBPR performance and to evaluate new process designs.

KEYWORDS:

Activated sludge model (ASM), Biological nutrient removal (BNR), Enhanced biological phosphorus removal (EBPR), metabolic modelling, polyphosphate accumulating organism (PAO) and glycogen accumulating organism (GAO).

PUBLISHED AS:

Santos, J.M.M., Rieger, L., Lanham, A.B., Carvalheira, M., Reis, M.A.M., Oehmen, A., 2020. A novel metabolic-ASM model for full-scale biological nutrient removal systems. Water Res. 171, 115373. doi:10.1016/J.WATRES.2019.115373

3.1 Introduction

Biological nutrient removal (BNR) is the most widely applied technology worldwide for the removal of nutrients such as nitrogen (N) and phosphorus (P) at water resource recovery facilities (WRRFs). In addition to meeting effluent discharge regulations, most WRRFs focus on achieving efficient BNR at relatively low operational costs. The application of mathematical models has been shown to be a useful tool in this regard, since their application provides a less time-consuming and less costly methodology for the design and optimisation of WRRFs. Currently there are three different model concepts used in the literature to describe BNR activated sludge systems: (i) the activated sludge models, ASMs, (ii) the metabolic models and (iii) the combination of these two approaches.

ASM models have been proposed as mechanistic models that represent the biochemical transformations in activated sludge through several simplified process descriptions (Hauduc et al., 2013). The ASM2 (Henze, et al. 1995) and ASM2d (Henze et al., 1999) are examples of ASMs developed by the International Water Association (IWA) to describe enhanced biological phosphorus removal (EBPR) together with chemical oxygen demand (COD) and N removal, oxygen consumption and sludge production. Other well-recognised ASMs were also developed for these purposes: the Barker & Dold model (Barker and Dold, 1997), also known as the BIOWIN biological model, ASM3+BioP (Rieger et al., 2001) and the most recent version of the University of Cape Town model, UCTPHO+ (Hu et al., 2007). These models have become the state-of-the-art reference for modelling BNR activated sludge systems and they have been implemented in most of the commercial software packages available (Van Loosdrecht et al., 2015).

On the other hand, the metabolic models rely on the understanding of the metabolic pathways active in the process in order to explain the biochemical transformations that take place within the cells, providing a better definition of the biological processes (Oehmen et al., 2010a). In this approach, most of the yield coefficients are calculated theoretically through substrate, energy and reducing power balances on well-established biochemical pathways for the processes involved in polyphosphate accumulating organism (PAO) and glycogen accumulating organism (GAO) metabolism. The stoichiometric yields estimated in existing PAO-GAO metabolic models are able to describe a wide range of operational and environmental conditions as reported by several experimental studies (Carvalheira et al., 2014a, 2014b; Carvalho et al., 2007; Lanham et al., 2013; Lu et al., 2006; Oehmen et al., 2005b, 2005a; Pijuan et al., 2004, 2008; Zeng et al., 2003b). The kinetic parameters of these models are the only parameters that require calibration because the metabolic approach mathematically correlates internal cellular reaction rates with observable conversion rates outside the cell to determine an overall stoichiometric reaction for each anaerobic, anoxic and aerobic condition (Lopez-Vazquez et al., 2009; Oehmen et al., 2010b; Oehmen et al., 2005c; Smolders et al., 1994a, 1994b; Zeng et al., 2003a). Therefore, this method not only increases the consistency and reliability of the model, but also facilitates the calibration process by reducing the number of parameters that require calibration.

The validation of existing PAO-GAO metabolic models to lab (Lopez-Vazquez et al., 2009; Oehmen et al., 2010b) and field studies (Lanham et al., 2014) demonstrated that the calibrated kinetic parameters are robust. In fact, these models only require recalibration of kinetic rates when the overall stoichiometric reactions and kinetic structure are modified to incorporate new process understanding.

The same capability is not observed with the application of current EBPR ASMs because they are lacking detailed and dynamic process understanding. In fact, some studies showed that these models require extensive stoichiometric and kinetic parameter changes (Dunlap et al., 2016; Menniti et al., 2016), which reduces their predictive power and limits their practical use, especially regarding the prediction of long-term EBPR performance.

Thereby, combining EBPR metabolic models with the heterotrophic, hydrolytic and autotrophic processes from ASMs may be seen as the most promising approach to achieve that goal, since it provides an overall platform to describe the activity of the key organisms and processes relevant to WRRFs. The most referenced example of this combination is the ASM2d + TUD model developed by the Delft University of Technology (Meijer, 2004), which is the last published version of the integrated ASM-TUD model. This model combines the ordinary heterotrophic, hydrolytic and autotrophic processes from ASM2d (Henze, et al., 1999) with the metabolic model for denitrifying and non-denitrifying EBPR developed by Murnleitner et al. (1997). There are several studies reporting that this model was successfully applied to domestic wastewater treatment plants with numerous configurations such as the University of Cape Town (UCT), modified UCT and 3-stage Phoredox (A2/O) process with the adjustment of only a few default parameters (Van Veldhuizen, et al., 1999; Brdjanovic, et al., 2000; Hao et al., 2001; Meijer, et al., 2001). Although the ASM2d+TUD model has demonstrated to indeed reduce the number of parameters requiring calibration, it is one of the least used models in practice (Hauduc et al., 2009).

In addition to these models, several experimental studies have improved, in recent years, the understanding of the mechanisms behind microbial population dynamics as a function of operational conditions in EBPR systems and suggested modifications to the currently available EBPR metabolic models. Examples of these developments include the description of the activity of various types of PAOs and their competitors, e.g. GAOs, under: i) different operational conditions such as substrate, temperature, pH and dissolved oxygen (DO) (Carvalheira et al., 2014a, 2014b; Lopez-Vazquez et al., 2009); ii) different electron acceptors such as oxygen, nitrate and nitrite (Burow et al., 2007; Camejo et al., 2019, 2016; Carvalho et al., 2007; Flowers et al., 2009; Kim et al., 2013; Lanham et al., 2011; McIlroy et al., 2014; Rubio-Rincón et al., 2019, 2017; Skennerton et al., 2015; Wang et al., 2008); iii) metabolic shifts, e.g. glycolysis and anaerobic tricarboxylic acid (TCA) cycle, as a function of storage polymer concentrations (Cokro et al., 2017; Lanham et al., 2014, 2013) as well as the role of these polymers in endogenous processes (Carvalheira et al., 2014c; Lanham et al., 2014; Liu et al., 2017; Lopez et al., 2006; Lu et al., 2007; Stokholm-Bjerregaard, 2016; Vargas et al., 2013). The incorporation

of these additional factors into a model will enable the prediction of EBPR behaviour over a wide range of operational and environmental conditions. Despite this available knowledge, these modifications have never been previously integrated into an overall activated sludge model and implemented in a commercial simulator. Therefore, the development of a valuable model (both in research and engineering) capable of covering EBPR dynamics in a predictive way is strongly needed.

This chapter intends to present an integrated metabolic-ASM model (referred to as META-ASM hereafter) for BNR activated sludge systems, capable of modelling EBPR processes in depth with minimal parameter adjustments. Table 3.1 synthesises the main limitations of the most well-known EBPR literature models reviewed by Hauduc et al. (2013) and the new developments included in META-ASM. This work aims to: 1) demonstrate the effectiveness of the META-ASM model, 2) calibrate and 3) validate this model with different data sets from experiments using enriched lab PAO-GAO cultures as well as full-scale sludge to provide a single set of default parameters. In doing this we will achieve a comprehensive combined metabolic-ASM model, that can be used as valuable tool in research and engineering applications of BNR systems.

Table 3.1. Synthesis of the main differences between the models: META-ASM, ASM2d + TUD, ASM2d, Barker & Dold and UCTPHO+.

	META-ASM (This study)	**ASM2d + TUD** (Meijer, 2004)	**ASM2d** (Henze, et al., 1999)	**Barker & Dold** (Barker and Dold, 1997)	**UCTPHO+** (Hu et al., 2007)
# of EBPR processes	PAOs: 41 Two GAO groups: CPOs[a]: 21 DFOs[b]: 16	PAOs: 11 (GAOs activity neglected)	PAOs: 8 (GAOs activity neglected)	PAOs: 19 (GAOs activity neglected)	PAOs: 18 (GAOs activity neglected)
Fermentation	Anaerobic growth process focused on distribution of fermentation products (Ac[c], Pr[d] and H_2) Different fermentation yields determined experimentally	Transformation (VFA[e])	Transformation (VFA)	Anaerobic growth process (VFA)	Transformation (VFA)
Nitrification	Two-step (NH_x[f]->NO_2[-g]->NO_3[-h])	One-step (NH_x->NO_x[i])	One-step (NH_x->NO_x)	One-step (NH_x->NO_x)	One-step (NH_x->NO_x)
OHO denitrification	Two-step (NO_3[-]->NO_2[-]->N_2[j])	One-step (NO_x ->N_2)	One-step (NO_x ->N_2)	One-step (NO_x ->N_2)	One-step (NO_x ->N_2)
Endogenous process in OHOs and ANOs[k]	Death-regeneration	Death-regeneration	Death-regeneration	Death-regeneration	Death-regeneration
Origin of reducing power and energy source in the anaerobic PAO metabolism	Reducing power: Glycolysis and others (e.g. TCA and propionyl-CoA conversion to acetyl-CoA); Energy: polyphosphate and glycogen	Reducing power: Glycolysis; Energy: polyphosphate and glycogen	Reducing power: neglected; Energy: polyphosphate	Reducing power: neglected; Energy: polyphosphate	Reducing power: neglected; Energy: polyphosphate
Effect of the electron acceptor on PAOs (Ox[l] and Ax[m] conditions)	Different yields	Different yields	Same yields	Different yields for the polyphosphate storage process; same yield for the biomass growth	Different yields
PAO denitrification capacity	Two PAO subgroups: DPAO (NO_3[-]->NO_2[-]->N_2) PAO (NO_2[-]->N_2)	Reduction factor to lower the aerobic kinetic rates	Reduction factor to lower the aerobic kinetic rates	Reduction factor to lower the aerobic kinetic rates	Reduction factor to lower the aerobic kinetic rates
GAO denitrification capacity	Two CPO subgroups: DCPO[n] (NO_3[-]->NO_2[-]->N_2) CPO (Cannot denitrify) Two DFO subgroups: DDFO[o] (NO_3[-]->NO_2[-])	-	-	-	-

	META-ASM (This study)	**ASM2d + TUD** (Meijer, 2004)	**ASM2d** (Henze, et al., 1999)	**Barker & Dold** (Barker and Dold, 1997)	**UCTPHO+** (Hu et al., 2007)
	DFO (Cannot denitrify)				
Endogenous process in PAOs and GAOs	Endogenous respiration/ cell maintenance and death-regeneration	PAO: endogenous respiration/ cell maintenance	PAO: death-regeneration	PAO: endogenous respiration/ cell maintenance and death-regeneration	PAO: endogenous respiration/ cell maintenance and death-regeneration
Energy source for anaerobic maintenance of PAOs and GAOs	PAO: polyphosphate and glycogen GAO: glycogen	PAO: Polyphosphate	No	PAO: Polyphosphate	PAO: Polyphosphate
Energy source for aerobic/ anoxic maintenance of PAOs and GAOs	PAO: PHAs, glycogen and polyphosphate GAO: PHAs and glycogen	PAO: PHAs	No	No	No
Effect of operational conditions on PAOs and GAOs	Stoichiometry and/or kinetics of PAOs and GAOs affected by type of carbon source and substrate competition, pH, temperature, DO	Effects of the pH and temperature on the stoichiometry and kinetics of PAOs, respectively	No	Effect of the temperature on kinetics	No

[a] *Competibacter*-lineage GAOs; [b] *Defluviicoccus* genus GAOs; [c] acetate; [d] propionate; [e] volatile fatty acid; [f] Ammonium plus ammonia nitrogen; [g] nitrite; [h] nitrate; [i] nitrate plus nitrite nitrogen; [j] nitrogen gas; [k] autotrophic nitrifying organisms; [l] oxic; [m] anoxic; [n] denitrifying CPO; [o] denitrifying DFO.

3.2 Material and Methods

3.2.1 Model description and development

The META-ASM model was implemented in SIMBA# (ifak, Germany) and describes the simultaneous removal of COD, N and P. It is composed of 109 processes and 41 components (23 particulate, 2 colloidal and 16 soluble), which describe the activity of the following six microbial groups: the ordinary heterotrophic organisms (X_{OHO}), the ammonia oxidizing organisms (X_{AOO}), the nitrite oxidizing organisms (X_{NOO}), *Accumulibacter* PAOs (X_{PAO}), *Competibacter*-lineage GAOs, (X_{CPO}) and *Defluviicoccus* genus GAOs (X_{DFO}). The standard processes and the state variables of META-ASM are described in Table 3.2 and in the list of abbreviations, respectively, while the observed interactions between microbial groups are represented in Figure 3.1.

The META-ASM model combines the heterotrophic, hydrolytic and autotrophic processes from the ASM-inCTRL model (inCTRL Solutions, Canada), a version based on the Barker & Dold model (Barker and Dold, 1997), with a metabolic EBPR model based on the previous developments of Lopez-Vazquez et al. (2009) and Oehmen et al. (2010b), and updated to include modifications proposed by Lanham et al. (2014). Both the Barker & Dold model and metabolic models were identified previously in the review of Hu et al. (2003) as having potential for further development, in addition to the UCTPHO model (Wentzel et al., 1992).

Overall, the META-ASM model incorporates more processes than the literature models to describe the observed EBPR dynamics summarised in Table 3.1. In this section, the new model developments implemented in META-ASM are described, highlighting the mechanisms that were simplified or are neglected by current models.

Table 3.2. List of standard processes and number of biological reactions (#) in META-ASM.

Standard processes	# of biological reactions	Standard processes	# of biological reactions
Hydrolysis	1	PHA oxidation by CPOs	3
Ammonification	1	Glycogen storage by CPOs	3
$S_{F,P}$[a] conversion to S_{PO4}[b]	1	PHA storage by DFOs	4
X_E[c] conversion to X_B[d]	1	PHA oxidation by DFOs	2
OHO growth and fermentation	10	Glycogen storage by DFOs	2
AOO growth	1	PAO maintenance	11
NOO growth	1	CPO maintenance	7
OHO decay	3	DFO maintenance	5
AOO and NOO decay	6	PAO decay	4
PHA storage by PAOs	8	CPO decay	4
PHA oxidation by PAOs	6	DFO decay	3
Glycogen storage by PAOs	6	NO_X[e] assimilative reduction	2
Polyphosphate storage	6	Adsorption	2
PHA storage by CPOs	4	Phosphorus precipitation	2

[a] Soluble biodegradable organic P from fermentable organic matter (S_F); [b] soluble inorganic phosphorus; [c] endogenous decay products; [d] slowly biodegradable substrate; [e] nitrate plus nitrite nitrogen.

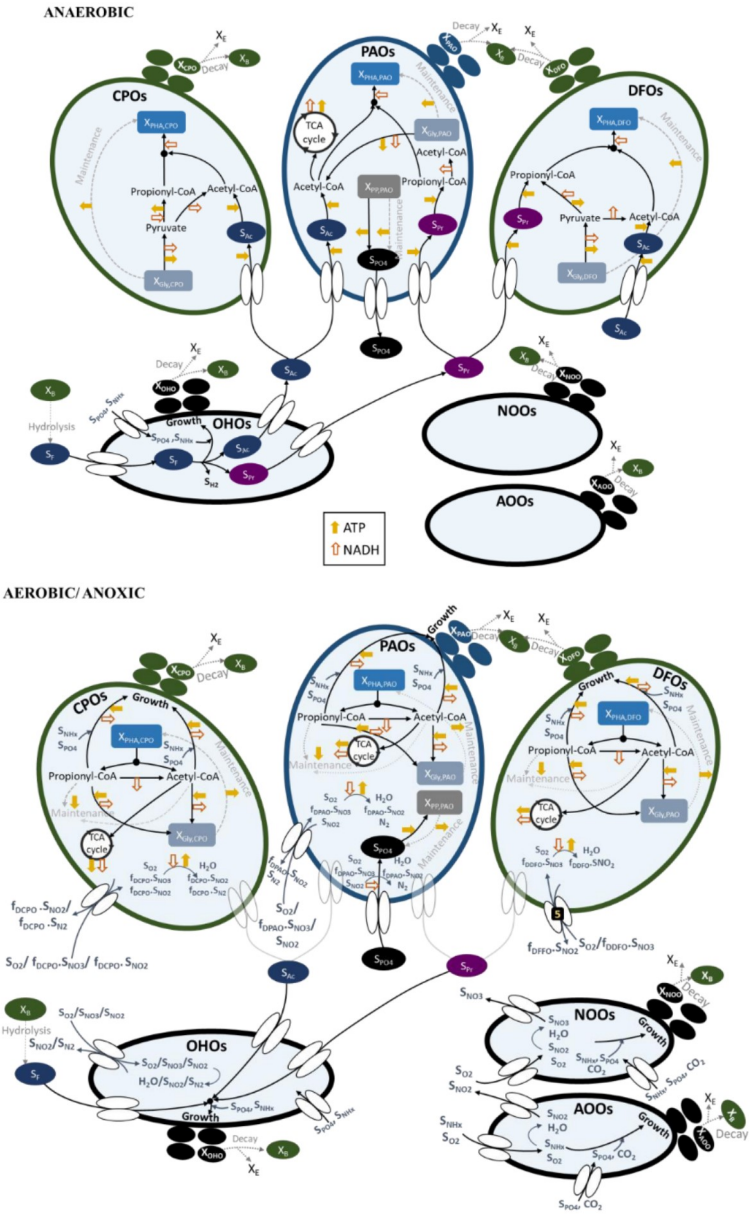

Figure 3.1. META-ASM conceptual model.

3.2.1.1 Fermentation

This process is modelled as a growth process similarly to the Barker & Dold model, but it is focused on the distribution of fermentation products (acetate, propionate and hydrogen), see Figure 3.2. This strategy correlates the "COD loss" mentioned by Barker and Dold (1997) with the hydrogen (H_2) gas formation and describes the production of two types of volatile fatty acids (VFAs) due to the impact that these carbon sources have on the PAO-GAO competition (as detailed below). Note that the further description of H_2 consumption, by e.g. hydrogenotrophic methanogenic organisms, was considered beyond the scope of this study.

3.2.1.2 Nitrification and denitrification (ANO and OHO)

These processes are modelled as two-step processes (see Figure 3.2) because WRRFs are increasingly interested in implementing new technologies (such as shortcut nitrogen removal) or control strategies that require the precise description of nitrate and nitrite. Furthermore, the inclusion of the intermediate species is important to describe the observed interactions between autotrophic nitrifying organisms (ANOs) and heterotrophic organisms (OHO, PAOs and GAOs).

3.2.1.3 Endogenous processes in OHOs and ANOs

The decay of the OHO, AOO and NOO is modelled according to the death-regeneration concept with a component-based model (similarly to the Barker & Dold model) under anaerobic, anoxic and aerobic conditions (see Figure 3.2). This concept was adopted in META-ASM because it allows modelling the anaerobic decay, unlike the endogenous respiration concept. Kinetically, the decay rate coefficients are defined by considering only the contribution of the cell death rate, while the effect of decreasing cellular activity was implemented through slowing down the growth rates of AOOs, NOOs and OHOs according to the activity decay rates determined by Hao et al. (2009) under aerobic conditions. The aerobic cell death rates of AOOs, NOOs and OHOs were defined according to the same study.

Instead, the other models consider the total cell decay as the sum of the activity decay and cell death rates. However, this assumption overpredicts the conversion of dead cells to slowly biodegradable substrate (X_B) and endogenous decay products (X_E), which affects the other processes due to the potential increase of carbon bioavailability through hydrolysis and fermentation.

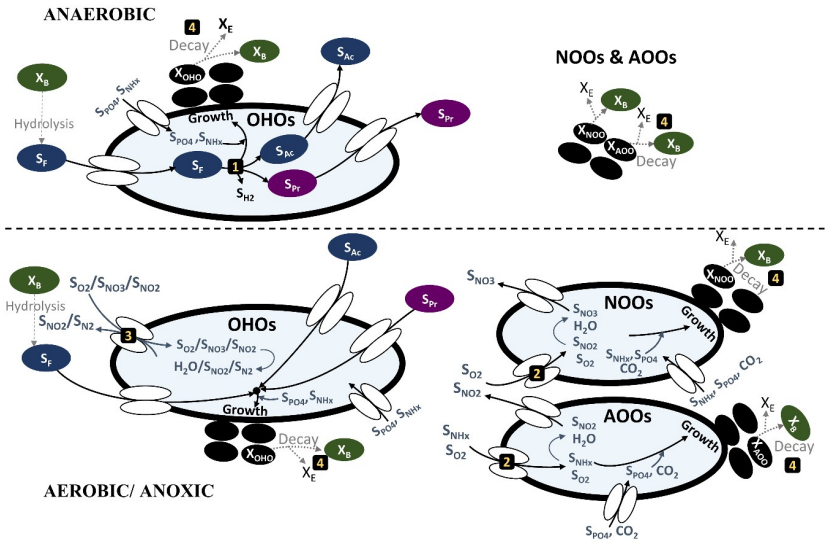

Figure 3.2. Simplified mechanisms for the processes of fermentation [1] (OHO growth under anaerobic conditions), nitrification [2] (NOO and AOO growth), OHO growth under aerobic and anoxic conditions [3] and decay [4] of OHO, AOO and NOO under anaerobic, aerobic and anoxic conditions. For further details on the description of model state variables, readers are referred to the list of abbreviations.

3.2.1.4 Origin of reducing power and energy for PAOs

The influence of the reducing power (i.e. NADH) on the stoichiometry of the poly-β-hydroxyalkanoates (PHA) storage processes of PAOs was incorporated in META-ASM. The reducing power is provided via glycolysis or TCA cycle pathways in the acetate uptake process according to Lanham et al. (2014), and via glycolysis or propionyl-CoA conversion to acetyl-CoA pathways in the propionate uptake process (see Figure 3.3-A). The latter pathway is proposed in this study by considering that PAO cells are able to generate NADH in the conversion of propionyl-CoA to acetyl-CoA, since propionyl-CoA is not a direct intermediate of the TCA cycle, and its conversion to acetyl-CoA generates ample NADH for PHA production.

These metabolic shifts are neglected in literature models and were incorporated in META-ASM because each pathway provides different yields for the anaerobic PHA formation and PO_4 release per VFA uptake. For instance, less PHA is produced and more PO_4 is released when the TCA cycle and propionyl-CoA conversion to acetyl-CoA pathways are active instead of glycolysis. In fact, the metabolic shifts between glycolysis and TCA cycle were observed in lab (Zhou et al., 2009) and full-scale plants (Cokro et al., 2017; Lanham et al., 2013; Pijuan et al., 2008), and are supported by recent metagenomics studies (Flowers et al., 2013; Martín et al., 2006; Skennerton et al., 2015) of

Accumulibacter organisms. Lanham et al. (2014) demonstrated through the application of metabolic models that lower VFA concentrations in the influent as well as longer aerobic retention times favour the dominance of the TCA metabolism over glycolysis.

The energy source (i.e. ATP) for the PHA storage processes of PAOs was considered in META-ASM to be mainly provided by hydrolysis of the intracellular polyphosphate, however, glycogen degradation was also considered to provide energy, similarly to the ASM2d+TUD model (see Figure 3.3-A). The other models only consider the hydrolysis of the intracellular polyphosphate as source of energy.

3.2.1.5 Effect of the electron acceptor on PAO yields

This effect was considered in META-ASM by defining distinct aerobic and anoxic yields as performed by Oehmen et al. (2010b). The same distinction is also considered in the UCTPHO+ and ASM2d+TUD models.

However, it is important to clarify that the aerobic and anoxic metabolism of PAOs consist of the following reactions as described in Murnleitner et al. (1997) and Smolders et al. (1994a): PHA catabolism, glycogen production, biomass growth, polyphosphate synthesis, phosphate transport across the cell membrane and oxidative phosphorylation (see Figure 3.3-B). From these reactions, only the last two depend on the electron acceptor, the others are independent and therefore identical for both conditions. In terms of stoichiometry, the amount of PO_4 transported per $NADH_2$ oxidized (ε), and the amount of ATP produced per $NADH_2$ oxidized (δ) differ under aerobic, anoxalic (i.e. in the presence of nitrate) and anoxilic conditions (i.e. in the presence of nitrite). Smolders et al. (1994a) and Kuba et al. (1996) determined experimentally these parameters under aerobic and anoxic conditions, respectively. According to Kuba et al. (1996), the anoxic (Ax) parameters δ_{Ax} and ε_{Ax} are approximately 50% lower than aerobic.

3.2.1.6 Capability of PAOs to denitrify

In addition to the effect of the electron acceptor in the anoxic yields of PAOs, two subgroups of PAOs were considered in META-ASM, where one subgroup performs nitrate reduction (hereafter DPAO) and both subgroups (henceforth PAO) perform nitrite reduction. These differences were modelled by multiplying a DPAO fraction (f_{DPAO}) to all stoichiometric coefficients in the nitrate reduction processes of PAOs (see Figure 3.3-B). This strategy is used to describe that some *Accumulibacter* species are capable of performing denitrifying PO_4 removal with nitrate, as suggested by recent studies (Camejo et al., 2019; Gao et al., 2019; Skennerton et al., 2015), while all known *Accumulibacter* clades are able to perform denitrification from nitrite onwards, as suggested by previous research in this area (Camejo et al., 2016; Flowers et al., 2013; Martín et al., 2006). Despite the

differences in the stoichiometries, it is considered that both subgroups denitrify at the same maximum kinetic rate.

The other literature models do not take into account the different denitrification capabilities of PAOs. Instead, they incorporate a reduction factor in the anoxic kinetic rate equations to lower the aerobic kinetic rates according to this factor.

3.2.1.7 Capability of GAOs to denitrify

Two subgroups were defined in META-ASM for *Competibacter* and *Defluviicoccus* GAOs to distinguish between the differences observed in their denitrification. As reported in literature (Burow et al., 2007; Kong et al., 2006; Wang et al., 2008), some *Competibacter* can denitrify from nitrate to N_2 gas (DCPO, hereafter) and others cannot denitrify (CPO), while some *Defluviicoccus* can denitrify from nitrate to nitrite (DDFO, hereafter), while others cannot denitrify at all (DFO). Following the same reasoning as PAOs, all stoichiometric coefficients in the nitrate and nitrite reduction processes of CPO were multiplied by the DCPO fraction (f_{DCPO}) and all stoichiometric coefficients in the nitrate reduction processes of DFO were multiplied by the DDFO fraction (f_{DDFO}), see Figure 3.3-B.

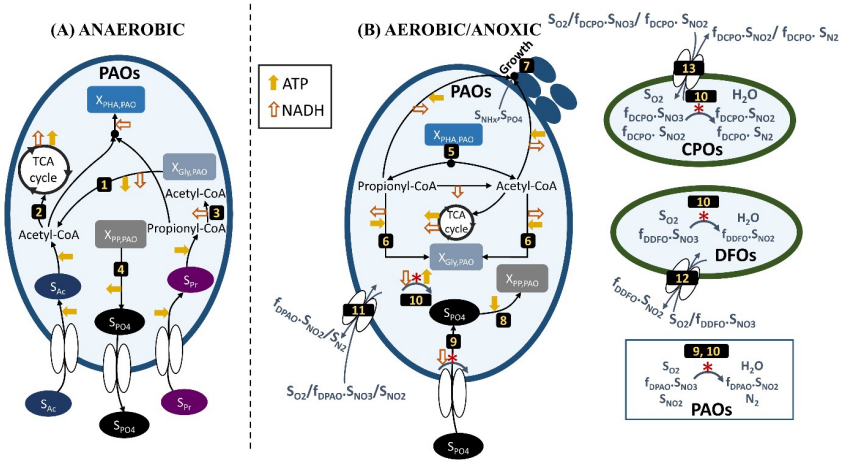

Figure 3.3. (A) Biochemical pathways for the PHA storage process by PAOs. (B) Biochemical pathways for the PHA oxidation, glycogen storage (both by PAOs and GAOs) and polyphosphate storage by PAOs under aerobic and anoxic conditions. Glycolysis [1]; TCA cycle [2]; propionyl-CoA conversion to acetyl-CoA [3]; hydrolysis of polyphosphate [4]; PHA catabolism (PAOs and GAOs) [5], glycogen production (PAOs and GAOs) [6], biomass growth (PAOs and GAOs) [7], polyphosphate synthesis (only in PAOs) [8], phosphate transport across the cell membrane (only in PAOs) [9] and oxidative phosphorylation [10]. Capabilities of PAOs [11], DFOs [12] and DCPOs [13] to denitrify. For further details on the description of model state variables, readers are referred to the list of abbreviations.

3.2.1.8 Endogenous processes in PAOs and GAOs

Two concepts were used sequentially in META-ASM to describe the endogenous processes for PAOs and GAOs: endogenous respiration/ cell maintenance (referred to as maintenance hereafter) and the death-regeneration concept (see Figure 3.4). This is consistent with available experimental studies (Carvalheira et al., 2014c; Hao et al., 2010; Liu et al., 2017; Lopez et al., 2006; Lu et al., 2007; Stokholm-Bjerregaard, 2016; Vargas et al., 2013; Wang et al., 2015, 2012) about the effect of starvation conditions and low organic loading rates on PAO and GAO metabolism. These studies have demonstrated that maintenance is the main endogenous process for PAOs and GAOs and that the cell death only corresponds to a minor fraction of the total decay (Hao et al., 2010; Lu et al., 2007; Vargas et al., 2013; Wang et al., 2012).

Literature models do not consider the use of different storage polymers by PAOs (and GAOs) as a survival strategy, prior to cell decay. For this reason, more details surrounding the maintenance processes are provided below for each process condition.

Energy source for anaerobic maintenance of PAOs and GAOs. In the META-ASM model, the anaerobic maintenance processes for PAOs were modelled according to Lanham et al. (2014), as polyphosphate hydrolysis (Smolders et al., 1994b) followed by glycogen degradation (Filipe et al., 2001; Zeng et al., 2003a), when low polyphosphate levels are attained. This sequential dependence was observed in several experimental studies (Lopez et al., 2006; Stokholm-Bjerregaard, 2016). It was considered that PAOs only decay when these storage polymers are exhausted (see Figure 3.4). In GAOs, glycogen is the only storage polymer source for the anaerobic maintenance (Carvalheira et al., 2014c; Stokholm-Bjerregaard, 2016; Vargas et al., 2013), and therefore, this process was modelled according to Filipe et al. (2001) and Zeng et al. (2003a). The anaerobic maintenance rates for PAOs and GAOs were calculated by taking into account the energy requirements obtained experimentally by Stokholm-Bjerregaard (2016). This study showed that GAOs have higher ATP requirements than PAOs under anaerobic conditions. Due to this reason, PAOs have an advantage over GAOs in periods of extended anaerobic starvation conditions, commonly observed in return sludge side-stream (RSS) hydrolysis/fermentation processes.

Energy source for aerobic/ anoxic maintenance of PAOs and GAOs. In the META-ASM model, the aerobic, anoxalic and anoxilic maintenance processes for PAOs were modelled in order to include sequential dependence on PHA, glycogen and polyphosphate (Carvalheira et al., 2014c; Lanham et al., 2014; Liu et al., 2017; Lu et al., 2007; Vargas et al., 2013). The same dependence was considered in the aerobic, anoxalic and anoxilic maintenance processes for GAOs, except that these organisms do not rely on polyphosphate (Carvalheira et al., 2014c; Vargas et al., 2013). It was considered that PAOs and GAOs start to decay with a maximum kinetic rate after PHA, glycogen and polyphosphate pools are exhausted (see Figure 3.4). The aerobic and anoxic maintenance rates for PAOs and GAOs were

calculated by taking into account the energy requirements obtained experimentally by Carvalheira et al. (2014c) and Carvalho et al. (2007). The analysis of these results showed that GAOs also have higher ATP requirements than PAOs under aerobic and anoxic conditions. Therefore, PAOs also have an advantage over GAOs in extended periods of aerobic and anoxic starvation conditions.

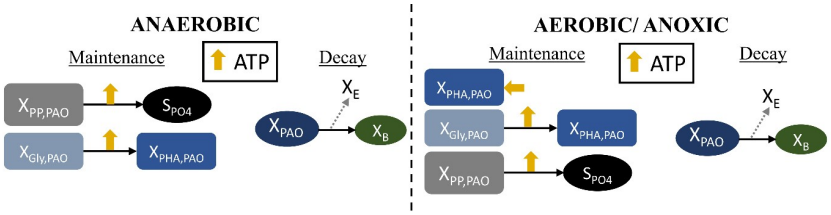

Figure 3.4. Simplified mechanisms for the maintenance and decay processes of PAOs under anaerobic, aerobic and anoxic conditions. GAOs perform the same processes, except the maintenance on polyphosphate under anaerobic, aerobic and anoxic conditions. For further details on the description of model state variables, readers are referred to the list of abbreviations.

3.2.1.9 Effect of operational conditions on PAOs and GAOs: type of carbon source and substrate competition, pH, temperature and DO.

The effect of type of carbon source and substrate competition, pH and temperature were incorporated in the processes of PAOs and GAOs as described in the models of Lopez-Vazquez et al. (2009) and Oehmen et al. (2010b). The effect of the DO was incorporated by determining the oxygen half-saturation coefficients of PAOs and GAOs through the experimental results of Carvalheira et al. (2014a).

Although some literature models incorporate the effect of the temperature on the kinetics of PAOs (Barker & Dold and ASM2d+TUD) and the effect of pH on the model stoichiometry (ASM2d+TUD), none of these models consider the effect of different types of carbon sources and DO in the stoichiometry and/or kinetics of PAOs (and GAOs). Consequently, these models fail to describe the competition commonly observed between PAOs and GAOs for the carbon source and the substrate preferences of each organism (Carvalheira et al., 2014b; Oehmen et al., 2005b). These models also fail to describe that PAOs have a higher affinity for oxygen, which provide them a kinetic advantage over GAOs at low DO levels, as studied by Carvalheira et al. (2014a) through lab studies and observed by Keene et al. (2017) in their pilot and full-scale experiments.

3.2.2 Model calibration and validation

The META-ASM model was calibrated and validated through the procedure shown in Figure 3.5 to derive a reliable default parameter set capable of predicting EBPR behaviour over a wide range of

selected operational and environmental conditions. The procedure followed is briefly described in this section and is consistent with the definition of model validation as stated by the *IWA Guidelines for Using Activated Sludge Models* (Rieger et al., 2012).

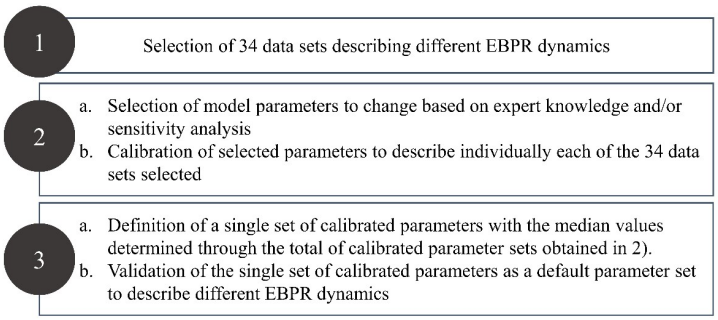

Figure 3.5. Procedure for the calibration of the META-ASM model and validation of the model default parameter set. Adapted from the IWA *Guidelines for Using Activated Sludge Models* (Rieger et al., 2012).

3.2.2.1 Data sets selection and their relevance to describe EBPR dynamics

A total of 34 data sets describing different EBPR dynamics were selected from bench-scale batch tests inoculated with lab-scale enriched PAO-GAO cultures and full-scale sludge from five WRRFs (from Portugal, PT, and Denmark, DK). Table 3.3 and Table 3.4 synthesize the characteristics of these sludges, respectively. For further details about the setup of these batch tests, readers are referred to the cited studies.

The experiments described in Table 3.3 were selected because they describe the dynamics of changing the carbon source and the DO on the competition between PAOs and GAOs, as well as the denitrification capability of PAOs.

The experiments in Table 3.4 describe the EBPR activity of five WRRFs (from Portugal and Denmark) with different process configurations: three conventional A2/O and two adapted Biodenitro™ combined with a RSS hydrolysis tank. These tests describe the different denitrification capabilities of PAOs and GAOs, the role of storage polymers in anoxic and aerobic endogenous processes and the metabolic shifts in PAOs as function of storage polymer concentrations (e.g. glycolysis pathway vs TCA cycle). In addition, these data sets also assess the effect of temperature on the activity of PAOs and GAOs, since the full-scale sludge was collected in winter and summer for the Portuguese WRRFs and only in winter for the Danish WRRFs.

Table 3.3. Characteristics of the lab-scale enriched PAO-GAO cultures used for the calibration of META-ASM and their relevance to describe EBPR dynamics.

Enriched culture[a]	Operational conditions							System	# data sets	Relevance	Ref.
	VFAs (mg COD.L^{-1})	% Acetate:Propionate	pH	T (ºC)	DO (mg O_2L^{-1})	SRT[b] (D)	HRT[c] (h)				
PAO culture 85% *Accumulibacter* 17% *Competibacter-lineage*	200	100:0 75:25 50:50 25:75 0:100	7.5	20	~8.0	8	12	Lab SBR A/O[d]	5	Study the effect of carbon source and substrate competition on the PAO-GAO competition	(Carvalheira et al., 2014b)
PAO culture 90% *Accumulibacter* 0.7% *Competibacter-lineage*	200	75:25	7.5	20	7.8 3.1 2.1 1.0 0.6 0.3 0.1	8	12	Lab SBR A/O	7	Study the impact of aeration on PAO metabolism	(Carvalheira et al., 2014a)
DPAO culture 76% *Accumulibacter* 1% *Defluviicoccus vanus*	300	0:100	8.2	24	-	10	24	Lab SBR A2[e]	1	Study the capability of PAOs to denitrify	(Carvalho et al., 2007)
CPO culture < 1% *Accumulibacter* 65% *Competibacter-lineage*	200	100:0	7.0	20	8.1 3.1 2.2 1.0 0.6	8	12	Lab SBR A/O	6	Study the impact of aeration on GAO metabolism	(Carvalheira et al., 2014a)

[a] Characterized by quantitative fluorescence *in situ* hybridisation (qFISH); [b] sludge retention time; [c] hydraulic retention time; [d] alternating anaerobic/ aerobic sequencing batch reactor (SBR); [e] alternating anaerobic/ anoxic sequencing batch reactor.

Table 3.4. Characteristics of the WRRFs used to perform batch tests for the calibration of the META-ASM with full-scale sludge and their relevance to describe EBPR dynamics.

	Beirolas (PT1)		**Setúbal (PT2)**		**Aalborg West (DK1)**	**Aalborg East (DK2)**	**Hjørring (DK3)**
Operational conditions							
Layout	A2/O		A2/O		Biodenitro + RSS	Biodenitro + RSS	A2/O
Average flow (10^3 $m^3.d^{-1}$)	48 ± 7		12 ± n/a		49 ± 8	17 ± 5	13 ± 6
Supplementary chemical precipitation	No		No		Yes ($FeCl_3$)	Yes ($FeCl_3$)	Yes ($FeCl_3$)
SRT (d)	12		5		19	30	43
Microbial composition by qFISH	Winter	Summer	Winter	Summer	Winter	Winter	Winter
% *Accumulibacter*	3.3	3.4	4.0	3.1	3.2	6.6	4.5
-Fraction *Accumulibacter* type I	0.46	0.15	0.66	0.13	0.49	0.28	0.32
-Fraction *Accumulibacter* type II	0.46	0.21	0.70	0.36	0.54	0.25	0.28
% *Competibacter-lineage*	< 1	< 1	5.1	< 1	< 1	< 1	< 1
% *Defluviicoccus* genus	0.0	< 1	3.1	4.9	0.0	0.0	3.2
-Fraction *Defluviicoccus vanus* Cluster I	-	-	0.08	0.05	-	-	0.18
Active DPAOs fraction, f_{DPAO}[a]	0.50	0.93	0.69	0.30	0.87	0.62	0.87
# Data sets	2	2	2	2	3	2	2
Relevance	-Study the EBPR activity in conventional and side-stream EBPR systems -Assess the capability of PAO to denitrify and remove P simultaneously -Evaluate the role of storage polymers in anoxic and aerobic endogenous processes -Evaluate the metabolic shifts in PAOs as function of storage polymer concentrations (e.g. glycolysis pathway vs TCA cycle)						
Ref.	(Lanham et al., 2018, 2013)						

[a] Estimated by the analytical method described in Lanham et al. (2018): $f_{DPAO}=(\Delta P_{ax}/\Delta P_{ox}).(\delta_{ox}/\delta_{ax})$ and $f_{DPAO}+f_{PAO}=1$.

3.2.2.2 Calibration process

The criteria for the selection of parameters requiring calibration was based on expert knowledge on metabolic models and sensitivity analyses performed in previous studies focussed on metabolic modelling (Lopez-Vazquez et al., 2009; Oehmen et al., 2010b), as discussed in section 3.3.1.1. The default parameters of AOOs, NOOs and OHOs were not calibrated in this study because the experiments described in section 3.2.2.1 were designed to: i) inhibit nitrification through the addition of allyl-N thiourea (ATU) and ii) reduce the activity of OHOs due to the existence of an anaerobic phase preceding the anoxic and aerobic phases, which favours the uptake of VFAs by PAOs (and GAOs) and limits the availability of this carbon source to OHOs in the subsequent phases.

The kinetic rates of PAOs and GAOs were the only parameters calibrated in this study to describe individually each of the 34 data sets selected. The method used for the calibration of each kinetic parameter was the minimum error search using Nelder Mead optimizer and least squares. Each phase (anaerobic, aerobic, and anoxic) was calibrated separately in order to avoid error propagation, and for this reason the initial model concentrations correspond to the initial experimental values (see definition of initial conditions in Appendix A.1), except the concentrations of X_{PAO}, X_{CPO}, $X_{DFO,}$ X_{OHO}, stored polyphosphates in PAOs ($X_{PAO,PP}$), inorganic suspended solids (X_{IG}), particulate unbiodegradable organics (X_U) and X_B in the aerobic and anoxic phases that were defined according to the last value simulated in the anaerobic phase.

The anaerobic kinetic rates of PAOs were determined first by fitting the measured anaerobic PO_4 release due to the fact that GAOs were present in some experiments, and therefore, they also contributed for the observable VFA uptake, PHA production and glycogen consumption. When PAOs are only present in the sludge, any of these anaerobic conversions could also be used for the calibration of the anaerobic kinetic rates of PAOs because they are described by the same stoichiometric reaction in META-ASM. However, it is recommendable to use the most reliable measurements (PO_4 or VFAs) for the calibration of this parameter. Furthermore, it should be noted that the anaerobic kinetic rates of PAOs were the only parameters calibrated in the anaerobic phase because those of CPO and DFO were indirectly determined through the correlations defined in equations A12-A17 (see Appendix A.1). These correlations assume the different substrate preferences obtained experimentally by Carvalheira et al. (2014b) and Lopez-Vazquez et al. (2009) with enriched PAO and GAO cultures.

The aerobic and anoxic kinetic rates of each organism were determined in subsequent simulations by fitting the respective measured PHA consumption, glycogen production and PO_4 removal (only in PAOs).

The effect of the DO on the PAO and GAO competition was determined by calibrating the maximum aerobic kinetic rates and oxygen half-saturation coefficients of these organisms with the data

sets of Carvalheira et al. (2014a), as the authors studied the effect of different DO concentrations in enriched PAO and CPO cultures.

Due to the contrasting findings about the capability of PAOs to use nitrate (Kim et al., 2013; Rubio-Rincón et al., 2017; Saad et al., 2016; Zeng et al., 2016), the parameter f_{DPAO} was firstly defined as zero (assuming that few full-scale *Accumulibacter* species are able to reduce nitrate) and then defined according to the active DPAO fraction estimated by the analytical method described in Lanham et al. (2018), see Table 3.4. These two parallel calibrations were performed to confirm whether PAOs are able or not to reduce nitrate. Note that Lanham et al. (2018) did not find any correlation between the parameter f_{DPAO} estimated through chemical batch tests and the microbial composition determined by quantitative fluorescence *in situ* hybridisation (qFISH), especially when compared with *Accumulibacter* Type I and type II, *Competibacter*-lineage and *Defluviicoccus* genus. This study suggested instead that chemical batch tests are the best methodology for quantifying the potential of anoxic P removal in full-scale WRRFs. The fraction of *Defluviicoccus* genus (f_{DDFO}) able to reduce nitrate and the fraction of *Competibacter* (f_{DCPO}) able to denitrify were assumed with a default value of 0.5, as discussed later. For the same reasons, the parameter f_{DDFO} was not defined according to the fraction of *Defluviicoccus vanus* Cluster I determined by qFISH.

3.2.2.3 Validation process

A single set of calibrated parameters was defined with the median values determined through the total of calibrated parameter sets obtained during the calibration process. In addition, the parameter f_{DPAO} was fixed with the median fraction of 0.69 determined analytically through the offline batch tests, and f_{DDFO} and f_{DCPO} were fixed with the assumed fraction of 0.5. Sensitivity analysis was performed on these fractions by changing the fixed values ± 30% in order to evaluate the impact of these fractions on the model predictions (see Table 3.5).

Table 3.5. Sensitivity analysis of the parameters f_{DPAO}, f_{DCPO} and f_{DDFO} on the PT2-Winter data set. This data set was selected because PAOs, CPOs and DFOs were simultaneously present in this test.

	Simulation A			**Simulation B**			**Simulation C**		
Parameter	**f_{DPAO}**	**f_{DCPO}**	**f_{DDFO}**	**f_{DPAO}**	**f_{DCPO}**	**f_{DDFO}**	**f_{DPAO}**	**f_{DCPO}**	**f_{DDFO}**
Default	0.69	0.5	0.5	0.69	0.5	0.5	0.69	0.5	0.5
Default - 30%	0.48	-	-	-	0.35	-	-	-	0.35
Default + 30%	0.9	-	-	-	0.65	-	-	-	0.65

Full-cycle simulations were performed on the same data sets (Table 3.3 and 3.4) to validate if the selected single set of calibrated parameters can be used as a default parameter set. In these simulations, the anoxic and aerobic phases were initiated with the final anaerobic concentrations predicted, as opposed to initiating these phases with the experimentally determined value. This procedure was

followed to assess the impact of error propagation between phases when a single set of default parameters is used.

The prediction quality of the model was assessed by plotting the predicted versus measured anaerobic PO_4^{3-}-P release, aerobic and anoxic PO_4^{3-}-P uptake, anaerobic PHA production, aerobic and anoxic PHA consumption, anaerobic glycogen consumption, aerobic and anoxic glycogen production, anaerobic VFAs consumption and anoxic NO_3^--N removal. The goodness-of-fit of the model versus measured data to an ideal match (y=x) was assessed by the adjusted R^2 (adj. R^2) parameter.

3.2.2.4 Performance comparison between models

The predictive power of META-ASM, Barker & Dold and ASM2d was evaluated by performing full-cycle simulations to the data sets of the WRRFs: PT1-Winter-1, DK2-Winter-2 and PT2-Winter-1.

The default parameter set validated in this study was used in the META-ASM, while the parameters defined in matrices reviewed by Hauduc et al. (2010) were used in the Barker & Dold and ASM2d models. The initial conditions in the anaerobic phase were defined as described in the Appendix A.1, except that in these models the concentrations of CPO and DFO were added to the concentration of OHO (X_{OHO}) and the total concentration of PHA measured was defined in the PHA stored by PAO ($X_{PAO,stor}$).

3.3 Results and discussion

3.3.1 Model calibration and validation

The procedure followed for the calibration and validation of the META-ASM was based on the *IWA Guidelines for Using Activated Sludge Models* (Rieger et al., 2012). This book defines a model parameter as default when it refers to a consensus value that can be used as a starting point in a calibration process, and a model parameter set as default when it has been validated on different wastewater treatment plants and has a clear explanation of how each proposed value was obtained. Therefore, this chapter discusses in detail 1) how the calibrated parameter sets were obtained in META-ASM and 2) how a single set of calibrated parameters can be derived and validated as a default parameter set.

3.3.1.1 Calibration of model parameters

The PAO-GAO metabolic models only require the calibration of kinetic parameters through well-designed experiments due to the fact that most of the yield coefficients are calculated theoretically through substrate, energy and reducing power balances on well-established biochemical pathways for the processes involved in the anaerobic, anoxic and aerobic PAO and GAO metabolism (Oehmen et al.,

2005c; Smolders et al., 1994a, 1994b; Zeng et al., 2003a). However, the obtained yields depend on a few metabolic ratios, such as the amount of ATP produced per $NADH_2$ oxidized (δ), amount of phosphate (PO_4) transported per $NADH_2$ oxidized (ε) and ATP necessary for biomass synthesis (K_1 and K_2), that were experimentally determined by previous studies with enriched PAO and/or GAO cultures (Smolders et al., 1994a; Zeng et al., 2003a). The impact of changing some of these metabolic ratios, e.g. δ and K_1 and K_2, was shown to have a marginal effect on the model predictions and overall stoichiometry, as demonstrated by Lopez-Vazquez et al. (2009) and Zeng et al. (2003a), respectively. Based on these results, the authors recommended not to change the original values of these parameters. In fact, several experimental studies (Carvalheira et al., 2014a, 2014b; Carvalho et al., 2007; Lanham et al., 2013; Lu et al., 2006; Oehmen et al., 2005b, 2005a; Pijuan et al., 2008, 2004; Zeng et al., 2003b) conducted at different environmental and operational conditions, including the data sets selected in this study, have reported that the measured yield coefficients are very well described by the theoretical stoichiometric yields of previous PAO-GAO metabolic models (Lanham et al., 2014; Lopez-Vazquez et al., 2009; Oehmen et al., 2010b).

The data sets selected in Table 3.3 and Table 3.4 describe a variety of process dynamics and changes of operational conditions. Due to this reason, the maximum kinetic rates for PAOs and GAOs were calibrated for each data set to describe individually each process dynamic. This procedure allowed a better understanding of the variations of each set of calibrated parameters and evaluate if, with the model structure proposed, it would be possible to derive a reliable and robust default parameter set capable of predicting these EBPR dynamics within an acceptable level of confidence. Table 3.6 shows the mean, median and standard deviation values obtained for each kinetic rate calibrated. Note that the number of data sets depicted in Table 3.6 used to calibrate each kinetic rate is less than 34, due to the fact that the experimental studies with the enriched cultures were not designed for all environmental conditions and in some full-scale sludge tests some parameters were not available.

The capability of PAOs to reduce nitrate was also assessed during the calibration of the maximum kinetic rates through the f_{DPAO} stoichiometric parameter. When this parameter is defined as zero the processes of nitrate reduction by PAOs are deactivated, which means that PAOs are only able to perform anoxic P uptake using nitrite as electron acceptor. Some literature studies suggested that PAOs are not able to reduce nitrate and that the observed anoxic P uptake results from the utilization of nitrite produced by side populations, such as denitrifying GAOs (DGAOs) or denitrifying OHOs (DOHOs) (Kim et al., 2013; Rubio-Rincón et al., 2017; Saad et al., 2016; Zeng et al., 2016). In this study, this theory was tested with the available data sets from Lanham et al. (2018). Table 3.6 shows that the model in this scenario only fitted the experimental results when the maximum anoxic kinetic rates of PAOs were increased to unrealistic values that are much higher than those calibrated under aerobic conditions. This happens because GAOs were not detected, for instance, in the tests performed with sludge from WRRFs PT1, DK1 and DK2 and the activity of DOHOs was inhibited, as no external carbon source was

added in the anoxic phase. Thus, the production of nitrite by side populations is not supported from this data. Although other PHA-storing denitrifiers could also have been involved in the reduction of nitrate, as suggested in section 3.3.1.2, this would not be enough to explain all the observed nitrate removal. Therefore, these results from META-ASM suggest that there are *Accumulibacter* species in WRRFs able to use nitrate and perform PO_4 uptake, as confirmed recently by Camejo et al. (2019), Gao et al. (2019) and Skennerton et al. (2015).

Table 3.6. Mean and median values for the anaerobic, aerobic and anoxic kinetic parameters determined after calibration of 34 different case-studies. (Stdev is the standard deviation and N is the number of data sets used for calibration. The values in parentheses correspond to the calibrations performed with f_{DPAO} = 0. ANA, Ox and Ax mean anaerobic, oxic and anoxic conditions, respectively).

Maximum kinetic rates			Units	Overall			
				Mean	Median	Stdev	N
PAO	$q_{PAO.AC,PHA,Max}$	ANA acetate uptake	d^{-1}	6.83	5.99	3.42	20
	$q_{PAO,Pr,PHA,Max}$	ANA propionate uptake	d^{-1}	6.30	6.72	1.71	5
	$q_{PAO,PHA,Max,Ox}$	Ox PHA degradation rate	d^{-1}	6.81	6.64	2.11	26
	$q_{PAO,Gly,Max,Ox}$	Ox glycogen production rate	d^{-1}	1.68	1.61	0.80	24
	$q_{PAO,PP,Max,Ox}$	Ox polyphosphate formation	g $P.gCOD^{-1}.d^{-1}$	4.23	3.18	3.05	26
	$q_{PAO,PHA,Max,Ax}$	Ax PHA degradation	d^{-1}	1.89 *(987.62)*	1.83 (686.67)	0.80 (1341.63)	16
	$q_{PAO,Gly,Max,Ax}$	Ax glycogen production	d^{-1}	0.87 *(394.42)*	0.50 *(207.96)*	0.90 *(589.37)*	13
	$q_{PAO,PP,Max,Ax}$	Ax polyphosphate formation	g $P.gCOD^{-1}.d^{-1}$	1.03 *(593.94)*	0.57 *(172.15)*	0.94 *(898.39)*	16
CPO, DFO	$q_{CPO,PHA,Max,Ox}$ $q_{DFO,PHA,Max,Ox}$	Ox PHA degradation	d^{-1}	18.72	18.81	0.81	6
	$q_{CPO,Gly,Max,Ox}$ $q_{DFO,Gly,Max,Ox}$	Ox glycogen production	d^{-1}	7.23	7.67	2.95	6
	$q_{CPO,PHA,Max,Ax}$ $q_{DFO,PHA,Max,Ax}$	Ax PHA degradation	d^{-1}	5.27	5.29	0.91	2
	$q_{CPO,Gly,Max,Ax}$ $q_{DFO,Gly,Max,Ax}$	Ax glycogen production	d^{-1}	3.81	4.04	-	1

In addition to the kinetic rates, the oxygen half-saturation coefficients of PAOs ($K_{O2,PAO}$=0.2) and GAOs ($K_{O2,GAO}$=0.5) were calibrated through the experimental results of Carvalheira et al. (2014a). The obtained parameters indicate that PAOs have a higher affinity for oxygen, which provide them a kinetic advantage over GAOs at low DO levels, as discussed in detail in Carvalheira et al. (2014a).

Figure 3.6 shows the META-ASM model describing successfully different case-studies using the calibrated parameter sets. However, it was still necessary to determine a single set of parameters and validate if it can be used as a default parameter set for future model applications.

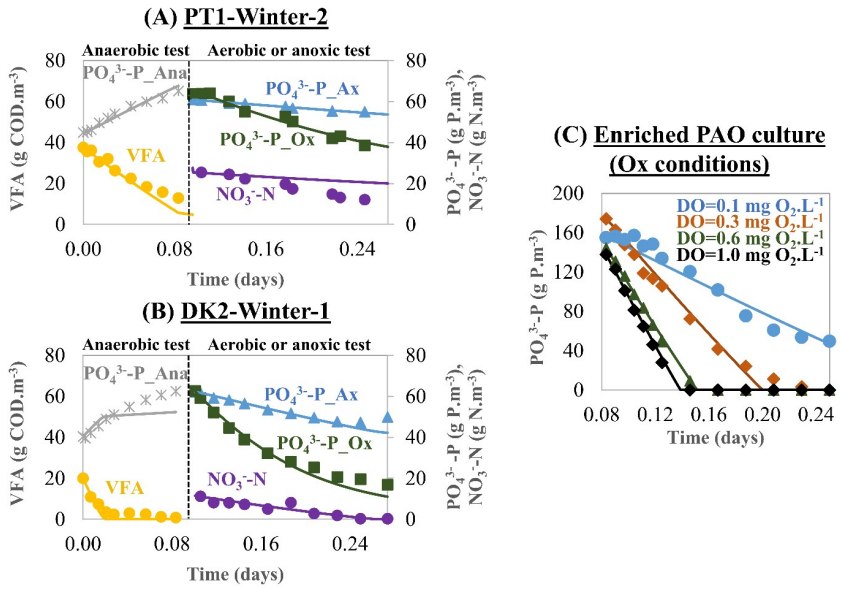

Figure 3.6. META-ASM model calibration in different case-studies. A) PT1-Winter-2, B) DK2-Winter-1 described in Table 3.4 and C) Enriched PAO culture described in Table 3.3. ANA, Ox and Ax mean anaerobic, oxic and anoxic conditions, respectively.

3.3.1.2 Validation of the default parameter set

Full-cycle simulations of the 34 data sets were performed using a single set of calibrated parameters defined with the median values determined during the calibration process (see Table 3.6), as well as the fixed fractions for the parameters f_{DCPO} and f_{DDFO}.

Despite the variations obtained in the calibration of the kinetic parameters, Figure 3.7-11 show that, overall, the single set of default parameters selected are reliable and robust, as demonstrated by the good correlations obtained when the predicted versus measured EBPR profiles from different data sets of enriched PAO-GAO cultures and full-scale sludge were plotted. These results suggest that the model structure proposed in this study is appropriated for all systems studied.

The typical enriched PAO-GAO and DPAO profiles were very well described for all parameters, even when different ratios of propionate to acetate and DO concentrations were tested ($0.844 \leq$ adj. $R^2 \leq 0.975$). This was only possible because the model incorporates the key biochemical pathways for the uptake of propionate and acetate on the overall anaerobic stoichiometric reactions of PAOs and GAOs, as described in Lopez-Vazquez et al. (2009) and Oehmen et al. (2010b), as well as the different oxygen affinities of these organisms calibrated in this study. Furthermore, the model predicted very well the PO_4^{3-}-P profiles in the tests with different full-scale sludge ($0.742 \leq$ adj. $R^2 \leq 0.872$, Figure 3.7-B, D, F),

which strongly supports the capability of META-ASM to describe different EBPR configurations (A2/O and side-stream EBPR systems). The goodness-of-fit of the predicted versus measured PHA to an ideal match in the tests with full-scale sludge needs to be interpreted individually. This parameter is reasonably described under anaerobic (adj. R^2=0.759, Figure 3.8-B) and aerobic (adj. R^2=0.601, Figure 3.8-D) conditions and less well described under anoxic (adj. R^2=0.409, Figure 3.8-F) conditions. Figure 3.8-B clearly shows that the anaerobic PHA production was slightly underpredicted at the end of the anaerobic phase, especially in the data sets PT2-Summer-2 and PT2-Winter-1. These deviations may indicate the presence of other organisms in the sludge that were also able to store and consume PHA in the subsequent phases. The predictions of the aerobic and anoxic PHA consumption were consequently affected by this anaerobic PHA underestimation, whose impact on adj. R^2 is most notable under anoxic conditions because less PHA is consumed. The slight underestimation observed in the prediction of NO_3^--N removal (adj. R^2=0.560) can also be explained by the impact that other PHA-storing denitrifiers could have had on the anoxic test (see Figure 3.11-B). Figure 3.10-B shows that the anaerobic VFA consumption was overall well described (adj. R^2=0.929). Glycogen is typically the most difficult parameter to be modelled accurately, as has been previously pointed out in the literature (Lopez-Vazquez et al., 2009; Meijer et al., 2002; Murnleitner et al., 1997). Even so, the predictions obtained in the tests with enriched PAO-GAO cultures were very reasonable (see Figure 3.9-A, C and E), as were the anaerobic and aerobic experiments with full-scale sludge in this study (see Figure 3.9-B and D).

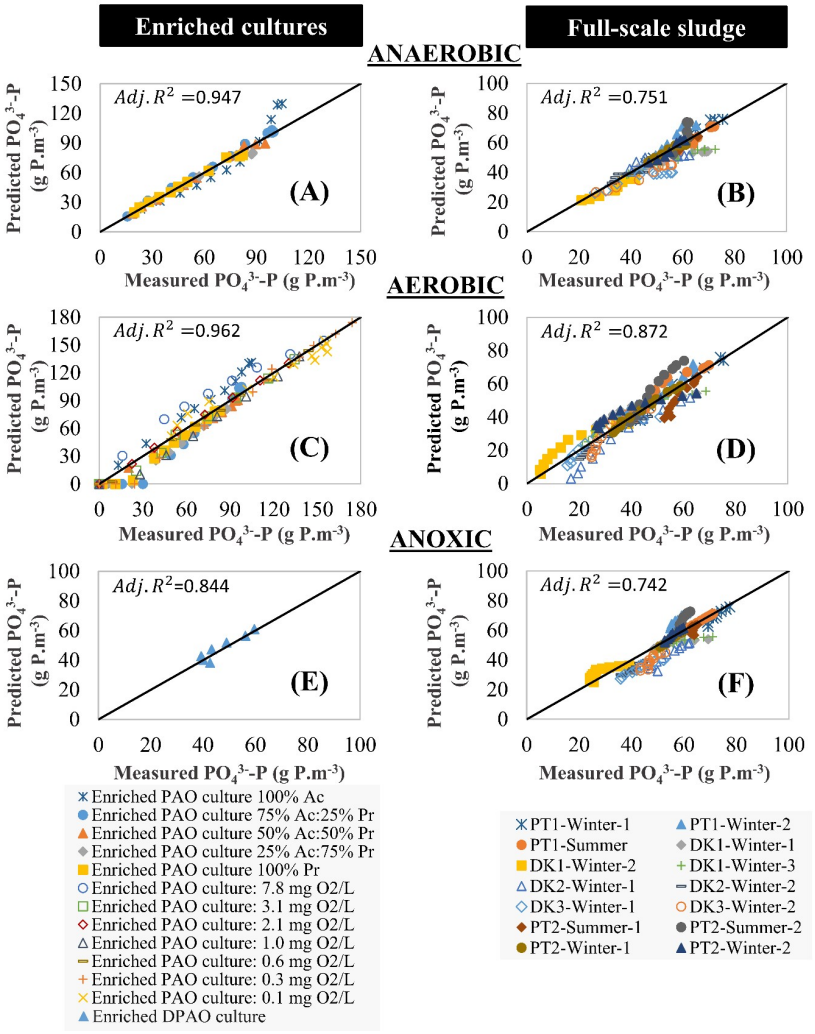

Figure 3.7. Predicted versus measured results for anaerobic PO_4^{3-}-P release (A and B), and aerobic (C and D) and anoxic (E and F) PO_4^{3-}-P uptake from different data sets described in Table 3.3 and Table 3.4. In these simulations the overall median values determined in Table 3.6 were used as default parameters. The solid line represents an ideal match (y=x). The goodness-of-fit was assessed by the adjusted R^2.

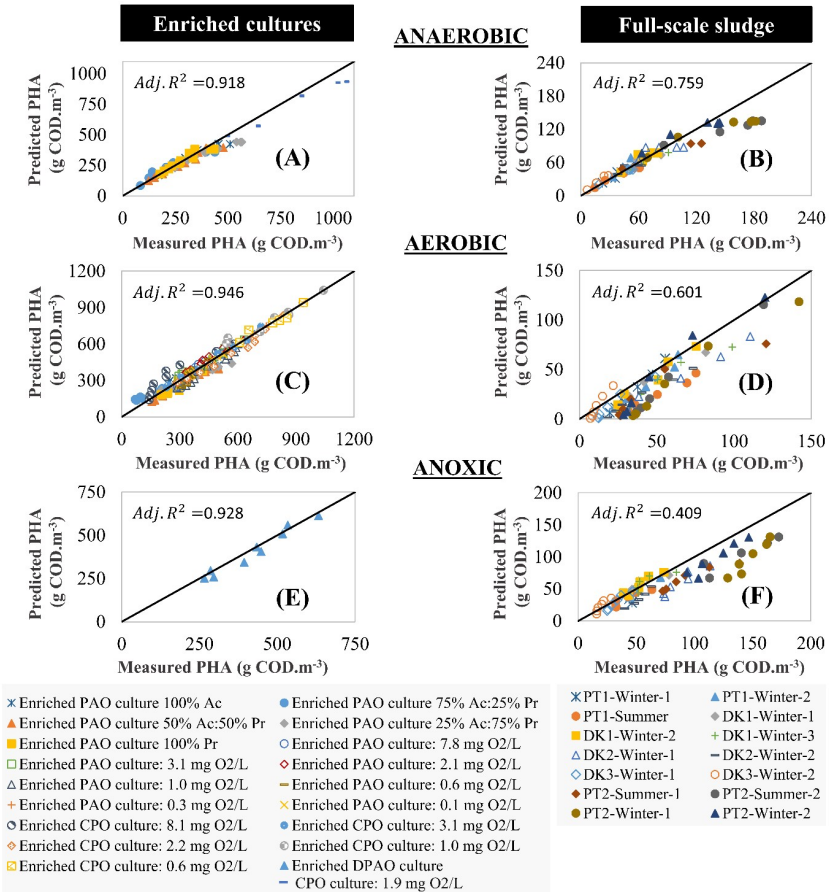

Figure 3.8. Predicted versus measured results for anaerobic PHA production (A and B), and aerobic (C and D) and anoxic (E and F) PHA consumption from different data sets described in Table 3.3 and Table 3.4. In these simulations the overall median values determined in Table 3.6 were used as default parameters. The solid line represents an ideal match (y=x). The goodness-of-fit was assessed by the adjusted R^2.

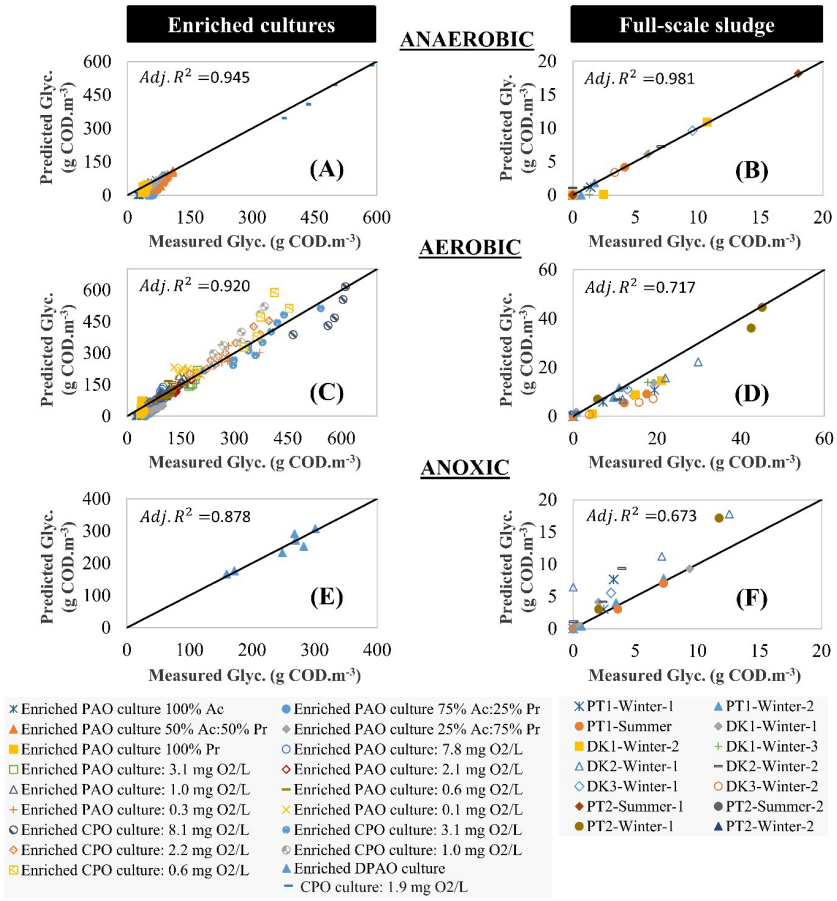

Figure 3.9. Predicted versus measured results for anaerobic glycogen consumption (A and B), and aerobic (C and D) and anoxic (E and F) glycogen production from different data sets described in Table 3.3 and Table 3.4. In these simulations the overall median values determined in Table 3.6 were used as default parameters. The solid line represents an ideal match (y=x). The goodness-of-fit was assessed by the adjusted R^2.

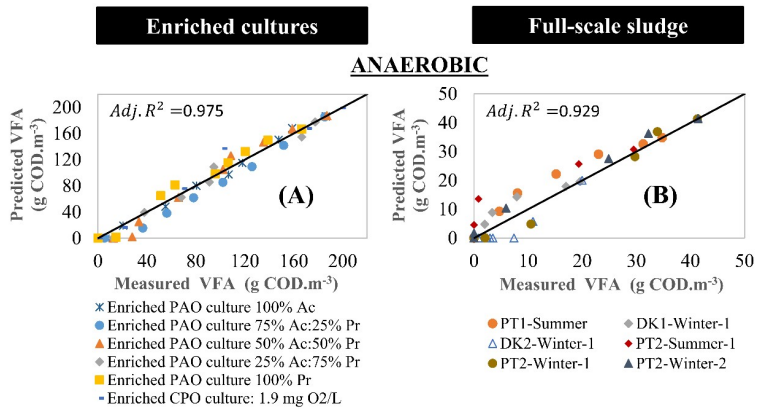

Figure 3.10. Predicted versus measured results for VFAs consumption (A and B) from different data sets described in Table 3.3 and Table 3.4. In these simulations the overall median values determined in Table 3.6 were used as default parameters. The solid line represents an ideal match (y=x). The goodness-of-fit was assessed by the adjusted R^2.

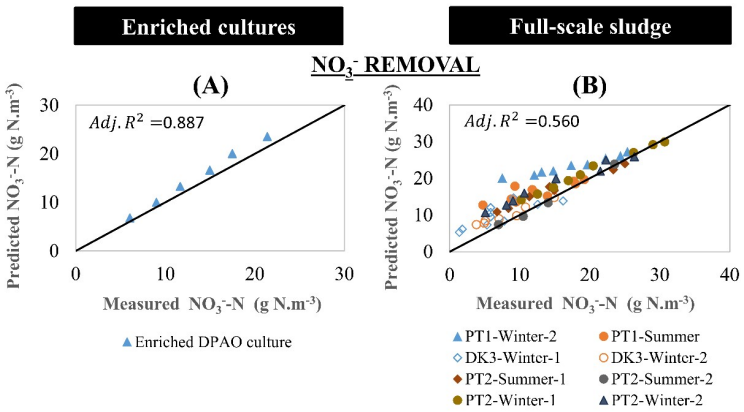

Figure 3.11. Predicted versus measured results for NO_3^--N removal (A and B) from different data sets described in Table 3.3 and Table 3.4. In these simulations the overall median values determined in Table 3.6 were used as default parameters. The solid line represents an ideal match (y=x). The goodness-of-fit was assessed by the adjusted R^2.

Furthermore, a sensitivity analysis was performed in this work for the f_{DPAO}, f_{DCPO} and f_{DDFO} parameters that were defined for the first time in the present study. The effect of changing each parameter by ± 30% was assessed and the results show that this variation had a residual impact on the model predictions (see Figure 3.12). It should also be pointed out that Oehmen et al. (2010b) had

previously performed a sensitivity analysis to the maximum kinetic rates that were calibrated in this study and observed that an increase or decrease of 10% of these parameters led only to a small increase (≤3%) in the deviation between the experimental measurements and predictions. Thus, small changes to the parameters calibrated in this study are unlikely to contribute substantial deviations to the model predictions.

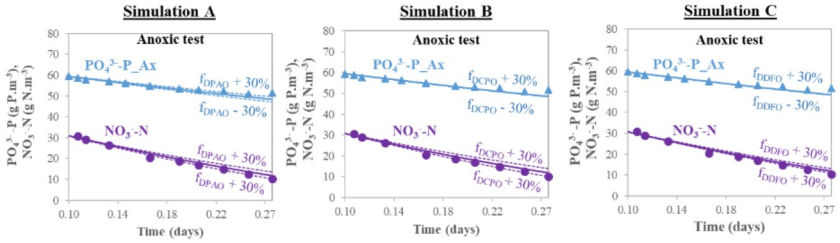

Figure 3.12. Sensitivity analysis of the parameters f_{DPAO}, f_{DCPO} and f_{DDFO} on the PT2-Winter data set (see Table 3.5).

3.3.1.3 Performance comparison between models

The predictive power of the META-ASM, Barker & Dold and ASM2d was evaluated by performing full-cycle simulations to the data sets of the WRRFs: PT1-Winter-1, PT2-Winter-1 and DK2-Winter-2. Figure 3.13-A, D, G show that the META-ASM model is able to describe all variables using the same default parameter set in the three case-studies evaluated, while the other two models do not. The Barker & Dold and ASM2d models were able to describe the anaerobic PO_4 release and the aerobic PO_4 uptake, except in the case-study PT1-winter-1. The observed deviations are possibly explained by the fact that in this WRRF the glycogen pools in the cells were exhausted and PAOs used the TCA cycle as alternative source of reducing power instead of glycolysis, as explained in Lanham et al. (2013). This shift is responsible for the increase of the yield of PO_4 release per VFA utilized, and this effect is well described in the META-ASM model. Both models were not able to describe the anaerobic VFA consumption (Figure 3.13-B, C, E, F, H and I). The main reason for this deviation is due to the predicted high anaerobic decay of ordinary heterotrophic organisms, which increased the concentration of slowly biodegradable substrate, affecting sequentially the anaerobic hydrolysis and fermentation processes. Even so, the anaerobic VFA consumption was better described in the Barker & Dold model than in the ASM2d model because the former describes the fermentation as an anaerobic growth process instead of a transformation process as described in the latter. To overcome this deviation and calibrate the anaerobic VFA consumption, it would be expected to change first the decay rate of OHO in both models or define different decay processes as a function of the environmental conditions. If these modifications are not enough to explain the measured anaerobic VFA consumption, it would be required to change the

kinetic rate for VFA uptake by PAOs in both models. However, this modification would cause an overprediction of the anaerobic release of PO_4 and PHA production. As a consequence, the stoichiometric parameters of this process would have to be modified in order to describe the subsequent phases.

On the other hand, both models fail to describe the simultaneous anoxic PO_4 and nitrate removal. The previous observed deviation in the anaerobic VFA consumption is partly responsible for this failure, due to the fact that the presence of VFAs under anoxic conditions promotes the competition between OHOs and PAOs for the electron acceptor, which increases the removal of nitrate. In addition to this correction, it would be required to modify the reduction factor for anoxic growth in both models to fit the measured nitrate, as illustrated in Figure 3.13-H, wherein the anaerobic VFA consumption was reasonably described by the Barker & Dold model. As a consequence of this modification, the anoxic yields of PAOs would also have to be changed in the Barker & Dold model and defined in the ASM2d model because the initial trend of the anoxic PO_4 uptake seems to be well explained in both models by the current reduction factor.

Overall, the results of Figure 3.13 support that current literature models are lacking detailed and dynamic process understanding and require extensive parameters changes, as demonstrated by the application of the Barker & Dold and ASM2d models. On the other hand, modelling EBPR processes in depth reduces calibration efforts, as demonstrated by the application of the META-ASM model. The effect of operational conditions on the competition between PAOs and GAOs, the capability of PAOs and GAOs to denitrify, the metabolic shifts as a function of storage polymer concentrations, as well as the role of these polymers in endogenous processes, and a better description of the fermentation process are suggestions of modifications that should be incorporated in the literature models to increase their predictive power.

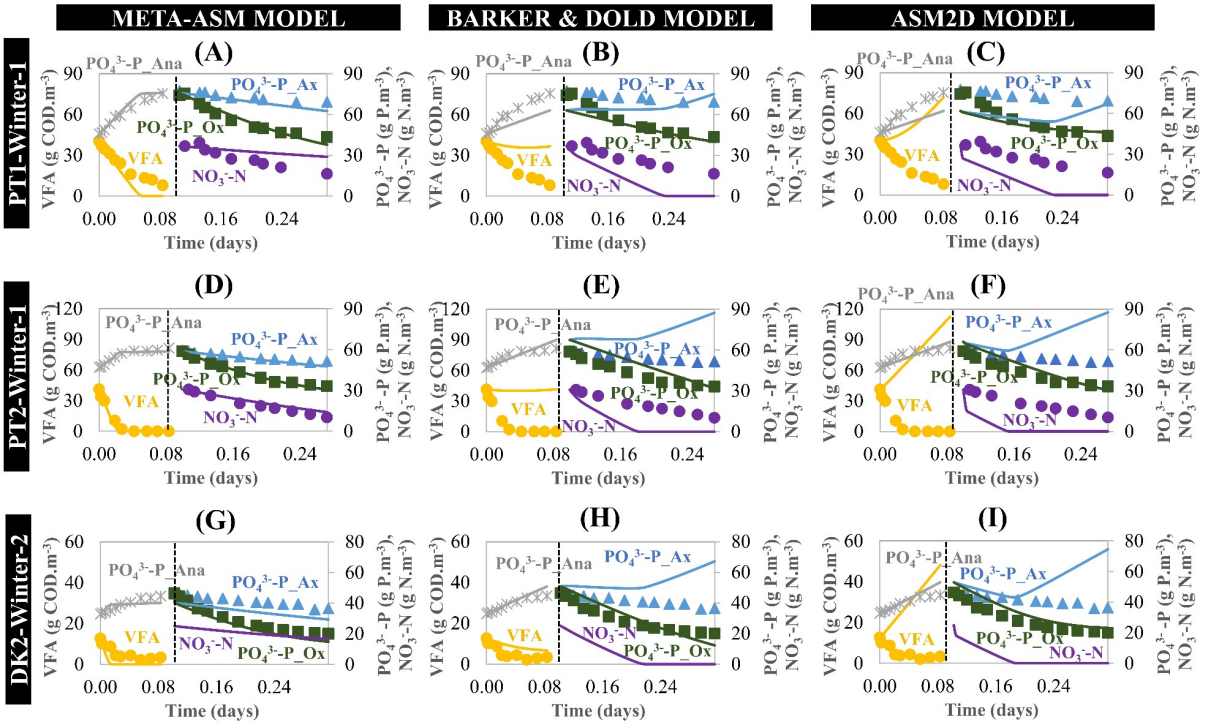

Figure 3.13. Performance comparison between the models: META-ASM (A, D and G), Barker & Dold (B, E and H) and ASM2d (C, F, and I) in the WRRFs PT1-Winter-1, PT2-Winter-1 and DK2-Winter-2. Ana: anaerobic; Ox: aerobic; Ax: anoxic. In these simulations the default parameter set validated in this study was used for the META-ASM model and the parameters defined in matrices reviewed by Hauduc et al. (2010) were used in the Barker & Dold and ASM2d models. The measured NO_3^--N data in DK2-Winter-2 was not available.

3.3.2 Challenges and limitations of the proposed approach

The authors have reviewed critically the limitations of previous literature models and gathered information from targeted experiments and available literature to develop a model capable of providing an in-depth understanding of EBPR systems operated at medium to long sludge retention times (SRTs, 5 to 43 days). The available experiments published over the last 20 years focus mainly on the most well-studied PAO (genus *Accumulibacter*) and GAO (*Competibacter*-lineage and the *Defluviicoccus* genus) organisms in lab and full-scale systems (hereafter referred to as classical PAO and GAO organisms). However, researchers have made efforts to improve the understanding of the ecophysiology of new putative PAO and GAO organisms, such as the genera *Tetrasphaera* and *Accumulimonas* PAOs (Kong et al., 2005; Nguyen et al., 2011) and *Micropruina* GAO (McIlroy et al., 2018; Shintani et al., 2000). In recent years, they have been found in significant abundance in WRRFs, sometimes outnumbering the classical PAO and GAO organisms (Lanham et al., 2013; Stokholm-Bjerregaard et al., 2017; Wu et al., 2019). Despite the abundance of *Tetrasphaera* in some systems, the quantification of its contribution to store intracellular P remains unclear and warrants further research.

It should be noted that the genera *Tetrasphaera* and *Micropruina* do not exhibit the typical phenotypes of PAO and GAO described in the META-ASM model. Their metabolism does not rely on PHA and they appear to be less competitive for VFA uptake (Kong et al., 2008; Kristiansen et al., 2013; Nguyen et al., 2011). Instead, they can grow anaerobically by fermenting amino acids or sugars and aerobically through the oxidation of glycogen (*Micropruina* spp.) or intracellular metabolites, such as amino acids, sugars and possibly fermentation products (*Tetrasphaera* spp.) (Nielsen et al., 2019). Due to these reasons, their impact on VFA-driven EBPR, which is the focus of META-ASM, is likely to be low. Moreover, the profile of PO_4 is still unclear in *Tetrasphaera* PAOs. An enriched lab-scale study showed that these organisms are able to uptake PO_4 anaerobically through energy generated by fermentation of some carbon sources (Marques et al., 2017), whereas other studies showed that they release PO_4 anaerobically, and uptake PO_4 aerobically and anoxically (Kristiansen et al., 2013; Nguyen et al., 2015). Due to the need for further research, the authors decided not to include these organisms in this version of the META-ASM model.

Furthermore, the validation of the META-ASM with the data sets presented in this study suggested that other organisms are capable of storing PHA anaerobically or aerobically and could compete with PAO and GAO for the carbon source and contribute to denitrification. If needed, future work in this area could incorporate PHA storage by ordinary heterotrophs into the model, as performed in ASM3 (Gujer et al., 1999). On the other hand, the META-ASM model structure enables the incorporation of similar PAOs to *Accumulibacter* (e.g. *Accumulimonas*) to be considered as part of the same group of PAO organisms, which would not necessitate any structural change to the model itself.

In recent years, some studies have focused on high-rate EBPR systems operated with SRTs lower than 4 days, where the microbial ecology and ecophysiology was observed to be different than the traditional EBPR systems (Ge et al., 2015; Valverde-Pérez et al., 2016). To describe these systems, the development of new mathematical models or adaptation of existing models is still required.

3.3.3 Implications for EBPR full-scale systems: control and optimisation tool

The META-ASM model summarises quantitatively the current state-of-knowledge of EBPR systems. It has the capability of predicting EBPR performance as a function of the PAO-GAO competition, various environmental temperatures and pHs, different DO concentrations, different COD/P ratios in the influent, and periods of low organic loading or starvation conditions commonly observed in WRRFs, without the need for extensive parameter adjustments. These capabilities make the META-ASM model a powerful tool for a better understanding, design and control of BNR systems. Potential applications include side-stream processes (return activated sludge, RAS, fermentation and shortcut nitrogen removal) coupled with EBPR and denitrifying and low DO operated EBPR systems, in addition to conventional EBPR processes.

The description of the known conditions that affect the PAO-GAO competition allow to estimate VFAs requirements for different configurations and choose the best operating modes or process configurations. The description of metabolic shifts as function of storage polymers concentrations, as well as the role of these polymers in endogenous processes, allow to select optimal SRT and hydraulic retention time (HRT) conditions in the anaerobic, anoxic and aerobic zones. This is particularly relevant for side-stream RAS fermentation systems because the model captures dynamically GAOs exhausting their storage polymers and decay much faster than PAOs in periods of extended anaerobic starvation conditions. These features make the model suitable to estimate the fraction of RAS diversion to fermentation, as well as the optimal HRT and SRT for fermentation.

The description of different PAO and GAO denitrification capabilities as well as the growth advantages of PAOs over GAO under low DO conditions (0.1-0.6 mg $O_2.L^{-1}$) allow the optimisation of EBPR systems with low energy and carbon consumption.

The next steps for further validation of the model are to: 1) perform long-term dynamic EBPR simulations and provide guidelines for future users of the model and 2) demonstrate the above features by applying the model in various engineering applications.

3.4 Conclusions

- This study produced a new integrated metabolic activated sludge model, the META-ASM model, that provides an overall platform to describe the activity of the key organisms and processes relevant to BNR systems with a robust single-set of default parameters.
- The advances described here overcome many of the limitations in terms of limited predictive power and extensive parameter changes required in currently available EBPR models. Examples of these improvements are: the effect of operational conditions in the competition between PAOs and GAOs, the capability of PAOs and GAOs to denitrify, the metabolic shifts as a function of storage polymer concentrations, as well as the role of these polymers in endogenous processes, and a better description of the fermentation process.
- The META-ASM model was tested against 34 different data sets obtained from bench-scale batch tests inoculated with lab-scale enriched PAO-GAO cultures and full-scale sludge from five WRRFs with two different process configurations: A2/O and adapted Biodenitro^{TM} combined with a return sludge side-stream hydrolysis tank.
- The overall good correlations obtained when the predicted versus measured EBPR profiles from different data sets were compared, support that this new model, which is based on in-depth understanding of EBPR, reduces calibration efforts.
- The theory that PAOs are able to use nitrate and perform anoxic P uptake was tested by activating or deactivating these processes during model calibration. The anoxic kinetic rates of PAOs obtained when these processes were activated suggest that there are *Accumulibacter* clades in WRRFs able to use nitrate and perform P uptake.
- The META-ASM model has the capability of predicting EBPR performance as a function of the PAO-GAO competition, various environmental temperatures and pHs, different DO concentrations, different COD/P ratios in the influent, and periods of low organic loading or starvation conditions commonly observed in WRRFs.
- This study suggests that the META-ASM model is a powerful tool to predict and mitigate EBPR upsets as well as to optimise EBPR performance.

3.5 References

Barker, P.., Dold, P.L., 1997. General model for biological nutrient removal activated-sludge systems: model presentation. Water Environ. Res. 69, 969–984. doi:doi:10.2175/106143097X125669

Brdjanovic, D., 2000. Modeling COD, N and P removal in a full-scale wwtp Haarlem Waarderpolder. Water Res. 34, 846–858. doi:10.1016/S0043-1354(99)00219-5

Burow, L.C., Kong, Y., Nielsen, J.L., Blackall, L.L., Nielsen, P.H., 2007. Abundance and ecophysiology of Defluviicoccus spp., glycogen-accumulating organisms in full-scale wastewater treatment processes. Microbiology. doi:10.1099/mic.0.2006/001032-0

Camejo, P.Y., Owen, B.R., Martirano, J., Ma, J., Kapoor, V., Santo Domingo, J., McMahon, K.D., Noguera, D.R., 2016. Candidatus Accumulibacter phosphatis clades enriched under cyclic

anaerobic and microaerobic conditions simultaneously use different electron acceptors. Water Res. doi:10.1016/j.watres.2016.06.033

Camejo, P.Y., Oyserman, B.O., McMahon, K.D., Noguera, D.R., 2019. Integrated Omic Analyses Provide Evidence that a "Candidatus Accumulibacter phosphatis" Strain Performs Denitrification under Microaerobic Conditions. mSystems. doi:10.1128/msystems.00193-18

Carvalheira, M., Oehmen, A., Carvalho, G., Eusébio, M., Reis, M.A.M., 2014a. The impact of aeration on the competition between polyphosphate accumulating organisms and glycogen accumulating organisms. Water Res. 66C, 296–307. doi:10.1016/j.watres.2014.08.033

Carvalheira, M., Oehmen, A., Carvalho, G., Reis, M.A.M., 2014b. The effect of substrate competition on the metabolism of polyphosphate accumulating organisms (PAOs). Water Res. 64, 149–59. doi:10.1016/j.watres.2014.07.004

Carvalheira, M., Oehmen, A., Carvalho, G., Reis, M.A.M., 2014c. Survival strategies of polyphosphate accumulating organisms and glycogen accumulating organisms under conditions of low organic loading. Bioresour. Technol. 172, 290–296. doi:10.1016/j.biortech.2014.09.059

Carvalho, G., Lemos, P.C., Oehmen, A., Reis, M.A.M., 2007. Denitrifying phosphorus removal: Linking the process performance with the microbial community structure. Water Res. 41, 4383–4396. doi:10.1016/j.watres.2007.06.065

Cokro, A.A., Law, Y., Williams, R.B.H., Cao, Y., Nielsen, P.H., Wuertz, S., 2017. Non-denitrifying polyphosphate accumulating organisms obviate requirement for anaerobic condition. Water Res. 111, 393–403. doi:10.1016/j.watres.2017.01.006

Dunlap, P., Martin, K., Stevens, G., Tooker, N., Barnard, J., Gu, A., Takacs, I., Onnis-Hayden, A., Li, Y., 2016. Rethinking EBPR: What do you do when the model will not fit real- world evidence? 5th IWA/WEF Wastewater Treat. Model. Semin. Annecy, Fr. 39–62.

Filipe, C.D., Daigger, G.T., Grady, C.P.J., 2001. A metabolic model for acetate uptake under anaerobic conditions by glycogen accumulating organisms: Stoichiometry, kinetics, and the effect of pH. Biotechnol. Bioeng. 76, 17–31.

Flowers, J.J., He, S., Malfatti, S., del Rio, T.G., Tringe, S.G., Hugenholtz, P., McMahon, K.D., 2013. Comparative genomics of two 'Candidatus Accumulibacter' clades performing biological phosphorus removal. ISME J. 7, 2301–2314. doi:10.1038/ismej.2013.117

Flowers, J.J., He, S., Yilmaz, S., Noguera, D.R., McMahon, K.D., 2009. Denitrification capabilities of two biological phosphorus removal sludges dominated by different "Candidatus Accumulibacter" clades. Environ. Microbiol. Rep. 1, 583–588. doi:10.1111/j.1758-2229.2009.00090.x

Gao, H., Mao, Y., Zhao, X., Liu, W.-T., Zhang, T., Wells, G., 2019. Genome-centric metagenomics resolves microbial diversity and prevalent truncated denitrification pathways in a denitrifying PAO-enriched bioprocess. Water Res. 155, 275–287. doi:10.1016/J.WATRES.2019.02.020

Ge, H., Batstone, D.J., Keller, J., 2015. Biological phosphorus removal from abattoir wastewater at very short sludge ages mediated bynovel PAO clade Comamonadaceae. Water Res. doi:10.1016/j.watres.2014.11.026

Gujer, W., Henze, M., Mino, T., Van Loosdrecht, M., 1999. Activated Sludge Model No. 3, in: Water Science and Technology. pp. 183–193. doi:10.1016/S0273-1223(98)00785-9

Hao, X., Van Loosdrecht, M.C., Meijer, S.C., Qian, Y., 2001. Model-based evaluation of two BNR processes--UCT and A2N. Water Res. 35, 2851–2860. doi:10.1016/S0043-1354(00)00596-0

Hao, X., Wang, Q., Cao, Y., Van Loosdrecht, M.C.M., 2010. Experimental evaluation of decrease in the activities of polyphosphate/glycogen-accumulating organisms due to cell death and activity decay in activated sludge. Biotechnol. Bioeng. 106, 399–407. doi:10.1002/bit.22703

Hao, X., Wang, Q., Zhang, X., Cao, Y., Mark Loosdrecht, C.M. van, 2009. Experimental evaluation of decrease in bacterial activity due to cell death and activity decay in activated sludge. Water Res. 43, 3604–3612. doi:10.1016/j.watres.2009.05.019

Hauduc, H., Gillot, S., Rieger, L., Ohtsuki, T., Shaw, A., Takács, I., Winkler, S., 2009. Activated sludge modelling in practice: An international survey. Water Sci. Technol. 60, 1943–1951. doi:10.2166/wst.2009.223

Hauduc, H., Rieger, L., Oehmen, A., van Loosdrecht, M.C.M., Comeau, Y., Héduit, A., Vanrolleghem, P.A., Gillot, S., 2013. Critical review of activated sludge modeling: State of process knowledge, modeling concepts, and limitations. Biotechnol. Bioeng. doi:10.1002/bit.24624

Hauduc, H., Rieger, L., Takács, I., Héduit, A., Vanrolleghem, P.A., Gillot, S., 2010. A systematic

approach for model verification: Application on seven published activated sludge models. Water Sci. Technol. doi:10.2166/wst.2010.898

Henze, M., Gujer, W., Mino, T., Matsuo, T., Wentzel, M. C. , Marais, G.V.R., 1995. Activated Sludge Model No. 2. IAWQ Scientific and Technical Report No. 3. IAWQ, London, UK., UK.

Henze, M., Gujer, W., Mino, T., Matsuo, T., Wentzel, M.C., Marais, G.V.R., Van Loosdrecht, M.C.M., 1999. Activated Sludge Model No.2d, ASM2d, in: Water Science and Technology. pp. 165–182. doi:10.1016/S0273-1223(98)00829-4

Hu, Z.-R., Wentzel, M.C., Ekama, G.A., 2003. Modelling biological nutrient removal activated sludge systems—a review. Water Res. 37, 3430–3444. doi:10.1016/S0043-1354(03)00168-4

Hu, Z., Wentzel, M., Ekama, G., 2007. A general kinetic model for biological nutrient removal activated sludge systems: Model development. Biotechnol. 98. doi:10.1002/bit21508

Keene, N.A., Reusser, S.R., Scarborough, M.J., Grooms, A.L., Seib, M., Santo Domingo, J., Noguera, D.R., 2017. Pilot plant demonstration of stable and efficient high rate biological nutrient removal with low dissolved oxygen conditions. Water Res. 121, 72–85. doi:10.1016/j.watres.2017.05.029

Kim, J.M., Lee, H.J., Lee, D.S., Jeon, C.O., 2013. Characterization of the denitrification-associated phosphorus uptake properties of "Candidatusaccumulibacter phosphatis" clades in sludge subjected to enhanced biological phosphorus removal. Appl. Environ. Microbiol. 79, 1969–1979. doi:10.1128/AEM.03464-12

Kong, Y., Nielsen, J.L., Nielsen, P.H., 2005. Identity and ecophysiology of uncultured actinobacterial polyphosphate-accumulating organisms in full-scale enhanced biological phosphorus removal plants. Appl. Environ. Microbiol. doi:10.1128/AEM.71.7.4076-4085.2005

Kong, Y., Xia, Y., Nielsen, J.L., Nielsen, P.H., 2006. Ecophysiology of a group of uncultured Gammaproteobacterial glycogen-accumulating organisms in full-scale enhanced biological phosphorus removal wastewater treatment plants. Environ. Microbiol. doi:10.1111/j.1462-2920.2005.00914.x

Kong, Y., Xia, Y., Nielsen, P.H., 2008. Activity and identity of fermenting microorganisms in full-scale biological nutrient removing wastewater treatment plants. Environ. Microbiol. doi:10.1111/j.1462-2920.2008.01617.x

Kristiansen, R., Nguyen, H.T.T., Saunders, A.M., Nielsen, J.L., Wimmer, R., Le, V.Q., McIlroy, S.J., Petrovski, S., Seviour, R.J., Calteau, A., Nielsen, K.L., Nielsen, P.H., 2013. A metabolic model for members of the genus Tetrasphaera involved in enhanced biological phosphorus removal. ISME J. 7, 543–554. doi:10.1038/ismej.2012.136

Kuba, T., Murnleitner, E., Van Loosdrecht, M.C.M., Heijnen, J.J., 1996. A metabolic model for biological phosphorus removal by denitrifying organisms. Biotechnol. Bioeng. 52, 685–695. doi:10.1002/(SICI)1097-0290(19961220)52:6<685::AID-BIT6>3.3.CO;2-M

Lanham, A.B., Moita, R., Lemos, P.C., Reis, M.A.M., 2011. Long-term operation of a reactor enriched in Accumulibacter clade I DPAOs: Performance with nitrate, nitrite and oxygen. Water Sci. Technol. 63, 352–359. doi:10.2166/wst.2011.063

Lanham, A.B., Oehmen, A., Carvalho, G., Saunders, A.M., Nielsen, P.H., Reis, M.A.M., 2018. Denitrification activity of polyphosphate accumulating organisms (PAOs) in full-scale wastewater treatment plants. Water Sci. Technol. 78, 2449–2458. doi:10.2166/wst.2018.517

Lanham, A.B., Oehmen, A., Saunders, A.M., Carvalho, G., Nielsen, P.H., Reis, M.A.M., 2014. Metabolic modelling of full-scale enhanced biological phosphorus removal sludge. Water Res. 66C, 283–295. doi:10.1016/j.watres.2014.08.036

Lanham, A.B., Oehmen, A., Saunders, A.M., Carvalho, G., Nielsen, P.H., Reis, M.A.M., 2013. Metabolic versatility in full-scale wastewater treatment plants performing enhanced biological phosphorus removal. Water Res. 47, 7032–7041. doi:10.1016/j.watres.2013.08.042

Liu, W., Peng, Y., Ma, B., Ma, L., Jia, F., Li, X., 2017. Dynamics of microbial activities and community structures in activated sludge under aerobic starvation. Bioresour. Technol. 244, 588–596. doi:10.1016/j.biortech.2017.07.131

Lopez-Vazquez, C.M., Oehmen, A., Hooijmans, C.M., Brdjanovic, D., Gijzen, H.J., Yuan, Z., van Loosdrecht, M.C.M., 2009. Modeling the PAO-GAO competition: Effects of carbon source, pH and temperature. Water Res. 43, 450–462. doi:10.1016/j.watres.2008.10.032

Lopez, C., Pons, M.N., Morgenroth, E., 2006. Endogenous processes during long-term starvation in activated sludge performing enhanced biological phosphorus removal. Water Res. 40, 1519–1530.

doi:10.1016/j.watres.2006.01.040
Lu, H., Keller, J., Yuan, Z., 2007. Endogenous metabolism of Candidatus Accumulibacter phosphatis under various starvation conditions. Water Res. 41, 4646–4656. doi:10.1016/j.watres.2007.06.046
Lu, H., Oehmen, A., Virdis, B., Keller, J., Yuan, Z., 2006. Obtaining highly enriched cultures of Candidatus Accumulibacter phosphates through alternating carbon sources. Water Res. 40, 3838–3848. doi:10.1016/j.watres.2006.09.004
Marques, R., Santos, J., Nguyen, H., Carvalho, G., Noronha, J.P., Nielsen, P.H., Reis, M.A.M., Oehmen, A., 2017. Metabolism and ecological niche of Tetrasphaera and Ca. Accumulibacter in enhanced biological phosphorus removal. Water Res. 122, 159–171. doi:10.1016/j.watres.2017.04.072
Martín, H.G., Ivanova, N., Kunin, V., Warnecke, F., Barry, K.W., McHardy, A.C., Yeates, C., He, S., Salamov, A.A., Szeto, E., Dalin, E., Putnam, N.H., Shapiro, H.J., Pangilinan, J.L., Rigoutsos, I., Kyrpides, N.C., Blackall, L.L., McMahon, K.D., Hugenholtz, P., 2006. Metagenomic analysis of two enhanced biological phosphorus removal (EBPR) sludge communities. Nat. Biotechnol. 24, 1263–1269. doi:10.1038/nbt1247
McIlroy, S.J., Albertsen, M., Andresen, E.K., Saunders, A.M., Kristiansen, R., Stokholm-Bjerregaard, M., Nielsen, K.L., Nielsen, P.H., 2014. 'Candidatus Competibacter'-lineage genomes retrieved from metagenomes reveal functional metabolic diversity. ISME J. doi:10.1038/ismej.2013.162
McIlroy, S.J., Onetto, C.A., McIlroy, B., Herbst, F.A., Dueholm, M.S., Kirkegaard, R.H., Fernando, E., Karst, S.M., Nierychlo, M., Kristensen, J.M., Eales, K.L., Grbin, P.R., Wimmer, R., Nielsen, P.H., 2018. Genomic and in Situ Analyses reveal the Micropruina spp. as Abundant fermentative glycogen accumulating organisms in enhanced biological phosphorus removal systems. Front. Microbiol. doi:10.3389/fmicb.2018.01004
Meijer, S., 2004. Theoretical and practical aspects of modelling activated sludge processes. Delft Univ. Technol. Netherlands 204.
Meijer, S.C.F., Van Loosdrecht, M.C.M., Heijnen, J.J., 2002. Modelling the start-up of a full-scale biological phosphorous and nitrogen removing WWTP. Water Res. 36, 4667–4682. doi:10.1016/S0043-1354(02)00192-6
Meijer, S.C.F., Van Loosdrecht, M.C.M., Heijnen, J.J., 2001. Metabolic modelling of full-scale biological nitrogen and phosphorus removing wwtp's. Water Res. 35, 2711–2723. doi:10.1016/S0043-1354(00)00567-4
Menniti, A., Schauer, P., Tackas, I., Shaw, A., 2016. Online Instrumentation for Monitoring and Control of Biological Phosphorus Removal. Proc. Water Environ. Fed. 2016, 3552–3561. doi:10.2175/193864716819713213
Murnleitner, E., Kuba, T., Van Loosdrecht, M.C.M., Heijnen, J.J., 1997. An integrated metabolic model for the aerobic and denitrifying biological phosphorus removal. Biotechnol. Bioeng. 54, 434–450. doi:10.1002/(SICI)1097-0290(19970605)54:5<434::AID-BIT4>3.0.CO;2-F
Nguyen, H.T.T., Kristiansen, R., Vestergaard, M., Wimmer, R., Nielsen, P.H., 2015. Intracellular Accumulation of Glycine in Polyphosphate-Accumulating Organisms in Activated Sludge, a Novel Storage Mechanism under Dynamic Anaerobic-Aerobic Conditions. Appl. Environ. Microbiol. doi:10.1128/aem.01012-15
Nguyen, H.T.T., Le, V.Q., Hansen, A.A., Nielsen, J.L., Nielsen, P.H., 2011. High diversity and abundance of putative polyphosphate-accumulating Tetrasphaera-related bacteria in activated sludge systems. FEMS Microbiol. Ecol. doi:10.1111/j.1574-6941.2011.01049.x
Nielsen, P.H., McIlroy, S.J., Albertsen, M., Nierychlo, M., 2019. Re-evaluating the microbiology of the enhanced biological phosphorus removal process. Curr. Opin. Biotechnol. 57, 111–118. doi:10.1016/J.COPBIO.2019.03.008
Oehmen, A, Carvalho, G., Lopez-Vazquez, C.M., van Loosdrecht, M.C.M., Reis, M.A.M., 2010a. Incorporating microbial ecology into the metabolic modelling of polyphosphate accumulating organisms and glycogen accumulating organisms. Water Res. 44, 4992–5004. doi:10.1016/j.watres.2010.06.071
Oehmen, A., Lopez-Vazquez, C.M., Carvalho, G., Reis, M.A.M., van Loosdrecht, M.C.M., 2010b. Modelling the population dynamics and metabolic diversity of organisms relevant in anaerobic/anoxic/aerobic enhanced biological phosphorus removal processes. Water Res. 44, 4473–4486. doi:10.1016/j.watres.2010.06.017
Oehmen, A., Vives, M.T., Lu, H., Yuan, Z., Keller, J., 2005a. The effect of pH on the competition

between polyphosphate-accumulating organisms and glycogen-accumulating organisms. Water Res. 39, 3727–3737. doi:10.1016/j.watres.2005.06.031

Oehmen, A., Yuan, Z., Blackall, L.L., Keller, J., 2005b. Comparison of acetate and propionate uptake by polyphosphate accumulating organisms and glycogen accumulating organisms. Biotechnol. Bioeng. 91, 162–168. doi:10.1002/bit.20500

Oehmen, A., Zeng, R.J., Yuan, Z., Keller, J., 2005c. Anaerobic metabolism of propionate by polyphosphate-accumulating organisms in enhanced biological phosphorus removal systems. Biotechnol. Bioeng. 91, 43–53. doi:10.1002/bit.20480

Pijuan, M., Oehmen, A., Baeza, J.A., Casas, C., Yuan, Z., 2008. Characterizing the biochemical activity of full-scale enhanced biological phosphorus removal systems: A comparison with metabolic models. Biotechnol. Bioeng. 99, 170–179. doi:10.1002/bit

Pijuan, M., Saunders, A.M., Guisasola, A., Baeza, J.A., Casas, C., Blackall, L.L., 2004. Enhanced Biological Phosphorus Removal in a Sequencing Batch Reactor Using Propionate as the Sole Carbon Source. Biotechnol. Bioeng. doi:10.1002/bit.10813

Rieger, L., Gillot, S., Langergraber, G., Ohtsuki, T., Shaw, A., Takacs, I., Winkler, S., 2012. Guidelines for Using Activated Sludge Models: IWA Task Group on Good Modelling Practice., Scientific and Technical Report No. 22. IWA Publishing, London, UK.

Rieger, L., Koch, G., Kuhni, M., Gujer, W., Siegrist, H., 2001. The EAWAG Bio-P module for activated sludge model No. 3. Water Res. 35, 3887–3903.

Rubio-Rincón, F.J., Lopez-Vazquez, C.M., Welles, L., van Loosdrecht, M.C.M., Brdjanovic, D., 2017. Cooperation between Candidatus Competibacter and Candidatus Accumulibacter clade I, in denitrification and phosphate removal processes. Water Res. 120, 156–164. doi:10.1016/j.watres.2017.05.001

Rubio-Rincón, F.J., Weissbrodt, D.G., Lopez-Vazquez, C.M., Welles, L., Abbas, B., Albertsen, M., Nielsen, P.H., van Loosdrecht, M.C.M., Brdjanovic, D., 2019. "Candidatus Accumulibacter delftensis": A clade IC novel polyphosphate-accumulating organism without denitrifying activity on nitrate. Water Res. 161, 136–151. doi:10.1016/J.WATRES.2019.03.053

Saad, S.A., Welles, L., Abbas, B., Lopez-Vazquez, C.M., van Loosdrecht, M.C.M., Brdjanovic, D., 2016. Denitrification of nitrate and nitrite by 'Candidatus Accumulibacter phosphatis' clade IC. Water Res. 105, 97–109. doi:10.1016/j.watres.2016.08.061

Shintani, T., Liu, W.T., Hanada, S., Kamagata, Y., Miyaoka, S., Suzuki, T., Nakamura, K., 2000. Micropruina glycogenica gen. nov., sp. nov., a new Gram-positive glycogen-accumulating bacterium isolated from activated sludge. Int. J. Syst. Evol. Microbiol. doi:10.1099/00207713-50-1-201

Skennerton, C.T., Barr, J.J., Slater, F.R., Bond, P.L., Tyson, G.W., 2015. Expanding our view of genomic diversity in *C andidatus* Accumulibacter clades. Environ. Microbiol. 17, 1574–1585. doi:10.1111/1462-2920.12582

Smolders, G.J., van der Meij, J., van Loosdrecht, M.C., Heijnen, J.J., 1994a. Stoichiometric model of the aerobic metabolism of the biological phosphorus removal process. Biotechnol. Bioeng. 44, 837–848. doi:10.1002/bit.260440709

Smolders, G.J., van der Meij, J., van Loosdrecht, M.C., Heijnen, J.J., 1994b. Model of the anaerobic metabolism of the biological phosphorus removal process: Stoichiometry and pH influence. Biotechnol. Bioeng. 43, 461–470. doi:10.1002/bit.260430605

Stokholm-Bjerregaard, M., 2016. Control of GAOs in wastewater treatment plants with enhanced biological phosphorus removal. PhD thesis. Aalborg University, Aalborg, Denmark, Denmark.

Stokholm-Bjerregaard, M., McIlroy, S.J., Nierychlo, M., Karst, S.M., Albertsen, M., Nielsen, P.H., 2017. A critical assessment of the microorganisms proposed to be important to enhanced biological phosphorus removal in full-scale wastewater treatment systems. Front. Microbiol. doi:10.3389/fmicb.2017.00718

Valverde-Pérez, B., Wágner, D.S., Lóránt, B., Gülay, A., Smets, B.F., Plósz, B.G., 2016. Short-sludge age EBPR process – Microbial and biochemical process characterisation during reactor start-up and operation. Water Res. doi:10.1016/j.watres.2016.08.026

Van Loosdrecht, M.C.M., Lopez-Vazquez, C.M., Meijer, S.C.F., Hooijmans, C.M., Brdjanovic, D., 2015. Twenty-five years of ASM1: past, present and future of wastewater treatment modelling. J. Hydroinformatics 17.

Van Veldhuizen, H.M., Van Loosdrecht, M.C.M., Heijnen, J.J., 1999. Modelling biological phosphorus and nitrogen removal in a full scale activated sludge process. Water Res. 33, 3459–3468. doi:10.1016/S0043-1354(99)00064-0

Vargas, M., Yuan, Z., Pijuan, M., 2013. Effect of long-term starvation conditions on polyphosphate- and glycogen-accumulating organisms. Bioresour. Technol. 127, 126–131. doi:10.1016/j.biortech.2012.09.117

Wang, X., Zeng, R.J., Dai, Y., Peng, Y., Yuan, Z., 2008. The denitrification capability of cluster 1 Defluviicoccus vanus-related glycogen-accumulating organisms. Biotechnol. Bioeng. doi:10.1002/bit.21711

Wang, Y., Geng, J., Peng, Y., Wang, C., Guo, G., Liu, S., 2012. A comparison of endogenous processes during anaerobic starvation in anaerobic end sludge and aerobic end sludge from an anaerobic/anoxic/oxic sequencing batch reactor performing denitrifying phosphorus removal. Bioresour. Technol. 104, 19–27. doi:10.1016/j.biortech.2011.09.049

Wang, Y., Zhou, S., Wang, H., Ye, L., Qin, J., Lin, X., 2015. Comparison of endogenous metabolism during long-term anaerobic starvation of nitrite/nitrate cultivated denitrifying phosphorus removal sludges. Water Res. 68, 374–386. doi:10.1016/j.watres.2014.09.044

Wentzel, M.C., Ekama, G.A., Marai, G.V.R., 1992. Processes and modelling of nitrification denitrification biological excess phosphorus removal systems - A review, in: Water Science and Technology. pp. 59–82.

Wu, Linwei, Ning, D., Zhang, B., Li, Y., Zhang, P., Shan, X., Zhang, Qiuting, Brown, Mathew, Li, Z., Van Nostrand, J.D., Ling, F., Xiao, N., Zhang, Ya, Vierheilig, J., Wells, G.F., Yang, Y., Deng, Y., Tu, Q., Wang, A., Acevedo, D., Agullo-Barcelo, M., Alvarez, P.J.J., Alvarez-Cohen, L., Andersen, G.L., de Araujo, J.C., Boehnke, K., Bond, P., Bott, C.B., Bovio, P., Brewster, R.K., Bux, F., Cabezas, A., Cabrol, L., Chen, S., Criddle, C.S., Deng, Y., Etchebehere, C., Ford, A., Frigon, D., Gómez, J.S., Griffin, J.S., Gu, A.Z., Habagil, M., Hale, L., Hardeman, S.D., Harmon, M., Horn, H., Hu, Z., Jauffur, S., Johnson, D.R., Keller, J., Keucken, A., Kumari, S., Leal, C.D., Lebrun, L.A., Lee, J., Lee, M., Lee, Z.M.P., Li, Y., Li, Z., Li, M., Li, X., Ling, F., Liu, Y., Luthy, R.G., Mendonça-Hagler, L.C., de Menezes, F.G.R., Meyers, A.J., Mohebbi, A., Nielsen, P.H., Ning, D., Oehmen, A., Palmer, A., Parameswaran, P., Park, J., Patsch, D., Reginatto, V., de los Reyes, F.L., Rittmann, B.E., Robles, A.N., Rossetti, S., Shan, X., Sidhu, J., Sloan, W.T., Smith, K., de Sousa, O.V., Stahl, D.A., Stephens, K., Tian, R., Tiedje, J.M., Tooker, N.B., Tu, Q., Van Nostrand, J.D., De los Cobos Vasconcelos, D., Vierheilig, J., Wagner, M., Wakelin, S., Wang, A., Wang, B., Weaver, J.E., Wells, G.F., West, S., Wilmes, P., Woo, S.-G., Wu, Linwei, Wu, J.-H., Wu, Liyou, Xi, C., Xiao, N., Xu, M., Yan, T., Yang, Y., Yang, M., Young, M., Yue, H., Zhang, B., Zhang, P., Zhang, Qiuting, Zhang, Ya, Zhang, T., Zhang, Qian, Zhang, W., Zhang, Yu, Zhou, H., Zhou, J., Wen, X., Curtis, T.P., He, Q., He, Z., Brown, Matthew, Zhang, T., He, Z., Keller, J., Nielsen, P.H., Alvarez, P.J.J., Criddle, C.S., Wagner, M., Tiedje, J.M., He, Q., Curtis, T.P., Stahl, D.A., Alvarez-Cohen, L., Rittmann, B.E., Wen, X., Zhou, J., Consortium, G.W.M., 2019. Global diversity and biogeography of bacterial communities in wastewater treatment plants. Nat. Microbiol. doi:10.1038/s41564-019-0426-5

Zeng, R.J., Van Loosdrecht, M.C.M., Yuan, Z., Keller, J., 2003a. Metabolic Model for Glycogen-Accumulating Organisms in Anaerobic/Aerobic Activated Sludge Systems. Biotechnol. Bioeng. 81, 92–105. doi:10.1002/bit.10455

Zeng, R.J., Yuan, Z., Keller, J., 2003b. Enrichment of denitrifying glycogen-accumulating organisms in anaerobic/anoxic activated sludge system. Biotechnol. Bioeng. doi:10.1002/bit.10484

Zeng, W., Zhang, J., Wang, A., Peng, Y., 2016. Denitrifying phosphorus removal from municipal wastewater and dynamics of “Candidatus Accumulibacter” and denitrifying bacteria based on genes of ppk1, narG, nirS and nirK. Bioresour. Technol. 207, 322–331. doi:10.1016/j.biortech.2016.02.016

Zhou, Y., Pijuan, M., Zeng, R.J., Yuan, Z., 2009. Involvement of the TCA cycle in the anaerobic metabolism of polyphosphate accumulating organisms (PAOs). Water Res. 43, 1330–1340. doi:10.1016/j.watres.2008.12.008

4

LONG-TERM SIMULATION OF A FULL-SCALE EBPR WRRF WITH A NOVEL METABOLIC-ASM AND ITS USE AS A DIAGNOSTIC TOOL FOR PLANT UPSETS

SUMMARY:

This study evaluates the predictive capacity of the META-ASM model, a new integrated metabolic activated sludge model, in describing the long-term performance of a full-scale enhanced biological phosphorus removal (EBPR) system that suffers from unpredictable upsets.

In order to elucidate the causes of EBPR upsets and troubleshoot the process accordingly, the META-ASM model was tested as an operational diagnostic tool in a 1336-day long-term dynamic simulation, while its performance was compared with the ASM-inCTRL model, a version based on the Barker & Dold model. Overall, the predictions obtained with the META-ASM without changing default parameters were more reliable and effective at describing the active biomass of polyphosphate accumulating organisms (PAOs) and the dynamics of their storage polymers. The primary causes of the EBPR upsets were the high aerobic hydraulic retention times (HRTs) and low organic loading rates (OLRs) of the plant, which led to periods of starvation. The impact of these factors on EBPR performance were only identified with the META-ASM model. Furthermore, the first signs of process upsets were predicted by variations in the aerobic PAO maintenance rates, suggesting that the META-ASM model has potential to provide an early warning of process upset.

The simulation of two viable scenarios indicated that troubleshooting the process could be achieved by reducing the aerated volume by switching off air in the first half of the aeration tank. In this scenario, the META-ASM model predicted a simultaneous improvement in the biological phosphorus (P) and nitrogen (N) removal due to the enhancement of the hydrolysis and fermentation of the mixed liquor

sludge in the new unaerated zone, which increased the availability of volatile fatty acids (VFAs) for PAOs.

This study demonstrates that the META-ASM model is a powerful operational diagnostic tool for EBPR systems, capable of predicting and mitigating upsets, optimising performance and evaluating new process designs.

KEYWORDS:

Activated sludge models (ASMs), enhanced biological phosphorus removal (EBPR), full-scale water resource recovery facility (WRRF), metabolic modelling, polyphosphate accumulating organisms (PAOs) and process optimisation.

IN PREPARATION:

This work will be submitted to an international peer reviewed scientific journal as: Santos, J.M.M., Martins, A., Barreto, S., Rieger, L., Reis, M.A.M., Oehmen, A., 2020. Long-term simulation of a full-scale EBPR WRRF with a novel metabolic-ASM model and its use as a diagnostic tool for plant upsets.

4.1 Introduction

Enhanced biological phosphorus removal (EBPR) in activated sludge systems is a widely applied process at water resource recovery facilities (WRRFs) that economically and sustainably removes anthropogenic phosphorus (P), to prevent undesirable eutrophication in receiving waters, and potentially increases P recovery from sludge in downstream processes (Yang et al., 2017). Compared to chemical P removal, less sludge is produced and EBPR significantly reduces chemical and sludge disposal costs. The effectiveness of this process relies on the activity of polyphosphate accumulating organisms (PAOs), which grow under alternating anaerobic and aerobic (or anoxic) conditions.

It is known that EBPR plants with various configurations are able to achieve low P effluent levels (below 1 g $P.m^{-3}$) for long periods of time. However, several studies have reported that many of these EBPR facilities suffer from unpredictable upsets that can lead to temporary or even irreversible EBPR loss (Barnard et al., 2012; Barnard and Abraham, 2006; Barnard and Steichen, 2006; Bushee et al., 2019; Gu et al., 2008; Neethling, 2006; Oehmen et al., 2007; Rieger et al., 2001). Examples of factors commonly reported as primary causes of EBPR upsets include: i) influent load dynamics (e.g. periods of limited availability of readily biodegradable chemical oxygen demand, rbCOD, and nutrients); ii) inhibition of fermentation (due to presence of nitrates, nitrites or oxygen in anaerobic zones); iii) competition for substrate in anaerobic zones (e.g. between PAOs and glycogen accumulating organisms, GAOs, or with other denitrifiers if nitrate or nitrite are present); iv) individual or combined effect of selected operational conditions and environmental factors (e.g. high influent soluble $rbCOD_{INF}/P_{Tot,INF}$ ratio, carbon composition, high dissolved oxygen (DO), excessive return activated sludge (RAS) recycle rates, long hydraulic retention times (HRTs) in aerobic tanks and secondary clarifiers, high environmental temperatures, overdosing of metals, etc).

Mitigating a process upset (break-through of phosphate, PO_4-P, in effluent) is difficult, because the trigger for an upset typically happens 1-2 days before elevated P levels are detectable in the effluent. Therefore, in response to an upset event, EBPR facilities often times fall back to chemical P precipitation to meet effluent limits (Bushee et al., 2019). As most upsets are unpredictable due to lack of readily available data, or the data available for process diagnosis and decision-making are of insufficient quality, chemicals are often added constantly and in excess as a corrective measure. Increasing chemical dosage directly and negatively impact EBPR performance due to limited availability of phosphorus. Consequently, the operational costs of these EBPR facilities increase (chemical and sludge disposal costs) and the potential to recover P from sludge is reduced. In fact, only a few parameters useful for process diagnosis are routinely measured through grab or composite samples of influent and effluent, whereas monitoring of biological tanks is usually limited to upset events (Schauer et al., 2018). This is too late to link root cause and effect, due to the very dynamic nature of the EBPR process.

Increasingly stringent regulations for P removal (less than 0.1 $g.m^{-3}$) in some regions (Bunce et al., 2018; Oleszkiewicz and Barnard, 2006) have forced WRRFs with conventional EBPR configurations to i) develop novel strategies to maintain a more stable and consistent long-term EBPR operation and ii) develop early warning operational diagnostic tools for EBPR processes to support decision making in view of plant upsets.

Emerging strategies to improve EBPR stability consist of modifying conventional EBPR configurations by other alternatives that enhance sludge fermentation to overcome the issue of low availability of rbCOD in the influent (Barnard et al., 2017). Some examples described in the literature include upgrading conventional EBPR configurations with one of the following processes (Barnard et al., 2012, 2017; Barnard and Abraham, 2006; Sedlak, 1991; Tooker et al., 2016; Wang et al., 2019): i) fermentation of primary sludge, ii) side-stream fermentation of RAS and iii) mainstream mixed liquor fermentation by either switching off air in a small fraction of a plug-flow aeration tank or by switching off a mixer in an anaerobic zone.

Potential early warning operational diagnostic tools are still under investigation and their use in practice is still very limited. Only a few examples can be found in the literature, which include the use of: i) online PO_4-P analysers and PO_4-P uptake respirometers placed at strategic locations to assess the PO_4-P uptake rate capacity of the mixed liquor sludge, as an indirect measurement of the amount of PHA stored in the biomass (Bushee et al., 2019; Schauer et al., 2018) and ii) predictive models (i.e. more mechanistic) (Santos et al., 2020; Varga et al., 2018). The latter has been suggested to be a promising tool, as it potentially describes in detail the microbial and chemical transformations of different EBPR scenarios and predicts long-term EBPR performance, however, previous studies have not yet investigated if this is indeed the case.

The META-ASM, an integrated metabolic activated sludge model, was described in a previous publication (Santos et al., 2020) as a powerful tool to predict EBPR process behaviour, since it reduces calibration efforts needed for EBPR processes. This model improved various shortcomings of the existing EBPR models by incorporating: the effect of operational conditions on the PAO-GAO competition, the capability of PAOs and GAOs to denitrify, metabolic shifts as a function of storage polymer concentrations as well as the role of these polymers in endogenous processes, and a better description of the fermentation process. Although its effectiveness compared to existing models was successfully demonstrated by describing 34 different data sets from enriched and full-scale sludge, its performance in a long-term dynamic simulation of a full-scale EBPR system was still required to be demonstrated along with its utility as a diagnostic tool to predict EBPR upsets.

Therefore, two models, the META-ASM (Santos et al., 2020) and the ASM-inCTRL model (inCTRL Solutions, Canada), are tested in this study as operational diagnostic tools to predict EBPR instability in a long-term operation of a full-scale 3-stage Phoredox (A2/O) activated sludge system.

These models were chosen because the former was identified previously as a predictive model and the latter is based on the Barker & Dold model (Barker and Dold, 1997), which is still one of the most widely used EBPR models in engineering and implemented in most commercial software available. This work focusses on evaluating whether the structure of these biokinetic models and respective default parameters are capable of providing an early warning of process upsets and a reliable response over a long-term dynamic simulation. Furthermore, process troubleshooting is also performed with the most predictive model in order to offer viable strategies to improve the performance of the WRRF under study.

4.2 Material and methods

4.2.1 Objectives for the WRRF

The Boavista WRRF is located on the Algarve coast, where the flux of population to this region increases in summer due to the typical Portuguese and European vacation period. The objectives for the WRRF are to understand the causes of the EBPR upsets observed during the high season and to develop low cost mitigation solutions, applicable within the boundaries of the existing infrastructure available at the plant. Improving biological P removal to less than 1 g $P.m^{-3}$ without the need for chemical dosing are high priorities.

4.2.2 WRRF description

The Boavista WRRF was designed to serve 33180 population equivalents and has a capacity of 6843 $m^3.d^{-1}$. The biological treatment stage is an A2/O activated sludge process designed with two parallel lanes to remove biochemical oxygen demand (BOD), nitrogen (N) and P biologically. Currently, only one lane is working because the maximum influent flow measured during the high season is about half of the maximum capacity.

Figure 4.1 shows a simplified scheme of the Boavista WRRF, where only one lane is represented in the biological treatment. The preliminary treatment is composed of screening units and processes for the removal of grit, grease and oil. This plant has no primary treatment, and therefore, raw influent wastewater (INF) and reject water (RW) recycled from the sludge line after flow (Q_{INF+RW}) measurement, are directly fed into a plug flow tank. This tank is sequentially divided into anaerobic (R_{AN}), anoxic (R_{AX}) and aerobic (R_{OX}) tanks. The anaerobic and anoxic tanks are physically divided by walls into 2 stirred cells in series.

Aeration is achieved through 312 fine bubble membrane diffusers distributed equally in two grids placed at 0.5 m from the floor of the aerobic tank. The DO is controlled within the range of 0.42-1.0 g $O_2.m^{-3}$ (see DO profile in Figure 4.5). Nitrates and nitrites produced in the aerobic tank are recycled to

the first anoxic cell (R_{AX1}) with a fixed flow ($Q_{ROX-RAX1}$). Chemical P precipitation with a 43% solution of $Fe_2(SO_4)_3$ is applied at the outlet of the aerobic tank whenever the effluent levels of total phosphorus (P_{Tot}) are observed by operators above 3 g $P.m^{-3}$ through lab measurements (see Figure 4.4-B).

Part of the activated sludge settled in the secondary clarifier is returned to the first anaerobic cell via the RAS, with a recycle ratio proportional to the influent flow (Q_{RAS}/Q_{INF}=1.37 ± 0.34). Waste activated sludge (WAS) is concentrated in a thickener. The thickened WAS (TW) is dewatered by two centrifuges and transported from the WRRF. The reject water recovered from the thickening and dewatering process are recycled to the preliminary treatment.

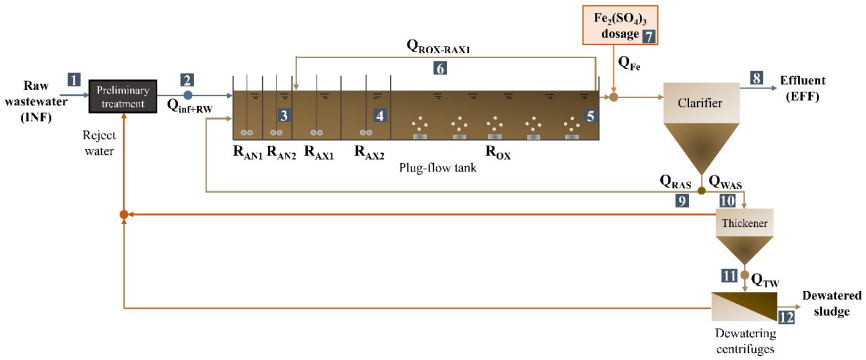

Figure 4.1. Flow scheme of the Boavista WRRF. R_{AN1} and R_{AN2}: anaerobic tank with 2 stirred cells in series; R_{AX1} and R_{AX2}: anoxic tank with 2 stirred cells in series; R_{OX}: aerobic tank; Q_{INF+RW}: influent flow composed of raw wastewater and reject water recycled from thickening and dewatering processes; $Q_{ROX-RAX1}$: internal recycle flow from R_{OX} to R_{AX1}; Q_{Fe}: $Fe_2(SO_4)_3$ dosage flow, Q_{WAS}: waste activated sludge (WAS) flow; Q_{RAS}: return activated sludge flow; Q_{TW}: thickened WAS flow. Numbers indicate locations for sampling or online measurement of the parameters identified in Table B.1 (see Appendix B).

4.2.3 Data collection, analysis and reconciliation

Plant data recorded from January 2012 to August 2015 was collected, analysed and reconciled. Table B.1 (see Appendix B) summarises the input and performance data used in this study and Table 4.1 contains the physical dimensions of each process unit.

Table 4.1. Flow rates and physical data of each process unit.

Flows	Average ± std ($m^3.d^{-1}$)	Process unit	Volume (m^3)	Side water Depth (m)	No. of diffusers
Q_{INF}	1486.82 ± 572.40	Anaerobic tank	360	6.09	-
Q_{RAS}	1948.16 ± 656.23	-Cell (R_{AN1})	180	6.09	-
Q_{WAS}	87.90 ± 48.91	-Cell (R_{AN2})	180	6.09	-
Q_{TW}	11.76 ± 10.71	Anoxic tank	600	6.00	-
$Q_{ROX-RAX1}$	8640.00	-Cell (R_{AX1})	300	6.00	-
		-Cell (R_{AX2})	300	6.00	-
		Aerobic tank	3000	6.00	312 (156 per grid)
		Secondary clarifier	1130	2.50	-
		Thickener	222.7	3.50	-

Figure 4.2, 4.3, 4.4-A, 4.4-B and 4.4-C show the dynamics and average values of the: influent $COD_{Tot,INF}$, $N_{Tot,INF}$ and $P_{Tot,INF}$ loads, HRTs of the anaerobic, anoxic and aerobic tanks, sludge retention time (SRT), metal dosage and temperature in the aerobic tank, respectively. The influent loading of the plant varies according to the typical pattern of population influx in the region, where the highest mass loads were commonly obtained in warmer months (high season) and the lowest mass loads were commonly obtained in cooler months (low season). These loading dynamics have been impacting the operational conditions of the plant (SRT and HRT of the anaerobic, anoxic and aerobic tanks) and affecting the resulting EBPR performance. Figure 4.4-B shows that metal dosing was always increased in the high seasons, suggesting that EBPR upsets may have occurred in these months. The variations of pH in the influent (7.46 ± 0.21) and effluent (7.59 ± 0.29) were very low.

Faults were detected and removed in the input and performance data by following the recommendations of the IWA Guidelines for Using Activated Sludge Models (Rieger et al., 2012). Briefly, outliers and gross errors were detected and removed after: 1) visualisation of data (flows, concentrations and mass loads) in time series plots; 2) analysis of descriptive statistics (averages, median, maximum, minimum and standard deviations) of data grouped by year and seasons (e.g. high and low); 3) checking simple relationships in data (e.g. N_{Tot}>NH_x-N, P_{Tot}>PO_4-P, COD_{Tot}>BOD_5, TSS>VSS and $MLSS_{RAS}$>MLSS R_{OX}); 4) comparison of raw wastewater influent ($N_{Tot,INF}/COD_{Tot,INF}$; $P_{Tot,INF}/COD_{Tot,INF}$; $COD_{Tot,INF}/BOD_{5,Tot,INF}$ and $TSS_{INF}/COD_{Tot,INF}$) and activated sludge ratios (COD_{Tot} R_{OX}/MLVSS R_{OX}) of the plant under study with a typical range of ratios found in municipal WRRFs (Rieger et al., 2012) and 5) overlapping mass balances on total suspended solids (TSS) and COD.

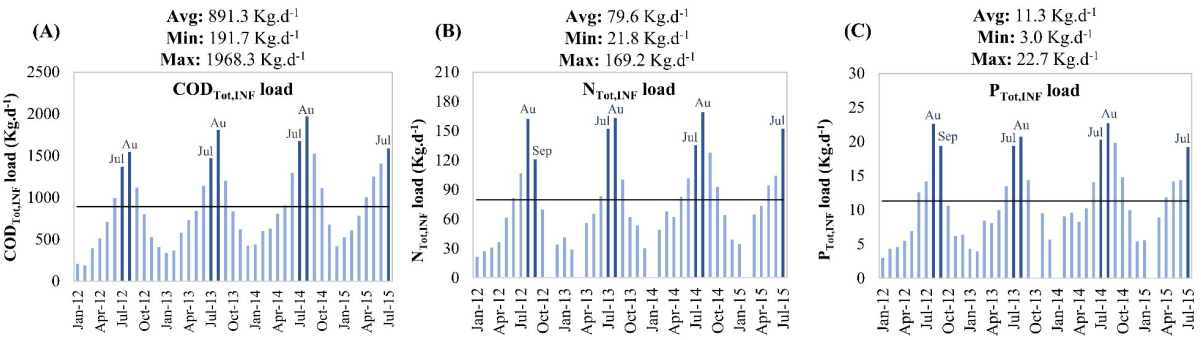

Figure 4.2. Influent $COD_{Tot,INF}$ (A), $N_{Tot,INF}$ (B), $P_{Tot,INF}$ (C) loading dynamics. Dark bars highlight the two months with the highest loads and line marks represent the average values.

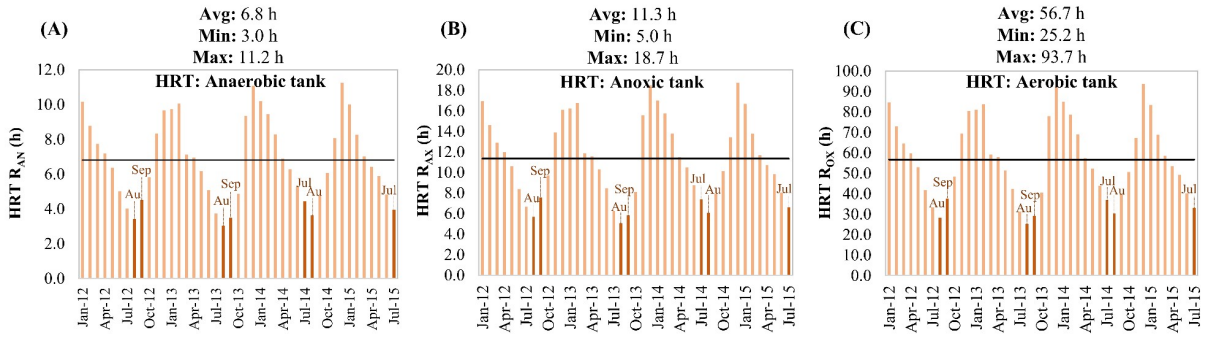

Figure 4.3. HRT dynamics of the anaerobic (A), anoxic (B) and aerobic (C) tanks. Dark bars highlight the two months with the lowest HRTs and line marks represent the average values.

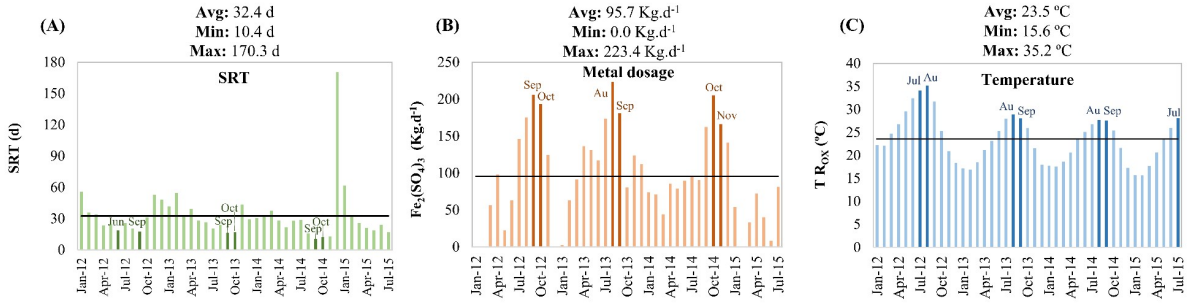

Figure 4.4. Dynamics of the SRT (A), metal dosage (B) and temperature (C). Dark bars highlight the two months with the lowest SRTs, the highest metal dosage and the highest temperature. Line marks represent the average values.

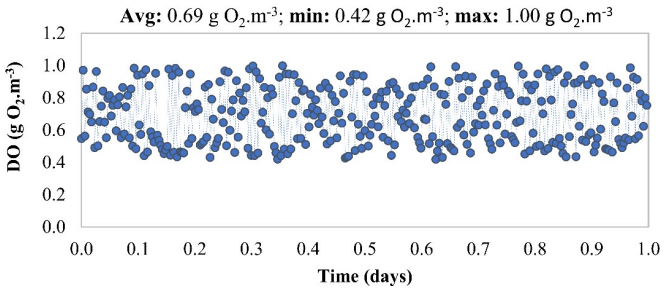

Figure 4.5. Diurnal variations of the DO in the aerobic tank.

4.2.4 Plant model setup

Two plant models differing only in the biokinetic models chosen to simulate the EBPR dynamics of the Boavista WRRF were set-up in SIMBA# (ifak, Germany) according to the flow scheme depicted in Figure 4.1**.** The biokinetic models META-ASM (Santos et al., 2020) and ASM-inCTRL (inCTRL Solutions, Canada) were chosen for this study.

The META-ASM is a novel integrated metabolic activated sludge model capable of predicting EBPR performance with a robust single set of default parameters (Santos et al., 2020) and was developed to overcome various shortcomings of existing EBPR models. Readers are referred to Santos et al. (2020) for a more detailed description of the META-ASM model. Briefly, this model incorporates the effect of operational conditions on the competition between PAOs and GAOs and their capability to denitrify, the metabolic shifts of PAOs/GAOs as a function of storage polymer concentrations, the role of storage polymers in endogenous processes, and a more detailed description of the fermentation process.

The ASM-inCTRL model (inCTRL Solutions, Canada) is a version based on the Barker & Dold model (Barker and Dold, 1997) (hereafter referred to as updated Barker & Dold model), which differs from the original in the description of the following processes: denitrification of ordinary heterotrophic organisms (OHOs) and PAOs as well as nitrification were modelled in two-steps and the endogenous processes of OHOs, ammonia oxidizing organisms (AOOs) and nitrite oxidizing organisms (NOOs) were modelled as a function of the electron acceptors. This version was chosen because the Barker & Dold model is still one of the most widely used EBPR models in practice and most commercial software available has these modifications implemented in their updated Barker & Dold models.

Each plant model was built as follows. The anaerobic and anoxic cells were modelled as a single continuous stirred tank reactor (CSTR), and the aerobic tank was split evenly into two CSTRs, each one with one grid containing 156 fine bubble membrane diffusers. The secondary clarifier was modelled as an ideal separator with volume (sludge blanket and clear water zone), where the TSS of the effluent was determined as a fraction (var_1) of the mixed liquor suspended solids (MLSS) of the aerobic tank. In addition, the biokinetic models were also activated at the top and bottom layers of the clarifier to describe the commonly observed biological reactions. The thickener was modelled as a point clarifier model, where TSS of the reject water was determined as a fraction (var_2) of TSS of the thickened WAS. The fractions var1 and var2 were defined based on the average values determined in the period under study (var1=0.154/100 and var2=7.060/100). The dewatering centrifuge was modelled by setting the final sludge TSS concentration and the efficiency of sludge removal from fluid flow with their average measured values of 162.256 $kg.m^3$ and 0.97, respectively. Influent models were configured to convert the influent daily average values of Q_{INF}, $COD_{Tot,INF}$, $N_{Tot,INF}$, $P_{Tot,INF}$ and inorganic suspended solids (ISS_{INF}) into state variables of the biokinetic models under study (see section 4.2.5). The Q_{RAS}, Q_{WAS} and Q_{TW} were set to the daily average flows measured (see Table 4.1). Furthermore, a typical DO profile

ranging from 0.42 to 1.00 g O_2 m^{-3} was used to control aeration (see Figure 4.5). The dosage of $Fe_2(SO_4)_3$ was not configured in both plant models due to the fact that chemical precipitation processes are described with very simple mathematical formulations in the selected biokinetic models (as in the ASM2d model). Although many studies have recently developed new precipitation models (Barat et al., 2011; Kazadi Mbamba et al., 2015; Solon et al., 2017), their integration into the selected biokinetic models was considered beyond the scope of this study.

4.2.5 Influent characterisation and definition of initial conditions

A week-long sampling campaign (from 15th to 22nd June 2015) was performed at the influent and effluent (see sampling locations nr. 1 and 8, respectively in Figure 4.1). This campaign aimed to collect additional data needed to complete the fractionation of the influent during the period under study and to develop influent models capable of converting measurements into model state variables.

The recommendations of the IWA Guidelines for Using Activated Sludge Models (Rieger et al., 2012) were followed to build the influent models. Table 4.2 summarises the average values of the parameters measured over the period under study, as well as the result of their conversion into state variables of META-ASM and updated Barker & Dold models.

The initial concentrations of the particulate variables in both plant models were defined with the values obtained after a 1336 day steady-state simulation and a 300 day dynamic simulation.

Table 4.2. Measurements needed for the characterisation of the influent and state variables of the META-ASM and ASM-inCTRL models.

Measurements		META-ASM				ASM-inCTRL			
	Average ± std	State variables	Value	State variables	Value	State variables	Value	State variables	Value
Influent		S_{O2} (g O_2.m^{-3})	1.00E-04	C_B (g COD.m^{-3})	104.41	S_{O2} (g O_2.m^{-3})	1.00E-04	X_B (g COD.m^{-3})	159.68
COD_{Tot} (g COD.m^{-3}) [a]	532.26 ± 157.20	S_F (g COD.m^{-3})	93.94	X_B (g COD.m^{-3})	159.68	S_F (g COD.m^{-3})	93.94	$X_{B,N}$ (g N.m^{-3})	1.60
COD_{Sol} (g COD.m^{-3}) [b]	140.60 ± 6.32	$S_{F,N}$ (g N.m^{-3})	0.94	$X_{B,N}$ (g N.m^{-3})	1.60	$S_{F,N}$ (g N.m^{-3})	0.94	$X_{B,P}$ (g P.m^{-3})	0.48
VFAs (g COD.m^{-3}) [b]	23.00	$S_{F,P}$ (g P.m^{-3})	0.75	$X_{B,P}$ (g P.m^{-3})	0.48	$S_{F,P}$ (g P.m^{-3})	0.75	X_E (g COD.m^{-3})	0.53
-Acetate + butyrate (g COD.m^{-3}) [b]	20.91	S_{Ac} (g COD.m^{-3})	20.91	X_E (g COD.m^{-3})	0.53	S_{VFA} (g COD.m^{-3})	23.00	X_{IG} (g TSS.m^{-3})	90.86
-Propionate + valerate (g COD.m^{-3}) [b]	2.09	S_{Pr} (g COD.m^{-3})	2.09	X_{IG} (g TSS.m^{-3})	90.86	S_U (g COD.m^{-3})	23.66	X_{OHO} (g COD.m^{-3})	53.23
$BOD_{5,Tot}$ (g COD.m^{-3}) [a]	309.36 ± 112.45	S_U (g COD.m^{-3})	23.66	X_{OHO} (g COD.m^{-3})	53.23	$S_{U,N}$ (g N.m^{-3})	0.24	X_{AOO} (g COD.m^{-3})	0.89
$BOD_{5,Sol}$ (g COD.m^{-3}) [b]	154.68 ± 10.95	$S_{U,N}$ (g N.m^{-3})	0.24	X_{AOO} (g COD.m^{-3})	0.53	$S_{U,P}$ (g P.m^{-3})	0.00	X_{NOO} (g COD.m^{-3})	0.89
N_{Tot} (g N.m^{-3}) [a]	47.68 ± 10.99	$S_{U,P}$ (g P.m^{-3})	0.00	X_{NOO} (g COD.m^{-3})	0.53	S_{NHx} (g N.m^{-3})	39.03	X_{PAO} (g COD.m^{-3})	0.89
NH_x-N (g N.m^{-3}) [b]	39.03 ± 3.02	S_{NHx} (g N.m^{-3})	39.03	X_{PAO} (g COD.m^{-3})	0.53	S_{NO3} (g N.m^{-3})	0.03	$X_{PAO,PHA}$ (g COD.m^{-3})	0.09
NO_3-N (g N.m^{-3}) [b]	0.03	S_{NO3} (g N.m^{-3})	0.03	X_{CPO} (g COD.m^{-3})	0.53	S_{NO2} (g N.m^{-3})	0.02	$X_{PP,Lo}$ (g P.m^{-3})	0.01
NO_2-N (g N.m^{-3}) [b]	0.02	S_{NO2} (g N.m^{-3})	0.02	X_{DFO} (g COD.m^{-3})	0.53	S_{N2} (g N.m^{-3})	1.00E-04	$X_{PP,Hi}$ (g P.m^{-3})	0.01
P_{Tot} (g P.m^{-3}) [a]	6.83 ± 1.51	S_{N2} (g N.m^{-3})	1.00E-04	$X_{PAO,PHA}$ (g COD.m^{-3})	0.05	S_{PO4} (g P.m^{-3})	4.36		
PO_4-P (g P.m^{-3}) [b]	4.36 ± 0.39	S_{H2} (g H.m^{-3})	1.00E-04	$X_{CPO,PHA}$ (g COD.m^{-3})	0.05	S_{Alk} (mol HCO_3^-.m^{-3})[c]	5.04		
TSS (g TSS.m^{-3}) [a]	266.81 ± 82.18	S_{PO4} (g P.m^{-3})	4.36	$X_{DFO,PHA}$ (g COD.m^{-3})	0.05	C_U (g COD.m^{-3})	21.12		
VSS (g VSS.m^{-3}) [c]	170.00	S_{Alk} (mol.m^3)	5.04	$X_{PAO,PP}$ (g P.m^{-3})	0.01	X_U (g COD.m^{-3})	49.94		
Alkalinity (mol HCO_3^-.m^{-3})[c]	5.04	C_U (g COD.m^{-3})	21.12	$X_{PAO,Gly}$ (g COD.m^{-3})	0.05	$X_{U,N}$ (g N.m^{-3})	0.75		
Effluent		X_U (g COD.m^{-3})	49.71	$X_{CPO,Gly}$ (g COD.m^{-3})	0.05	$X_{U,P}$ (g P.m^{-3})	0.15		
COD_{Sol} (g COD.m^{-3}) [b]	25.16 ± 2.71	$X_{U,N}$ (g N.m^{-3})	0.75	$X_{DFO,Gly}$ (g COD.m^{-3})	0.05	C_B (g COD.m^{-3})	104.41		
		$X_{U,P}$ (g P.m^{-3})	0.15						

[a] Measurements from January 2012 to August 2015; [b] measurements from a week-long sampling campaign (15th to 22nd June 2015); [c] assumed from typical range of ratios/ measurements found in municipal WRRFs.

4.2.6 Simulation studies

4.2.6.1 Model evaluation and prediction of EBPR upsets

A 1336-day long-term dynamic simulation was performed using the two plant models described in section 4.2.4 without changing any default parameters in the biokinetic models. The predictive power of the models was assessed by plotting the predicted and observed data of PO_4-P R_{AN2}, PO_4-P R_{OX}, mixed liquor volatile suspended solids (MLVSS R_{OX}) and COD_{Tot} R_{OX} in time series plots (see section 4.3.1). The capability of these two models to predict the causes for the EBPR upsets observed in the Boavista WRRF was also assessed in this simulation (see section 4.3.2).

4.2.6.2 Mitigation of EBPR upsets

The mitigation of the identified EBPR upsets was performed through two scenarios described in Table 4.3. Each scenario was designed with the aim of using existing infrastructure to improve biological P removal to less than 1 g $P.m^{-3}$ from September 2014 to August 2015 without the need for chemical dosing.

Table 4.3. Description of scenarios for the optimisation of the EBPR process.

Scenario	Modification [a]
1	Existing aerobic tank was split evenly into two CSTRs in series, one unaerated and the other aerated.
2	$Q_{ROX-RAX1}$ is controlled as a function of Q_{INF}.

[a] Implemented to the plant model setup described in section 4.2.4.

In order to compare the impact of each scenario with the historical operation simulated in section 4.2.6.1, the same input data and strategy for the definition of initial model concentrations described in sections 4.2.3 and 4.2.5, respectively, were used. The plant model setup described in section 4.2.4, using the META-ASM as a biokinetic model, was modified as follows. In the 1st scenario, the existing aerobic tank (with a HRT of 55.7 h ± 18.8 h) was split evenly into two CSTRs in series, one unaerated and the other aerated, due to the fact that the first grid of 156 air diffusors can be turned off. This modification reduced the previous HRT to 27.8 h ± 9.4 h in each new unaerated and aerated zone, respectively. The effect of changing the recycle of nitrates and nitrites, $Q_{ROX-RAX1}$, as a function of Q_{INF} and the ratio of aerobic to anoxic tank volumes [$Q_{ROx-RAX1}$= (Volume R_{OX}/Volume R_{AX}).Q_{INF}] was assessed in scenario 2.

4.3 Results and discussion

4.3.1 Model evaluation

A model is considered predictive and robust when it is capable to describe in detail the microbial and chemical transformations with minimal adjustment to parameters. These features were assessed in

this study by performing a 1336-day long-term dynamic simulation with the two plant models without changing any stoichiometric and kinetic default parameters in the selected biokinetic models. The goal was to determine the capacity of each model to predict the EBPR behaviour independently of a calibration procedure. It should be noted that the default parameters of the META-ASM model were calibrated and validated in previous work based on 34 data sets originating from other studies (Santos et al. 2020), but the effectiveness of these parameters to describe the long-term dynamics at a full-scale EBPR plant had not been performed.

Figure 4.6 shows that the average difference between model predictions and observed PO_4-P R_{AN2}, PO_4-P R_{OX}, COD_{Tot} R_{OX} and MLVSS R_{OX} in the period under study was +3.05 g $P.m^{-3}$, +0.31 g $P.m^{-3}$, +17.90% and +5.53% in the META-ASM model, respectively, and were +10.33 g $P.m^{-3}$, +0.97 g $P.m^{-3}$, -40.34% and -43.79% in the updated Barker & Dold model, respectively. Thus, the model performance of the META-ASM model showed significant improvement with respect to the description of each variable. The poor predictions of COD_{Tot} R_{OX} and MLVSS R_{OX} obtained with the latter model may suggest that this model fails to describe the active biomass and storage polymer concentrations, as will be discussed in section 4.3.2. Although deviations in PO_4-P were more significant in the updated Barker & Dold model, both models overpredicted the PO_4-P R_{AN2} and slightly overpredicted the PO_4-P R_{OX} concentrations. However, it should be noted that these simulations did not take into account the effect of $Fe_2(SO_4)_3$ dosage at the outlet of the aerobic tank. In fact, adding high doses of metals can contribute to the reduction of EBPR performance because available metals compete with PAOs for the soluble PO_4-P, since they are recirculated in RAS to the anaerobic zone. This competition over a long-term means that less polyphosphate is stored by PAOs and used as a source of energy for the consumption of VFAs, which explains the overpredictions of PO_4-P R_{AN2} obtained in both models.

Despite the deviations in the prediction of PO_4-P R_{AN2} caused by the dosing of chemical precipitants, Figure 4.6 highlights that the predictions obtained with the META-ASM model in the anaerobic and aerobic tanks are more reliable than those obtained with the updated Barker & Dold model. This result supports the hypothesis that the META-ASM model reduces the requirement for model calibration efforts.

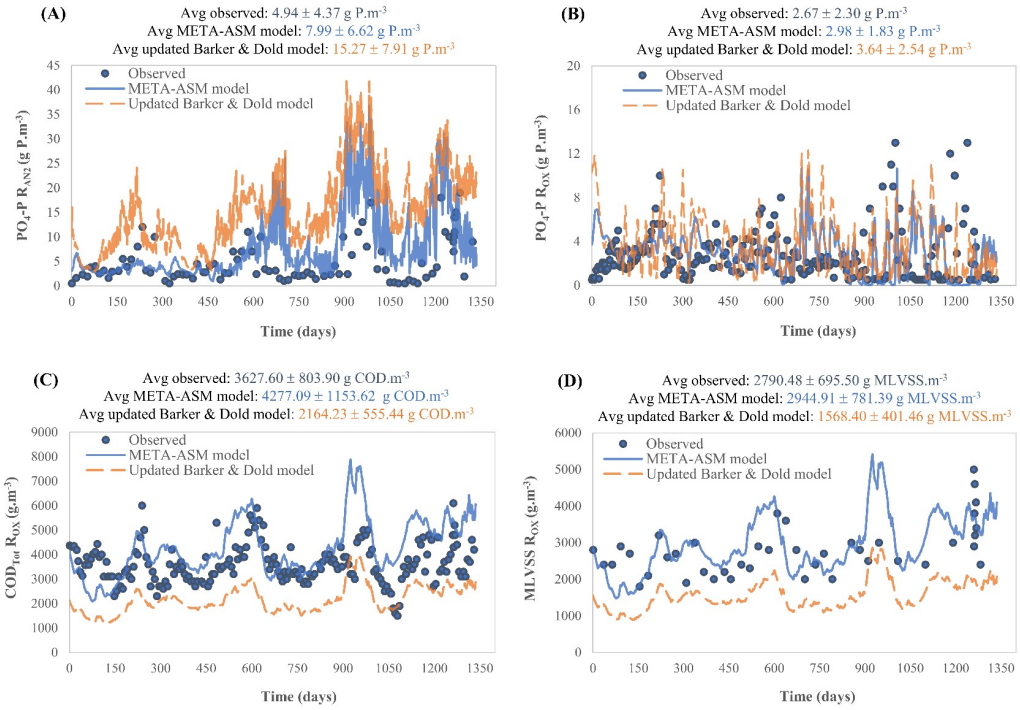

Figure 4.6. Observed and simulated data by META-ASM and updated Barker & Dold models without changing default parameters. (A) PO_4-P R_{AN2}; (B) PO_4-P R_{OX}, (C) COD_{Tot} R_{OX} and (D) MLVSS R_{OX}.

4.3.2 Prediction of EBPR upsets

Model predictions and observed data show the occurrence of break-throughs of PO_4-P in the aerobic tank (see Figure 4.6-B). As a corrective measure, the plant needed to increase chemical dosage at the outlet of the aerobic tank (see Figure 4.4-B), especially during the high seasons (warmer months).

The high temperatures observed in high seasons (see Figure 4.4-C) and the rapid increase of influent loads observed in the transition from low to high seasons (see Figure 4.2), accompanied by the decrease of the HRTs in the biological tanks (see Figure 4.3), appears to each have an impact on the microbial dynamics and EBPR performance. Due to the combined influence of these factors, the reasons for EBPR deterioration in high seasons were not clear, with potential reasons including the growth of GAOs, the metabolic shifts as a function of storage polymer concentrations and the role of these polymers in endogenous processes. Thus, both plant models were used to elucidate the causes for the EBPR upsets observed in the Boavista WRRF and the combined impact of all individual factors on the overall process.

Figure 4.7-A shows that the predicted percentage of PAOs and GAOs per total active biomass throughout the 1336 days averaged 2.1% and 0.5% with the META-ASM model, respectively. Different predictions were obtained with the updated Barker & Dold model, where PAOs averaged 15.1% (Figure 4.7-B) and GAOs are not described by this model. However, the predictions obtained with the META-ASM are in the same range as the microbial characterisation performed by Lanham et al. (2013) on this plant using quantitative fluorescence *in situ* hybridisation (qFISH). The authors observed that the percentages of *Accumulibacter* PAOs and *Competibacter-lineage* plus *Defluviicoccus vanus* GAOs were 3.2% and 0.3%, respectively. In addition, the observed percentage of *Accumulibacter* PAOs and predicted by the META-ASM model are also within the range of values observed in other microbial characterisation studies at full-scale EBPR plants (Stokholm-Bjerregaard et al., 2017; Wu et al., 2019). These results suggest that the updated Barker & Dold model overpredicts the activity of PAOs.

Several studies (Lopez-Vazquez et al., 2009a, 2009b; Panswad et al., 2003; Ren et al., 2011; Whang and Park, 2006) have shown that high temperatures can be detrimental to EBPR due to the fact that GAOs have kinetic advantages over PAOs at high temperatures. However, the model predictions demonstrated that GAOs had a residual impact at the Boavista WRRF, even in summer where temperatures were above 28 ºC. This might suggest that other operational conditions are exerting a higher selective pressure in favour of PAOs than the high temperature exerts in favour of GAOs, as reported in some studies and elucidated further with the META-ASM model (Qiu et al., 2019; Shen et al., 2017).

Figure 4.7 also confirms that the activity of PAOs increased in the high seasons and decreased in the low seasons, which correlates with the oscillations described in the influent loading, HRT, temperature and anaerobic PO_4-P release depicted in Figure 4.2, 4.3, 4.4 and 4.6-A, respectively.

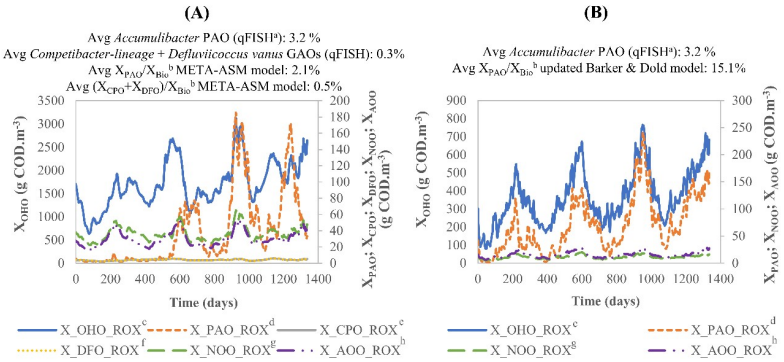

Figure 4.7. Simulated active biomass in the aerobic tank with the META-ASM model (A) and updated Barker & Dold model (B). [a] Quantitative fluorescence *in situ* hybridisation; [b] total active biomass; [c] ordinary heterotrophic organisms; [d] *Accumulibacter* PAOs; [e] *Competibacter*-lineage GAOs; [f] *Defluviicoccus* genus GAOs; [g] nitrite oxidizing organisms; [h] ammonia oxidizing organisms.

Figure 4.8 confirms that the preferred pathways for the origin of reducing power in the anaerobic metabolism of PAOs were the tricarboxylic acid (TCA) cycle, for the uptake of acetate and butyrate, and the conversion of propionyl-CoA to acetyl-CoA, for the uptake of propionate and valerate. The use of these pathways by PAOs is common in full-scale EBPR plants with low influent volatile fatty acid (VFA) concentrations and long aerobic retention times (Cokro et al., 2017; Lanham et al., 2013; Zhou et al., 2009). In this plant, the estimated VFA concentration in the influent and the aerobic HRT averaged 23.0 mg ± 6.8 g COD.m^{-3} and 56.7 ± 19.3 h, respectively, which led to a low replenishment of the glycogen pools in PAOs and to a limited reducing power for the conversion of VFAs to PHA via the glycolysis pathway. In these situations, PAOs tend to shift their metabolism to alternative pathways as survival strategy that favours the competition of PAOs over GAOs (Santos et al., 2020), since the origin of reducing power and energy in the latter comes essentially from the glycolysis pathway (Oehmen et al., 2010). The META-ASM model is the only EBPR model capable of describing this metabolic shift and elucidating that this competitive advantage of PAOs may also contribute to the reduction of the EBPR efficiency, because in both alternative pathways more PO_4-P is released and less PHA is produced under anaerobic conditions (Santos et al., 2020). This means that less PHA is available for the removal of PO_4-P under anoxic and aerobic conditions.

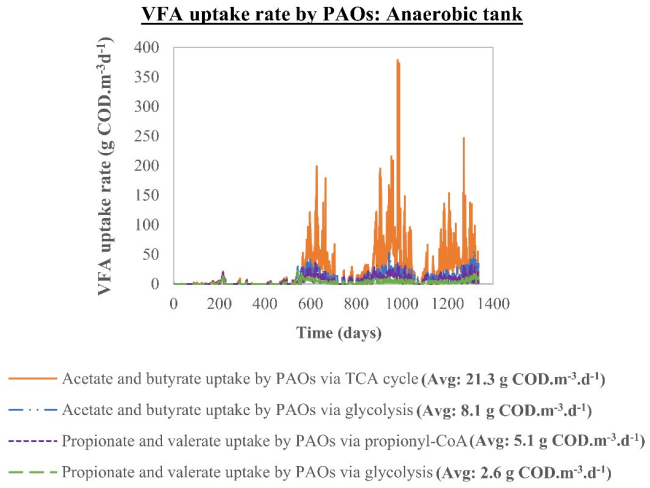

Figure 4.8. Simulated VFA uptake rate in anaerobic tank with META-ASM model.

In addition, the simulation of the PAOs endogenous rates in the aerobic tank with the META-ASM shows that the maintenance rate on PHA increased with the concentration of PAOs, while the maintenance rate on polyphosphate increased when the PHA rate decreased (see Figure 4.9-A). The application of the META-ASM suggests that PAOs are depleting their PHA pools, which limits simultaneously their growth, production of polyphosphate (and PO_4-P uptake) and maintenance on PHA. As a survival strategy to the high aerobic HRTs and low organic loading rate (OLR) conditions, especially observed in the transition from high to low seasons, PAOs consume stored polyphosphate as a source of energy prior to decay. In fact, the META-ASM predictions showed that the increase of the maintenance rate on polyphosphate is accompanied with the increase of PO_4-P R_{OX} concentrations in the aerobic tank, where concentrations higher than 3 mg $P.L^{-1}$ were achieved in certain periods, as illustrated in Figure 4.9 (A) at 693, 1007 and 1120 days. The same conclusions cannot be drawn with the simulation of the endogenous rates with the updated Barker & Dold (see Figure 4.9-B). This model explains the increase of PO_4-P R_{OX} concentration at 1007 days with the simultaneous reduction of the aerobic decay of PAO and lysis of releasable stored polyphosphate (PP_{Lo}), which happens due to the simultaneous decrease of PAOs active biomass and PP_{Lo}, respectively, occurring when no more PHA is available for their growth and production of polyphosphate (and PO_4-P uptake). However, this correlation was only established with the information obtained with the META-ASM model. By itself, the updated Barker & Dold model (Figure 4.9-B) did not show a clear correlation between the increase of PO_4-P R_{OX} concentrations in the aerobic tank and the reduction of PAO endogenous rates. Furthermore, the mechanisms described by the updated Barker & Dold are not supported by previous

experimental evidence (Carvalheira et al., 2014; Lanham et al., 2014; Liu et al., 2017; Lu et al., 2007; Vargas et al., 2013), since PAOs appear to deplete their PHA and polyphosphate storage polymers prior to decay (as well as glycogen when it is available).

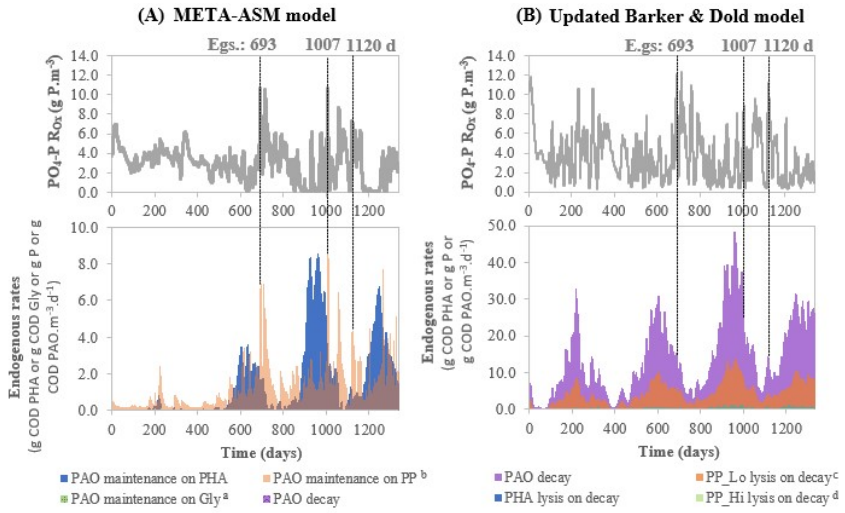

Figure 4.9. Simulated endogenous rates and PO_4-P_{ROX} in aerobic tank with META-ASM model (A) and updated Barker & Dold model (B). [a] Glycogen, [b] Polyphosphate, [c] releasable stored polyphosphate and [d] non-releasable stored polyphosphate.

Figure 4.10 also shows that the META-ASM can be used as an operational diagnostic tool capable of providing ~10 days of early warning of process upsets by predicting the variations in aerobic PAO maintenance rates. As shown, the maintenance on PHA began to decrease at 990 days when the PO_4-P R_{OX} concentration in the aerobic tank was still below 3 g $P.m^{-3}$. This maintenance rate reached minimum values at 1007 days, while the maintenance rate on polyphosphate and the concentration of PO_4-P reached maximum values. As the maintenance rate on PHA increased again (> 1007 days), meaning that PHA is available for PAO growth and production of polyphosphate (and PO_4-P uptake), the maintenance rate on polyphosphate and the PO_4-P R_{OX} concentration decreased.

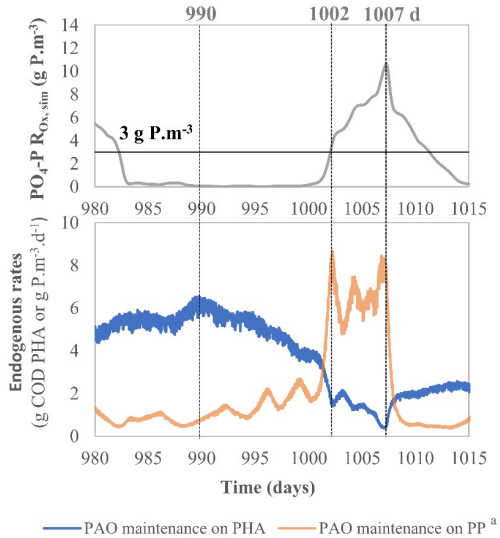

Figure 4.10. Early warning of process upset predicted with the META-ASM model.
[a] Polyphosphate.

Interestingly, Bushee et al. (2019) were also capable of providing about 10 days of early warning of process upsets by using information obtained from online PO_4-P analysers placed at the end of the anaerobic zone and the middle of the aerobic zone, and a PO_4-P uptake respirometer placed at the end of the anaerobic zone. The authors concluded that the system was moving toward instability when the PO_4-P uptake rate capacity of the mixed liquor sludge decreased. Similarly, they correlated the occurrence of an upset with the reduction of the amount of PHA stored in the biomass.

This study demonstrates the causes associated with high aerobic HRT and low OLRs were only possible to be identified with the application of the META-ASM model. This model predicted that in this plant more PO_4-P and less PHA is produced per VFA uptake under anaerobic conditions and that PAOs are depleting their PHA pools and consuming polyphosphate as a survival strategy under aerobic conditions. Therefore, the META-ASM model is a more powerful operational diagnostic tool to predict EBPR instability, allowing the development of mitigation strategies for the upsets identified in this plant.

4.3.3 Mitigation of EBPR upsets

The two scenarios described in Table 4.3 were designed to troubleshoot the EBPR upsets identified in the EBPR plant and mitigate their causes. The aim was to assess strategies, applicable within the boundaries of the existing infrastructure available at the plant, that improve biological P removal to less than 1 g $P.m^{-3}$ without the need for chemical dosing. The modifications implemented were specifically

designed to: reduce the observed consumption of polyphosphate caused by high aerobic HRTs (scenario 1), and enhance denitrification and prevent the recirculation of nitrates and nitrites to the anaerobic zone through the RAS (scenario 2). The impact of each scenario was compared with the historical operation simulated in section 4.2.6.1 (referred to as the base scenario hereafter), using the same influent characteristics and dynamics from September 2014 to August 2015.Figure 4.11-A compares the PO_4-P_{ROX} predictions at the aerobic tank outlet obtained in each simulated scenario. It can be observed that scenario 1 was the most efficient, where residual PO_4-P R_{OX} concentrations ($0.1 \pm 3.0E\text{-}02$ g $P.m^{-3}$) were continuously reached, while scenario 2 did not provide significant process improvements. In addition, Figure 4.11-B shows that scenario 1 also improved the removal of N (5.7 ± 0.6 g $N_{Tot,EFF}.m^{-3}$ compared to the 16.6 ± 1.7 g $N_{Tot,EFF}.m^{-3}$ predicted in the base scenario).

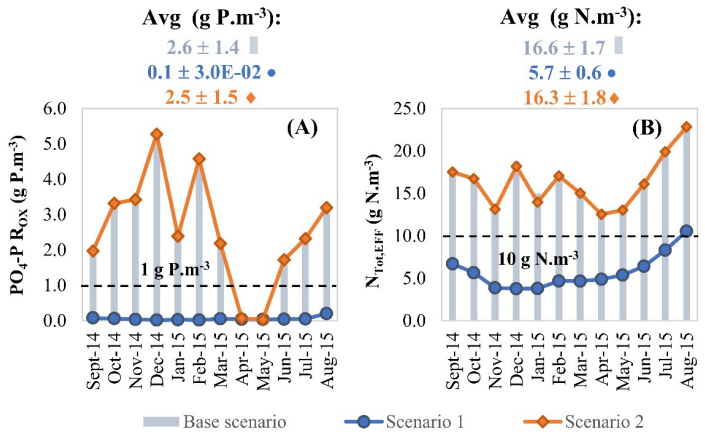

Figure 4.11. PO_4-P R_{OX} concentration at the aerobic tank outlet (A) and $N_{Tot,EFF}$ concentration in the effluent (B) predicted by the META-ASM model in each simulated scenario. The base scenario corresponds to the historical operation simulated in section 4.2.6.1.

The reasons for the simultaneous improvement of P and N removal in scenario 1 compared to the base scenario were elucidated with the META-ASM model. Switching off air in the first half of the existing aerobic tank created an unaerated zone with an average HRT of 27.8 h. Figure 4.12-A and B show that alternating anoxic and anaerobic conditions were created in this zone, leading to the production of VFAs through fermentation with an average rate of 17.5 g $COD.m^{-3}.d^{-1}$. PAOs were able to consume 41.6% of these VFAs, while the remaining fraction was consumed by denitrifying OHOs. The uptake of VFAs by PAOs in the additional unaerated zone corresponded to 11.4% of the VFAs consumed in the existing anaerobic tank (R_{AN2}). These conditions increased the average percentage of PAOs per total active biomass from 3.4% to 13.1% (see Figure 4.12-C) and increased the average total PHA at the aerobic tank outlet from 1.0 g $COD.m^{-3}$ to 5.7 g $COD.m^{-3}$ (see Figure 4.12-D) in the base

scenario and scenario 1, respectively, reducing the risk of PAOs depleting their PHA pools under aerobic conditions (and consuming polyphosphate). In fact, the alternating anoxic and anaerobic conditions in the unaerated zone maintained the PHA pools in PAOs constant during the HRT of 27.8 h. The META-ASM model predicted that only an average of 0.4 g $COD.m^{-3}$ and 0.6 g P m^{-3} were consumed and released during this period, respectively, which means that PAOs had enough PHA storage to remove all PO_4-P in the aerated zone. The removal of N was improved due to increased activity of denitrifying PAOs in the anoxic tank, since the activity of denitrifying OHOs remained similar to that of the base scenario (see Figure 4.12-E and F, respectively).

The results obtained in scenario 1 are also in line with those reported in Sedlak (1991), where biological P removal was successfully achieved and maintained below 0.6 g $P.m^{-3}$ over a period of three years at the Reedy Creek plant in Florida when aeration was switched off in the first half of the first pass of a plug-flow nitrifying plant. Similarly, N removal was also improved with this modification.

Overall, the implementation of scenario 1 compared to the base scenario has the potential to save the costs equivalent to 35.85 ton $Fe_2(SO_4)_3$/year. This value was estimated based on the amount of chemicals added to the process from September 2014 to August 2015, in order to comply with legislation limits. Moreover, scenario 1 would also be likely to decrease the total aeration demand of the WRRF.

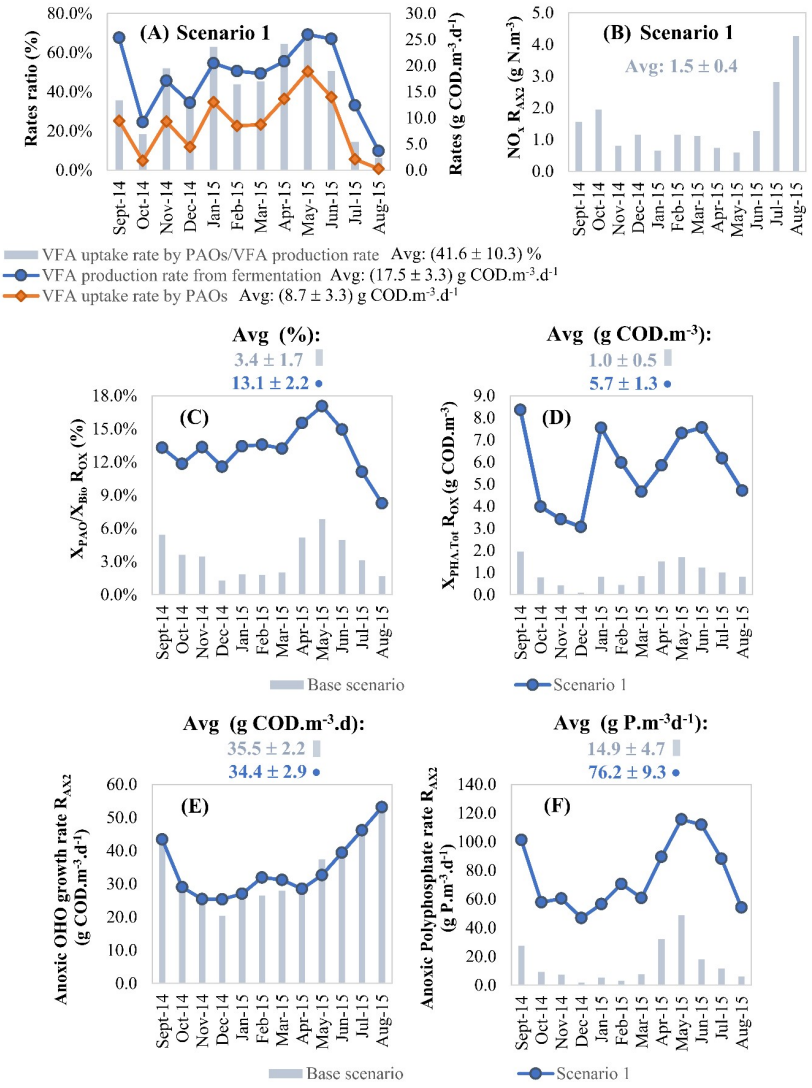

Figure 4.12. Differences between scenario 1 and base scenario predicted by the META-ASM model. VFA production rate from fermentation and VFA uptake rate by PAOs at the unaerated zone created in scenario 1 (A); nitrates plus nitrites (NO_x) at the second anoxic cell outlet, inlet of the unaerated zone in scenario 1, (B); *Accumulibacter* PAOs to total active biomass ratio, X_{PAO}/X_{Bio} (C) and PHA total, $X_{PHA,Tot}$ (D) at the aerobic tank outlet; anoxic OHO growth rate (E) and anoxic polyphosphate storage rate in PAOs (F) at the second anoxic cell outlet. The base scenario corresponds to the historical operation simulated in section 4.2.6.1.

4.4 Conclusions

This study evaluates the capacity of the META-ASM model to describe the long-term performance of a full-scale A2/O activated sludge system and to be used as an operational diagnostic tool for plant upsets. Its performance was compared with an updated version of the Barker & Dold model without changing default parameters. Overall, the META-ASM provided a better description of PAOs active biomass and storage polymers and was a more powerful operational diagnostic tool. The high aerobic HRTs and the low OLRs of the plant were only identified as the primary causes of the EBPR upsets because the META-ASM predicted that: i) the activity of GAOs was residual; ii) the replenishment of the glycogen pools in PAOs was low and PAOs used alternative metabolic pathways as a survival strategy that released more PO_4-P and produced less PHA per VFA uptake; iii) PAOs were depleting their PHA pools and consuming polyphosphate as a survival strategy under aerobic conditions.

The EBPR upsets were mitigated by switching-off air in the first half of the aeration tank. In this scenario, the META-ASM model predicted a simultaneous improvement in the biological P and N removal due to the enhancement of the hydrolysis and fermentation of the mixed liquor sludge in the created unaerated zone. The model predicted that PAOs were able to consume 41.6% of the VFAs produced, which favoured their growth and activity under anoxic and aerobic conditions.

This study establishes for the first time that the META-ASM model, previously identified as a predictive model, is a powerful operational diagnostic tool for EBPR systems, capable of predicting and mitigating upsets, optimising performance and evaluating new process designs.

4.5 References

Barat, R., Montoya, T., Seco, A., Ferrer, J., 2011. Modelling biological and chemically induced precipitation of calcium phosphate in enhanced biological phosphorus removal systems. Water Res. doi:10.1016/j.watres.2011.04.028

Barker, P.., Dold, P.L., 1997. General model for biological nutrient removal activated-sludge systems: model presentation. Water Environ. Res. 69, 969–984. doi:doi:10.2175/106143097X125669

Barnard, J., Houweling, D., Analla, H., Steichen, M., 2012. Saving phosphorus removal at the Henderson NV plant. Water Sci. Technol. doi:10.2166/wst.2012.022

Barnard, J.L., Abraham, K., 2006. Key features of successful BNR operation, in: Water Science and Technology. doi:10.2166/wst.2006.400

Barnard, J.L., Dunlap, P., Steichen, M., 2017. Rethinking the Mechanisms of Biological Phosphorus Removal. Water Environ. Res. doi:10.2175/106143017x15051465919010

Barnard, J.L., Steichen, M.T., 2006. Where is biological nutrient removal going now? Water Sci. Technol. doi:10.2166/wst.2006.088

Bunce, J.T., Ndam, E., Ofiteru, I.D., Moore, A., Graham, D.W., 2018. A review of phosphorus removal technologies and their applicability to small-scale domestic wastewater treatment systems. Front. Environ. Sci. doi:10.3389/fenvs.2018.00008

Bushee, G., Schauer, P., Menniti, A., 2019. An assessment of operational tools for Characterizing BPR activity and evaluating process health. Proc. 92nd Water Environ. Fed. Tech. Exhib. Conf. (WEFTEC 2019) 2, 838–856.

Carvalheira, M., Oehmen, A., Carvalho, G., Reis, M.A.M., 2014. Survival strategies of polyphosphate

accumulating organisms and glycogen accumulating organisms under conditions of low organic loading. Bioresour. Technol. 172, 290–296. doi:10.1016/j.biortech.2014.09.059

Cokro, A.A., Law, Y., Williams, R.B.H., Cao, Y., Nielsen, P.H., Wuertz, S., 2017. Non-denitrifying polyphosphate accumulating organisms obviate requirement for anaerobic condition. Water Res. 111, 393–403. doi:10.1016/j.watres.2017.01.006

Gu, A.Z., Saunders, A., Neethling, J.B., Stensel, H.D., Blackall, L.L., 2008. Functionally Relevant Microorganisms to Enhanced Biological Phosphorus Removal Performance at Full-Scale Wastewater Treatment Plants in the United States. Water Environ. Res. doi:10.2175/106143008x276741

Kazadi Mbamba, C., Batstone, D.J., Flores-Alsina, X., Tait, S., 2015. A generalised chemical precipitation modelling approach in wastewater treatment applied to calcite. Water Res. doi:10.1016/j.watres.2014.10.011

Lanham, A.B., Oehmen, A., Saunders, A.M., Carvalho, G., Nielsen, P.H., Reis, M.A.M., 2014. Metabolic modelling of full-scale enhanced biological phosphorus removal sludge. Water Res. 66C, 283–295. doi:10.1016/j.watres.2014.08.036

Lanham, A.B., Oehmen, A., Saunders, A.M., Carvalho, G., Nielsen, P.H., Reis, M.A.M., 2013. Metabolic versatility in full-scale wastewater treatment plants performing enhanced biological phosphorus removal. Water Res. 47, 7032–7041. doi:10.1016/j.watres.2013.08.042

Liu, W., Peng, Y., Ma, B., Ma, L., Jia, F., Li, X., 2017. Dynamics of microbial activities and community structures in activated sludge under aerobic starvation. Bioresour. Technol. 244, 588–596. doi:10.1016/j.biortech.2017.07.131

Lopez-Vazquez, C.M., Hooijmans, C.M., Brdjanovic, D., Gijzen, H.J., van Loosdrecht, M.C.M., 2009a. Temperature effects on glycogen accumulating organisms. Water Res. doi:10.1016/j.watres.2009.03.038

Lopez-Vazquez, C.M., Oehmen, A., Hooijmans, C.M., Brdjanovic, D., Gijzen, H.J., Yuan, Z., van Loosdrecht, M.C.M., 2009b. Modeling the PAO-GAO competition: Effects of carbon source, pH and temperature. Water Res. 43, 450–462. doi:10.1016/j.watres.2008.10.032

Lu, H., Keller, J., Yuan, Z., 2007. Endogenous metabolism of Candidatus Accumulibacter phosphatis under various starvation conditions. Water Res. 41, 4646–4656. doi:10.1016/j.watres.2007.06.046

Neethling, J.B., 2006. Factors Influencing the Reliability of Enhanced Biological Phosphorus Removal. doi:10.2166/9781780404479

Oehmen, A., Carvalho, G., Lopez-Vazquez, C.M., van Loosdrecht, M.C.M., Reis, M.A.M., 2010. Incorporating microbial ecology into the metabolic modelling of polyphosphate accumulating organisms and glycogen accumulating organisms. Water Res. 44, 4992–5004. doi:10.1016/j.watres.2010.06.071

Oehmen, A., Lemos, P.C., Carvalho, G., Yuan, Z.G., Keller, J., Blackall, L.L., Reis, M.A.M., 2007. Advances in enhanced biological phosphorus removal: From micro to macro scale. Water Res. 41, 2271–2300. doi:DOI 10.1016/j.watres.2007.02.030

Oleszkiewicz, J.A., Barnard, J.L., 2006. Nutrient removal technology in North America and the European Union: A review. Water Qual. Res. J. Canada. doi:10.1002/chin.200734273

Panswad, T., Doungchai, A., Anotai, J., 2003. Temperature effect on microbial community of enhanced biological phosphorus removal system. Water Res. doi:10.1016/S0043-1354(02)00286-5

Qiu, G., Zuniga-Montanez, R., Law, Y., Thi, S.S., Nguyen, T.Q.N., Eganathan, K., Liu, X., Nielsen, P.H., Williams, R.B.H., Wuertz, S., 2019. Polyphosphate-accumulating organisms in full-scale tropical wastewater treatment plants use diverse carbon sources. Water Res. doi:10.1016/j.watres.2018.11.011

Ren, N., Kang, H., Wang, X., Li, N., 2011. Short-term effect of temperature variation on the competition between PAOs and GAOs during acclimation period of an EBPR system. Front. Environ. Sci. Eng. China. doi:10.1007/s11783-010-0226-x

Rieger, L., Gillot, S., Langergraber, G., Ohtsuki, T., Shaw, A., Takacs, I., Winkler, S., 2012. Guidelines for Using Activated Sludge Models: IWA Task Group on Good Modelling Practice., Scientific and Technical Report No. 22. IWA Publishing, London, UK.

Rieger, L., Koch, G., Kuhni, M., Gujer, W., Siegrist, H., 2001. The EAWAG Bio-P module for activated sludge model No. 3. Water Res. 35, 3887–3903.

Santos, J.M.M., Rieger, L., Lanham, A.B., Carvalheira, M., Reis, M.A.M., Oehmen, A., 2020. A novel

metabolic-ASM model for full-scale biological nutrient removal systems. Water Res. 171, 115373. doi:10.1016/J.WATRES.2019.115373

Schauer, P., Bushee, G., Menniti, A., 2018. Characterizing BPR activity to understand overall process health. Proc. Water Environ. Fed. Nutr. Remov. Recover. 569–585.

Sedlak, R., 1991. Phosphorus and nitrogen removal from municipal wastewater: principles and practice, 2nd ed. Lewis Publishers/CRC Press: Boca Raton, Florida.

Shen, N., Chen, Y., Zhou, Y., 2017. Multi-cycle operation of enhanced biological phosphorus removal (EBPR) with different carbon sources under high temperature. Water Res. doi:10.1016/j.watres.2017.02.051

Solon, K., Flores-Alsina, X., Kazadi Mbamba, C., Ikumi, D., Volcke, E.I.P., Vaneeckhaute, C., Ekama, G., Vanrolleghem, P.A., Batstone, D.J., Gernaey, K. V., Jeppsson, U., 2017. Plant-wide modelling of phosphorus transformations in wastewater treatment systems: Impacts of control and operational strategies. Water Res. doi:10.1016/j.watres.2017.02.007

Stokholm-Bjerregaard, M., McIlroy, S.J., Nierychlo, M., Karst, S.M., Albertsen, M., Nielsen, P.H., 2017. A critical assessment of the microorganisms proposed to be important to enhanced biological phosphorus removal in full-scale wastewater treatment systems. Front. Microbiol. doi:10.3389/fmicb.2017.00718

Tooker, N.B., Barnard, J.L., Bott, C., Carson, K., Dombrowski, P., Dunlap, P., Martin, K., McQuarrie, J., Menniti, A., Phillips, H., Schauer, P., Shaw, A., Stevens, G., Takács, I., Onnis-Hayden, A., Gu, A.Z., 2016. Side-Stream Enhanced Biological Phosphorus Removal As A Sustainable And Stable Approach For Removing Phosphorus From Wastewater, in: Proceedings of WEF/IWA Nutrient Removal and Recovery 2016.

Varga, E., Hauduc, H., Barnard, J., Dunlap, P., Jimenez, J., Menniti, A., Schauer, P., Lopez Vazquez, C.M., Gu, A.Z., Sperandio, M., Takács, I., 2018. Recent advances in bio-P modelling - A new approach verified by full-scale observations. Water Sci. Technol. doi:10.2166/wst.2018.490

Vargas, M., Yuan, Z., Pijuan, M., 2013. Effect of long-term starvation conditions on polyphosphate- and glycogen-accumulating organisms. Bioresour. Technol. 127, 126–131. doi:10.1016/j.biortech.2012.09.117

Wang, D., Tooker, N.B., Srinivasan, V., Li, G., Fernandez, L.A., Schauer, P., Menniti, A., Maher, C., Bott, C.B., Dombrowski, P., Barnard, J.L., Onnis-Hayden, A., Gu, A.Z., 2019. Side-stream enhanced biological phosphorus removal (S2EBPR) process improves system performance - A full-scale comparative study. Water Res. doi:10.1016/j.watres.2019.115109

Whang, L., Park, J.K., 2006. Competition between Polyphosphate- and Glycogen-Accumulating Organisms in Systems : Effect of Temperature and Sludge Age. Water Environ. Res.

Wu, Linwei, Ning, D., Zhang, B., Li, Y., Zhang, P., Shan, X., Zhang, Qiuting, Brown, Mathew, Li, Z., Van Nostrand, J.D., Ling, F., Xiao, N., Zhang, Ya, Vierheilig, J., Wells, G.F., Yang, Y., Deng, Y., Tu, Q., Wang, A., Acevedo, D., Agullo-Barcelo, M., Alvarez, P.J.J., Alvarez-Cohen, L., Andersen, G.L., de Araujo, J.C., Boehnke, K., Bond, P., Bott, C.B., Bovio, P., Brewster, R.K., Bux, F., Cabezas, A., Cabrol, L., Chen, S., Criddle, C.S., Deng, Y., Etchebehere, C., Ford, A., Frigon, D., Gómez, J.S., Griffin, J.S., Gu, A.Z., Habagil, M., Hale, L., Hardeman, S.D., Harmon, M., Horn, H., Hu, Z., Jauffur, S., Johnson, D.R., Keller, J., Keucken, A., Kumari, S., Leal, C.D., Lebrun, L.A., Lee, J., Lee, M., Lee, Z.M.P., Li, Y., Li, Z., Li, M., Li, X., Ling, F., Liu, Y., Luthy, R.G., Mendonça-Hagler, L.C., de Menezes, F.G.R., Meyers, A.J., Mohebbi, A., Nielsen, P.H., Ning, D., Oehmen, A., Palmer, A., Parameswaran, P., Park, J., Patsch, D., Reginatto, V., de los Reyes, F.L., Rittmann, B.E., Robles, A.N., Rossetti, S., Shan, X., Sidhu, J., Sloan, W.T., Smith, K., de Sousa, O.V., Stahl, D.A., Stephens, K., Tian, R., Tiedje, J.M., Tooker, N.B., Tu, Q., Van Nostrand, J.D., De los Cobos Vasconcelos, D., Vierheilig, J., Wagner, M., Wakelin, S., Wang, A., Wang, B., Weaver, J.E., Wells, G.F., West, S., Wilmes, P., Woo, S.-G., Wu, Linwei, Wu, J.-H., Wu, Liyou, Xi, C., Xiao, N., Xu, M., Yan, T., Yang, Y., Yang, M., Young, M., Yue, H., Zhang, B., Zhang, P., Zhang, Qiuting, Zhang, Ya, Zhang, T., Zhang, Qian, Zhang, W., Zhang, Yu, Zhou, H., Zhou, J., Wen, X., Curtis, T.P., He, Q., He, Z., Brown, Matthew, Zhang, T., He, Z., Keller, J., Nielsen, P.H., Alvarez, P.J.J., Criddle, C.S., Wagner, M., Tiedje, J.M., He, Q., Curtis, T.P., Stahl, D.A., Alvarez-Cohen, L., Rittmann, B.E., Wen, X., Zhou, J., Consortium, G.W.M., 2019. Global diversity and biogeography of bacterial communities in wastewater treatment plants. Nat. Microbiol. doi:10.1038/s41564-019-0426-5

Yang, Y., Shi, X., Ballent, W., Mayer, B.K., 2017. Biological Phosphorus Recovery: Review of Current Progress and Future Needs. Water Environ. Res. doi:10.2175/106143017x15054988926424

Zhou, Y., Pijuan, M., Zeng, R.J., Yuan, Z., 2009. Involvement of the TCA cycle in the anaerobic metabolism of polyphosphate accumulating organisms (PAOs). Water Res. 43, 1330–1340. doi:10.1016/j.watres.2008.12.008

5

GENERAL CONCLUSIONS AND PERSPECTIVES

5.1 General conclusions

This PhD project focussed on the development, calibration, validation and application of a novel integrated metabolic activated sludge model, the META-ASM, that describes the activity of the key organisms and processes relevant to EBPR with a robust single set of default parameters. The advances on the EBPR mechanisms investigated over the last twenty years were integrated into the META-ASM model to overcome various shortcomings of existing EBPR models, which require extensive calibration. Examples of model improvements incorporated were: the effect of operational conditions on the competition between PAOs and GAOs, the capability of PAOs and GAOs to denitrify, the metabolic shifts as a function of storage polymer concentrations, as well as the role of these polymers in endogenous processes, and a better description of the fermentation process.

This PhD project demonstrated that the META-ASM model is:

i. **capable of dynamically predicting the microbial and chemical transformations in EBPR systems over a wide range of operational and environmental conditions** (e.g. various environmental temperatures and pHs, different DO concentrations, different rbCOD/P_{Tot} ratios and type of carbon sources in the influent, different SRTs and HRTs in the anaerobic, anoxic and aerobic zones). This capability was validated against 34 different data sets obtained from bench-scale batch tests inoculated with lab-scale enriched PAO-GAO cultures and full-scale sludge from five WRRFs. The overall strong agreement between the predicted versus measured EBPR profiles from different data sets support that this new model, which is based on in-depth understanding of EBPR, reduces calibration efforts. Furthermore, the applicability of one unique default parameter set to describe well all 34 data sets supports the robustness of the proposed model to a wide range of conditions relevant to EBPR systems. In addition, the comparison of the predictive power of the META-ASM with other existing literature models showed that existing literature models require extensive parameter changes to describe different EBPR dynamics, unlike META-ASM.
ii. **capable of dynamically predicting long-term EBPR performance.** This capability was evaluated in a 1336-day long-term dynamic simulation of a full-scale A2/O EBPR system, and the effectiveness of the META-ASM was compared with the ASM-inCTRL model, a version based on the Barker & Dold model without changing default parameters. In this study, the META-ASM provided a better description of the active biomass of PAOs and the dynamics of their storage polymers.
iii. **a powerful operational diagnostic tool that predicts EBPR upsets, optimises EBPR performance and evaluates new process designs.** These features were tested in a full-scale A2/O EBPR system that suffers from unpredictable EBPR upsets. The effectiveness of the META-ASM model was compared with the ASM-inCTRL model, where the high aerobic HRTs and the low OLRs of the plant were only identified as the primary causes of the EBPR upsets through the META-ASM model. The simulation of two viable scenarios, designed within the boundaries of the existing

infrastructure available at the plant, showed that the biological P and N removal could be improved without the need for chemical dosing by switching-off air in the first half of the aeration tank. In this scenario, the META-ASM predicted an enhancement of the hydrolysis and fermentation of the mixed liquor sludge in the created unaerated zone, which increased the availability of VFAs for PAOs.

5.2 Perspectives and future work

For future research on EBPR mechanisms, a better understanding of the metabolism of new putative PAO and GAO organisms, such as the genera *Tetrasphaera* and *Micropruina*, respectively, is recommended, as well as a better understanding of the interactions between these organisms and the classical PAO and GAO organisms studied in this PhD project. So far, it is known that the genera *Tetrasphaera* and *Micropruina* do not rely on PHA and they appear to be less competitive for VFA uptake. They can grow anaerobically by fermenting amino acids or sugars and it is hypothesized that they interact with the classical PAOs and GAOs under anaerobic conditions due to the VFAs produced through fermentation. These novel organisms can also grow aerobically through the oxidation of glycogen (*Micropruina* spp.) or intracellular metabolites, such as amino acids, sugars and possibly fermentation products (*Tetrasphaera* spp.). The impact of different operational and environmental conditions on their metabolism, such as different pHs, environmental temperatures, DO and anaerobic, anoxic and aerobic HRTs is still unclear. Further research is also required to better elucidate the denitrification capabilities of the different clades of these novel and classical PAO and GAO organisms. The incorporation of this improved knowledge in EBPR mathematical models, including the META-ASM model, will increase their predictive power due to the fact that these novel PAO and GAO organisms have been found in significant abundance in WRRFs, sometimes outnumbering the classical PAO and GAO organisms. On the other hand, recent studies have investigated the integration of high-rate EBPR systems operated with SRTs lower than 4 days in the A-stage of an A/B WRRF, as an energy-efficient alternative to the systems operated at medium to long SRTs (5-40 days). Although the ecology and ecophysiology of these systems are still under investigation, it is anticipated that a new mathematical model or the adaptation of existing models will be necessary to describe this configuration.

For further development of the META-ASM model, it is recommended the incorporation of a chemical P precipitation model to describe the impact that the dosage of chemicals have on the EBPR performance and P recovery from downstream processes. Furthermore, a better description of the hydrolysis processes and the incorporation of other anaerobic processes that describe the activity of hydrogenotrophic and acetoclastic methanogenic organisms is also required to model in detail side-stream fermentation systems. This work also suggested that there are other non-PAO and GAO organisms present in full-scale activated sludge that are capable of storing PHA anaerobically or aerobically and can compete with PAO and GAO for the carbon source and contribute to denitrification.

If needed, future work in this area could incorporate PHA storage by ordinary heterotrophs into the model, as performed in the ASM3 model.

Application of the META-ASM in other EBPR systems is also expected to further demonstrate the benefits as a diagnostic, optimisation and design tool. Increasing attention has been given to granular systems and side-stream processes (RAS fermentation and shortcut nitrogen removal) coupled with EBPR and denitrifying and low DO operated EBPR systems. The META-ASM model can provide important insights and guidelines for the design of these novel configurations, since it summarises the current state-of-knowledge of the most relevant biochemical transformations occurring in activated sludge processes.

The WRRF industry is also moving towards digitalisation to improve real time decision-making. This PhD work suggested that the META-ASM model has potential to provide an early warning of EBPR upset by predicting variations in the aerobic PAO maintenance rates. This feature should be better investigated to develop real time decision-making solutions for EBPR facilities.

On the other hand, the approach used in the META-ASM model can be extended to other non-EBPR systems, such as the three-stage process of PHA production by mixed microbial cultures (1st stage: acidogenic fermentation, 2nd stage: aerobic culture selection and 3rd stage: PHA production), as the metabolic approach proved to be very effective in describing highly dynamic processes. The development of a microbial community-based model and its use as an operational diagnostic tool, capable of optimising the acidogenic fermentation to produce the required VFA composition, would be very useful to maintain the long-term production of PHA within the desired properties.

APPENDIX A. MODEL CALIBRATION METHODOLOGY

A.1. Definition of initial conditions

The initial concentrations of the soluble components correspond to the experimental values of volatile fatty acids, VFAs (i.e. acetate and/or propionate), soluble inorganic phosphorus (PO_4^{3-}-P), nitrate (NO_3^--N) and ammonium plus ammonia nitrogen (NH_x-N) added in each test, except that a typical value of 7.0 mol.m^{-3} was assumed for the alkalinity. Note that, there is no effect of the soluble components and colloidals present in the inoculums of the full-scale WRRFs under study, since Lanham et al. (2013a, 2018) washed the sludge three times with mineral media. Carvalheira et al. (2014a, 2014b) and Carvalho et al. (2007) inoculated the tests with inoculum collected at the end of the aerobic and anoxic phases of enriched PAO or GAO SBRs, respectively. In these samples, the concentrations of VFAs, PO_4^{3-}-P or NO_3^--N were zero, except the concentration of NH_x-N that was residual, and therefore it was counted in the definition of the initial concentration of S_{NHx}.

The initial concentrations of the particulate components in each WRRF and enriched culture sludges were determined as follows. The active biomass concentration ($X_{VSS,BIO}$, g VSS.m^{-3}) was calculated through the difference between the measured volatile suspended solids (VSS_{exp}, g VSS.m^{-3}) and the respective measured concentrations of total PHA (PHA_{exp}, g COD.m^{-3}), total glycogen (Gly_{exp}, g COD.m^{-3}), slowly biodegradable substrate ($B_{X,exp}$, g COD.m^{-3}) and particulate unbiodegradable organics ($Ux_{,exp}$, g COD.m^{-3}), see equation A1. Note that this is an approximate estimation for the tests inoculated with full-scale sludge, since the contribution of X_E and water loss per metal are neglected in this equation. Nevertheless, this is still an accurate approximation for the tests inoculated with enriched cultures, since PAO and GAO are characterised by having low decay rates (as they tend to exhaust their storage polymers prior to decay) and metals were not added.

The conversion factors ($i_{CV,i}$) described in Table A1 were used for the unit conversions. PHA_{exp} and Gly_{exp} were measured according to the methodologies described in Lanham et al. (2012, 2013b), respectively. $Ux_{,exp}$ and $B_{X,exp}$ were determined after evaluation of historical data from the WRRF influents in the tests inoculated with full-scale sludge (see guidelines in Rieger et al., 2012). In the tests inoculated with enriched cultures, these concentrations were neglected because the parent SBRs were fed with synthetic media for a long period of time prior to the experiments.

$$X_{VSS,Bio}(g\ VSS.m^{-3}) \approx VSS_{exp} - \frac{PHA_{exp}}{i_{CV,PHA}} - \frac{Gly_{exp}}{i_{CV,Gly}} - \frac{B_{X,exp}}{i_{CV,B}} - \frac{U_{X,exp}}{i_{CV,U}} \quad \text{(A1)}$$

Table A1. Conversion factors used for the characterization of the particulate components.

Composition coefficients	Description	Value	Units	Reference
$i_{CV,Bio}$	COD to VSS ratio for X_{Bio}	1.42	g COD/g VSS	ASM_inCTRL model
$i_{CV,B}$	COD to VSS ratio for X_B	1.8	g COD/g VSS	ASM_inCTRL model
$i_{CV,U}$	COD to VSS ratio for X_U	1.3	g COD/g VSS	ASM_inCTRL model
$i_{CV,PHA}$	COD to VSS ratio for PHA	1.77	g COD/g VSS	This study
$i_{CV,Gly}$	COD to VSS ratio for glycogen	1.18	g COD/g VSS	This study
$i_{ISS,PP}$	TSS content of polyphosphate	3.23	g TSS/g P	ASM_inCTRL model

The concentrations of X_{PAO}, X_{CPO}, X_{DFO} and X_{OHO} were determined through equations A2-A5, wherein the active biomass fractions for the total *Accumulibacter*-PAOs ($f_{PAO,qFISH}$), *Competibacter-lineage*-GAOs ($f_{CPO,qFISH}$) and *Defluviicoccus vanus* GAOs ($f_{DFO,qFISH}$) were determined by quantitative fluorescence *in situ* hybridisation (qFISH).

$$X_{PAO}\ (g\ COD.m^{-3}) = X_{Bio} \times i_{CV,Bio} \times f_{PAO,qFISH} \quad \text{(A2)}$$

$$X_{CPO}(g\ COD.m^{-3}) = X_{Bio} \times i_{CV,Bio} \times f_{CPO,qFISH} \quad \text{(A3)}$$

$$X_{DFO}\ (g\ COD.m^{-3}) = X_{Bio} \times i_{CV,Bio} \times f_{DFO,qFISH} \quad \text{(A4)}$$

$$X_{OHO}\ (g\ COD.m^{-3}) \approx (X_{Bio} \times i_{CV,Bio}).(1 - f_{PAO,qFISH} - f_{CPO,qFISH} - f_{DFO,qFISH}) \quad \text{(A5)}$$

The activities of AOOs and NOOs were inhibited in these batch tests, since allyl-N thiourea (ATU) was added to prevent nitrification, while the OHOs are not able to take up VFAs anaerobically. However, the OHOs are able to hydrolyse the slowly biodegradable substrate present in the WRRF inoculum, ferment the fermentable organic matter produced in the previous step, and uptake the residual concentrations of acetate that, in some tests, passed from the anaerobic to the aerobic and anoxic reactors. To simulate these effects, the initial concentration of X_{OHO} was defined through the difference between the total active biomass concentration and the concentrations of PAOs and GAOs (see equation A5). It is important to highlight that equation A5 is valid only because the activity of OHOs was low and ANOs were inhibited and, therefore, their impact on kinetics is minimal.

In systems with the simultaneous presence of PAOs and GAOs, the initial concentrations of PHA and glycogen were fractionated according to equations A9 and A10, respectively, as performed by Lanham et al. (2014). In these equations, $Y_{VFA\text{-}PHA,i}$ corresponds to the yield for anaerobic formation of PHA from VFAs in PAOs or GAOs, while $Y_{VFA\text{-}Gly,i}$ corresponds to the yield for anaerobic consumption of glycogen from VFAs in PAOs or GAOs. These yields were determined according to the equations A7 and A8, respectively, wherein the weighted contribution of acetate and propionate to the determination of the overall yield is counted (see the individual stoichiometric yields defined in Table A2).

PAO, CPO and DFO are the only groups of microorganisms considered in META-ASM as being able to store PHAs and glycogen. Due to this reason, the fractions $f_{i,Stor}$ were calculated through equation A6, wherein i correspond to PAO, CPO or DFO.

$$f_{i,Stor} = \frac{f_{i,qFISH}}{f_{PAO,qFISH} + f_{CPO,qFISH} + f_{DFO,qFISH}}, i = PAO, CPO\ or\ DFO \quad (A6)$$

$$Y_{VFA-PHA,i} = Y_{Ac-PHA,i} \cdot \frac{Ac_{exp,in}}{VFAs_{exp,in}} + Y_{Pr-PHA,i} \cdot \frac{Pr_{exp,in}}{VFAs_{exp,in}}, i = PAO \text{ or GAO} \quad (A7)$$

$$Y_{VFA-Gly,i} = Y_{Ac-Gly,i} \cdot \frac{Ac_{exp,in}}{VFAs_{exp,in}} + Y_{Pr-Gly,i} \cdot \frac{Pr_{exp,in}}{VFAs_{exp,in}}, i = PAO \text{ or GAO} \quad (A8)$$

$$X_{i,PHA}(g\ COD.m^{-3}) = PHA_{exp} \cdot \frac{f_{i,Stor} \times Y_{VFA-PHA,i}}{f_{PAO,Stor} \times Y_{VFA-PHA,PAO} + f_{CPO,Stor} \times Y_{VFA-PHA,GAO} + f_{DFO,Stor} \times Y_{VFA-PHA,GAO}} \quad (A9)$$

$$X_{i,Gly}\ (g\ COD.m^{-3}) = Gly_{exp} \cdot \frac{f_{i,Stor} \times Y_{VFA,Gly,i}}{f_{PAO,Stor} \times Y_{VFA-Gly,PAO} + f_{CPO,Stor} \times Y_{VFA-Gly,GAO} + f_{DFO,Stor} \times Y_{VFA-Gly,GAO}} \quad (A10)$$

Table A2. Anaerobic stoichiometric yields of PAOs and GAOs.

Stoichiometric yields	Description	Value	Units	Reference
$Y_{Ac-PHA,PAO}$	Yield for anaerobic formation of PHA from acetate in PAOs	1.50	g COD. g COD^{-1}	(Smolders et al., 1994)
$Y_{Pr-PHA,PAO}$	Yield for anaerobic formation of PHA from propionate in PAOs	1.29	g COD. g COD^{-1}	(Oehmen et al., 2005)
$Y_{Ac-Gly,PAO}$	Yield for anaerobic consumption of glycogen from acetate in PAOs	0.50	g COD. g COD^{-1}	(Smolders et al., 1994)
$Y_{Pr-Gly,PAO}$	Yield for anaerobic consumption of glycogen from propionate in PAOs	0.29	g COD. g COD^{-1}	(Oehmen et al., 2005)
$Y_{Ac-PHA,GAO}$	Yield for anaerobic formation of PHA from acetate in GAOs	2.12	g COD. g COD^{-1}	(Zeng et al., 2003)
$Y_{Pr-PHA,GAO}$	Yield for anaerobic formation of PHA from propionate in GAOs	1.57	g COD. g COD^{-1}	(Oehmen et al., 2006)
$Y_{Ac-Gly,GAO}$	Yield for anaerobic consumption of glycogen from acetate in GAOs	1.12	g COD. g COD^{-1}	(Zeng et al., 2003)
$Y_{Pr-Gly,GAO}$	Yield for anaerobic consumption of glycogen from propionate in GAOs	0.57	g COD. g COD^{-1}	(Oehmen et al., 2006)

Stored polyphosphate in PAOs, $X_{PAO,PP}$, (gP.m^{-3}) was determined experimentally by quantifying the phosphorus released after a prolonged anaerobic phase and the inorganic suspended solids (X_{IG}) was determined by equation A11. The TSS content of polyphosphate ($i_{ISS,PP}$) is defined in Table A1. Note that the impact of metal-hydroxides (X_{MeOH}) and metal-phosphates (X_{MeP}) in equation A11 were

neglected in this study for the reasons explained above and because only the Danish WRRFs supplemented the P removal with precipitants.

$$X_{IG}(g.m^{-3}) \approx TSS_{exp} - VSS_{exp} - X_{PAO,PP}.i_{ISS,PP} \quad \text{(A11)}$$

The following equations were defined, and incorporated in the META-ASM model, for the calibration of the anaerobic acetate and propionate uptake rates of PAO and GAOs when both organisms were present.

$$q_{CPO,Ac,PHA,10\_20^{o}C} = q_{PAO,Ac,PHA} \quad \text{(A12)}$$

$$q_{CPO,Ac,PHA,20\_30^{o}C} = 1.091 \times q_{PAO,Ac,PHA} \quad \text{(A13)}$$

$$q_{DFO,Ac,PHA,10\_20^{o}C} = 0.55 \times q_{PAO,Ac,PHA} \quad \text{(A14)}$$

$$q_{DFO,Ac,PHA,20\_30^{o}C} = 0.65 \times q_{PAO,Ac,PHA} \quad \text{(A15)}$$

$$q_{DFO,Pr,PHA,10\_20^{o}C} = q_{PAO,Pr,PHA} \quad \text{(A16)}$$

$$q_{DFO,Pr,PHA,20\_30^{o}C} = 1.091 \times q_{PAO,Pr,PHA} \quad \text{(A17)}$$

Wherein $q_{PAO,AC,PHA}$, $q_{CPO,AC,PHA}$ and $q_{DFO,AC,PHA}$ correspond to the maximum anaerobic acetate uptake rates by PAOs, CPOs and DFOs, respectively. While $q_{PAO,Pr,PHA}$ and $q_{DFO,Pr,PHA}$ correspond to the maximum propionate uptake rates by PAOs and DFOs. The influence of the temperature was also incorporated. These assumptions are based on the experimental results obtained by Carvalheira et al. (2014b) and Lopez-Vazquez et al. (2009) with enriched PAOs and GAOs cultures. Through this methodology, the kinetic rates of PAOs are the only parameters calibrated in the anaerobic phase, the others are sequentially determined.

APPENDIX B. DATA COLLECTION

Table B.1. List of input and performance data collected.

Data type	Parameter	Sampling type	Sampling frequency	Sampling location	Data source
Input data					
-Influent organics and suspended solids	$COD_{Tot,INF}$ ($g.m^{-3}$)	composite	weekly	1	routine sampling
	$CBO5_{Tot,\ INF}$ ($g.m^{-3}$)		twice per month		
	TSS_{INF} ($g.m^{-3}$)		twice per month		
-Influent nutrients	TN_{INF} ($g\ N.m^{-3}$)	composite	twice per month	1	routine sampling
	$P_{Tot,INF}$ ($g\ P.m^{-3}$)				
-Influent flow	Q_{INF+RW} ($m^3.d^{-1}$)	online	daily	2	SCADA [a]
-Iron	C_{Fe} ($g\ Fe.m^{-3}$)	composite	monthly	7	routine sampling
-Iron dosage	Q_{Fe} ($m^3.d^{-1}$)	online	daily	7	SCADA [a]
-pH	pH_{INF}	composite	weekly	1	routine sampling
Performance data					
-Effluent organics and suspended solids	$COD_{Tot,EFF}$ ($g.m^{-3}$)	composite	weekly	8	routine sampling
	$CBO5_{Tot,EFF}$ ($g.m^{-3}$)		twice per month		
	TSS_{EFF} ($g.m^{-3}$)		twice per month		
-Effluent nutrients	TN_{EFF} ($g\ N.m^{-3}$)	composite	twice per month	8	routine sampling
	$P_{Tot,EFF}$ ($g\ P.m^{-3}$)		weekly		
-pH	pH_{EFF}	composite	weekly	8	routine sampling
-Mixed liquor (total and soluble fractions)	PO_4-P R_{AN2} ($g\ P.m^{-3}$)	grab	twice per month	3	routine sampling
	PO_4-P R_{OX} ($g\ P.m^{-3}$)		weekly	5	
	NO_3-N R_{AX2} ($g\ N.m^{-3}$)		monthly	4	
	NO_3-N R_{OX} ($g\ N.m^{-3}$)		monthly	5	
	NH_4-N R_{OX} ($g\ N.m^{-3}$)		monthly	5	
	COD_{Tot} R_{OX} ($g.m^{-3}$)		weekly	5	
	MLVSS R_{OX} ($g.m^{-3}$)		monthly	5	
-Temperature	T R_{OX} (ºC)	online	twice per day	5	SCADA [a]
-Dissolved oxygen	DO ($g\ O_2.m^{-3}$)	online	every 4 minutes	5	SCADA [a]
Internal recycle flow	$Q_{ROX\text{-}RAX1}$ ($m^3.d^{-1}$)	Fixed flow		6	
-RAS solids	TS_{RAS} ($g.m^{-3}$)	grab	weekly	9	routine sampling
-RAS flow	Q_{RAS} ($m^3.d^{-1}$)	online	daily	9	SCADA [a]
-WAS flow	Q_{WAS} ($m^3.d^{-1}$)	online	daily	10	SCADA [a]
-Sludge	Dry matter ($g.m^{-3}$)	grab	weekly	11 and 12	routine sampling
-Sludge flow	Q_{TW} ($m^3.d^{-1}$)	online	daily	11	SCADA [a]

[a] Supervisory control and data acquisition system.

APPENDIX C. REFERENCES FOR THE SUPPLEMENTARY MATERIAL

Carvalheira, M., Oehmen, A., Carvalho, G., Eusébio, M., Reis, M.A.M., 2014a. The impact of aeration on the competition between polyphosphate accumulating organisms and glycogen accumulating organisms. Water Res. 66C, 296–307. doi:10.1016/j.watres.2014.08.033

Carvalheira, M., Oehmen, A., Carvalho, G., Reis, M.A.M., 2014b. The effect of substrate competition on the metabolism of polyphosphate accumulating organisms (PAOs). Water Res. 64, 149–59. doi:10.1016/j.watres.2014.07.004

Carvalho, G., Lemos, P.C., Oehmen, A., Reis, M.A.M., 2007. Denitrifying phosphorus removal: Linking the process performance with the microbial community structure. Water Res. 41, 4383–4396. doi:10.1016/j.watres.2007.06.065

Lanham, A.B., Oehmen, A., Carvalho, G., Saunders, A.M., Nielsen, P.H., Reis, M.A.M., 2018. Denitrification activity of polyphosphate accumulating organisms (PAOs) in full-scale wastewater treatment plants. Water Sci. Technol. 78, 2449–2458. doi:10.2166/wst.2018.517

Lanham, A.B., Oehmen, A., Saunders, A.M., Carvalho, G., Nielsen, P.H., Reis, M.A.M., 2014. Metabolic modelling of full-scale enhanced biological phosphorus removal sludge. Water Res. 66C, 283–295. doi:10.1016/j.watres.2014.08.036

Lanham, A.B., Oehmen, A., Saunders, A.M., Carvalho, G., Nielsen, P.H., Reis, M.A.M., 2013a. Metabolic versatility in full-scale wastewater treatment plants performing enhanced biological phosphorus removal. Water Res. 47, 7032–7041. doi:10.1016/j.watres.2013.08.042

Lanham, A.B., Ricardo, A.R., Albuquerque, M.G.E., Pardelha, F., Carvalheira, M., Coma, M., Fradinho, J., Carvalho, G., Oehmen, A., Reis, M.A.M., 2013b. Determination of the extraction kinetics for the quantification of polyhydroxyalkanoate monomers in mixed microbial systems. Process Biochem. doi:10.1016/j.procbio.2013.07.023

Lanham, A.B., Ricardo, A.R., Coma, M., Fradinho, J., Carvalheira, M., Oehmen, A., Carvalho, G., Reis, M.A.M., 2012. Optimisation of glycogen quantification in mixed microbial cultures. Bioresour. Technol. doi:10.1016/j.biortech.2012.05.087

Lopez-Vazquez, C.M., Oehmen, A., Hooijmans, C.M., Brdjanovic, D., Gijzen, H.J., Yuan, Z., van Loosdrecht, M.C.M., 2009. Modeling the PAO-GAO competition: Effects of carbon source, pH and temperature. Water Res. 43, 450–462. doi:10.1016/j.watres.2008.10.032

Oehmen, A., Yuan, Z., Blackall, L.L., Keller, J., 2005. Comparison of acetate and propionate uptake by polyphosphate accumulating organisms and glycogen accumulating organisms. Biotechnol. Bioeng. doi:10.1002/bit.20500

Oehmen, A., Zeng, R.J., Saunders, A.M., Blackall, L.L., Keller, J., Yuan, Z., 2006. Anaerobic and aerobic metabolism of glycogen-accumulating organisms selected with propionate as the sole carbon source. Microbiology. doi:10.1099/mic.0.28065-0

Rieger, L., Gillot, S., Langergraber, G., Ohtsuki, T., Shaw, A., Takacs, I., Winkler, S., 2012. Guidelines for Using Activated Sludge Models: IWA Task Group on Good Modelling Practice., Scientific and Technical Report No. 22. IWA Publishing, London, UK.

Smolders, G.J., van der Meij, J., van Loosdrecht, M.C., Heijnen, J.J., 1994. Model of the anaerobic metabolism of the biological phosphorus removal process: Stoichiometry and pH influence. Biotechnol. Bioeng. 43, 461–470. doi:10.1002/bit.260430605

Zeng, R.J., Van Loosdrecht, M.C.M., Yuan, Z., Keller, J., 2003. Metabolic Model for Glycogen-Accumulating Organisms in Anaerobic/Aerobic Activated Sludge Systems. Biotechnol. Bioeng. 81, 92–105. doi:10.1002/bit.10455